

CIE4440 - HYDROLOGICAL MEASUREMENTS



ir. W.M.J. Luxemburg and dr. ir. A.M.J. Coenders
Lecture notes
Delft University of Technology

October 31, 2011

Contents

1. <i>Introduction</i>	1
1.1 Need for measurements	1
1.2 Scope of the lecture	2
2. <i>Theory of errors</i>	5
2.1 Nature of errors	5
2.1.1 Random Errors	5
2.1.2 Systematic errors	5
2.1.3 Spurious errors	5
2.2 Measure for errors	5
2.3 Error propagation from mathematical relations	6
2.3.1 Repetition of measurements	9
2.4 Error propagation from bivariate regression and correlation	9
2.4.1 Bivariate linear regression	9
2.4.2 Bivariate linear correlation	11
2.5 Error detection from measurements	15
2.5.1 Spatial inhomogeneities	15
2.5.2 Statistical time series analysis	18
3. <i>Precipitation</i>	27
3.1 The precipitation mechanisms	27
3.2 Measuring rainfall	28
3.2.1 Point observations of rainfall	28
3.2.2 Areal observations of rainfall	32
3.3 The correlation function	35
3.3.1 Example: Rainfall correlation in the Netherlands	37
4. <i>Evaporation</i>	41
4.1 Types of evaporation and definitions	41
4.2 The process of evaporation	42
4.2.1 Factors influencing evaporation	43
4.3 Measuring evaporation	49
4.3.1 Penman Equation	49

4.3.2	Penman-Monteith Equation	51
4.3.3	Pan evaporation	51
4.3.4	Lysimeters	52
4.3.5	Sapflow	52
4.3.6	Bowen ratio	52
4.3.7	Eddy correlation	54
4.3.8	Scintillometer	54
4.3.9	Energy balance	54
5.	<i>Soil water</i>	55
5.1	Capacitance Probe	55
5.2	Time Domain Reflectometry (TDR)	56
5.3	Frequency Domain Reflectometry (FDR)	56
5.4	Heat Pulse Sensors	57
5.5	Remote Sensing	57
5.5.1	Further readings	57
6.	<i>Measurements of stage</i>	59
6.1	Introduction	59
6.2	Selection of Location	59
6.3	Equipment pre-considerations	60
6.4	Principles of measurement equipment	61
6.4.1	Staff gauges	62
6.4.2	Float gauges	62
6.4.3	Bubble-type pneumatic gauge	63
6.4.4	Ultrasonic water level gauges	64
6.4.5	Electronic pressure transducers	64
6.5	Stilling well and intake	65
6.6	Water level recording devices	66
6.6.1	Manual recording	66
6.6.2	Autographic recorders	66
6.6.3	Solid-state recorders	67
6.6.4	Others	67
7.	<i>Stage-discharge relation</i>	69
7.1	Introduction	69
7.2	Site selection	69
7.3	Composition of Rating curves	70
7.3.1	Rating Curve Accuracy	73
7.4	Non-steady and non-uniform flow	76
7.4.1	The flood wave	77
7.4.2	Backwater curves	78

8. <i>Streamflow measurements</i>	83
8.1 Introduction	83
8.2 Velocity Area Method	84
8.2.1 Principles	84
8.2.2 Site selection	87
8.2.3 Instruments to measure point velocity	87
8.2.4 Current meter measurements by wading	95
8.2.5 Suspension systems	96
8.2.6 Moving boat	98
8.3 Dilution gauging	104
8.3.1 Principles	104
8.3.2 Constant rate injection method	104
8.3.3 Sudden or Gulp injection method	108
8.3.4 Range and accuracy	109
8.4 Ultra-sonic streamflow measurement	109
8.4.1 Theory	109
8.4.2 Site selection	112
8.4.3 Instrumentation	113
8.4.4 Accuracy	114
8.4.5 Existing installations	115
8.5 Electromagnetic streamflow measurement	115
8.5.1 Theory	115
8.5.2 Site selection	117
8.5.3 Design and construction	118
8.6 Flood surveys	119
8.6.1 Floats	119
8.6.2 Slope area method	122
8.6.3 Simplified slope area method	123
8.7 Structures	124
8.7.1 Principles	124
8.7.2 Description of structures	128
9. <i>Tracer Hydrology</i>	141
9.1 General overview on tracer hydrology	141
9.2 Applications	141
10. <i>Interpolation techniques</i>	143
10.1 Inverse distance	143
10.2 Thiessen polygons	144
10.3 Contouring	144
10.4 Kriging	145
10.4.1 Validation of Kriging results	148

<i>11. Design of networks</i>	151
11.1 Kriging	151
11.2 Kagan	151
 <i>Appendix</i>	 157
<i>A. Examples of statistical methods and distributions</i>	159
A.1 Detection of spatial inhomogeneities	160
A.2 Standard normal distribution	161
A.3 Students-t distribution	162
A.4 The Spearman's rank test	163
A.5 Fisher-F distribution	164
A.6 Split record tests	165

1

Introduction

1.1 Need for measurements

The concept of the hydrological cycle (Figure 1.1) forms the basis for the engineering hydrologist's understanding of the sources of water at or under the earth's surface and its consequent movement by various pathways back to the principle storage in the oceans. Two of the greatest problems for the hydrologist are quantifying the amount of water in the different phases in the cycle and evaluating the rate of transfer of water from one phase to another within the cycle. Thus measurement within the components of the cycle is a major function.

Four main purposes for measured data can be distinguished, each with its own requirements:

1. for planning, which requires long term records usually on large time scale
2. for design, which requires long term records usually on small time scale
3. for management, which requires real-time measurements and forecasting
4. for research, which generally requires high quality intensive data

The importance of any of these purposes and even more detailed uses may vary from country to country. Streamflow data, for example, within the context of water management can be used for pollution control, water supply, irrigation, flood control, energy generation and industrial use. The purpose of data often is related to where the main water related constraints lie in a country or region. Generally the constraints vary considerably worldwide, but can be classified into issues related to water shortage, abundance or water quality matters. Again this might change over time and vary within hydrological years.

The cost effectiveness of data collection is an important consideration. Therefore, it is wise to establish the purpose of the data and act accordingly in the planning of measurements and/or the design of networks. Cost-effectiveness may be measured by the benefit-cost ratio, but to estimate this ratio is difficult, due to the problems associated with assessing the benefits accruing. This problem often leaves the hydrological service at a disadvantage in bidding for funds. Direct

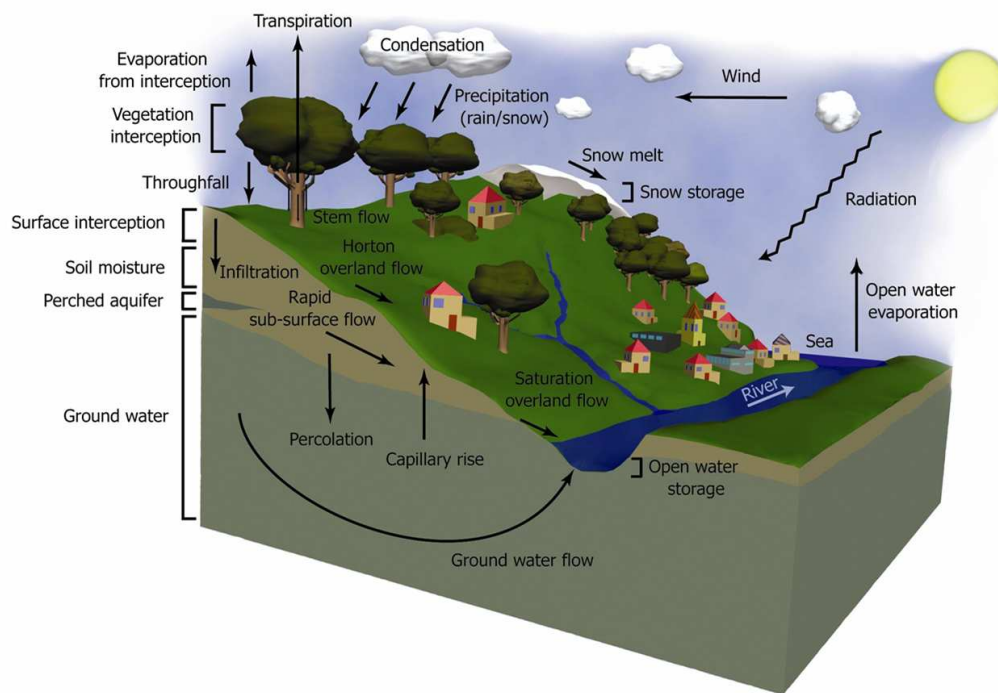


Fig. 1.1: The hydrological cycle.

benefits from data for planning and research purposes are often hard to justify. Quantifying the benefits of data required for reservoir design, water abstraction, flood control, irrigation, hydro-electric power generation, to mention a few possible uses, is usually easier.

1.2 Scope of the lecture

These lecture notes primarily attend to hydrological measurements in the field and not so much to the measurements performed under laboratory conditions. Nevertheless, some of the presented methods can be applied to laboratory measurements as well.

It has been explained, that whoever measures should realize that measurements bear a cost and hence must be justified according to the use of the data. Therefore, the required accuracy of the measurements has to be established and measurements have to be set up accordingly. In general, this involves considering the proper scales in time, so defining the relevant data requirement (hourly, daily, weekly, monthly, yearly, etc.) and scales in space (network density). For example, often a telemetric, real-time network is considered as an ideal monitoring system for e.g. flood management. However, considering cost and reliability has learned that this can only be justified when there is a real need for real-time data. This can be the case when data is used for flood warning. To the contrary, flood data is not required real time when it is used for design purposes such as design of culverts, spillways, etc. In that case capturing the event is important, but not the real time aspect of it.

Measuring requires knowledge on equipment and methods. Only when the equipment and

the measuring method are tuned, it will deliver an optimum result. For example, measuring streamflow by moving boat in rivers with an accurate and sophisticated acoustic Doppler current meter only makes sense if the positioning system is accurate as well. The moving boat method captures information on flow velocity during a transversal crossing of the boat over the river. Otherwise a current meter with propeller, mounted under the moving boat, can do the job. In that case a current meter with a propeller on horizontal axis is preferred above a cub current meter that revolves around a vertical axis. The latter is more sensitive for turbulence around the cubs as a result of the boat movement.

There is also the paradox of measurements that has to be solved when selecting equipment. The paradox is the fact that first of all the (unknown) characteristics of the parameter to measure are required to be able to select the proper equipment. But one can only familiarize with the parameter after having measured it. An example of the paradox is the measurement of streamflow with an Ott current meter. This current meter measures with a propeller revolting on a horizontal axis when placed into stream. The revolutions over a specific period of time have been calibrated against flow velocities, within certain ranges only. For different ranges of flow velocities, different propellers have to be mounted. For low velocities the current meter anyhow has low accuracy. Hence some pre-knowledge on the stream flow is required to mount the proper propeller, or to decide to use another type of current meter. Another example is the use of tracers for discharge measurement. The method is based on the dilution of a certain concentration of a tracer (e.g. a salt or radioactive material) when added to a stream. To be able to measure the diluted quantities one needs information on the discharge on the first place. Summarized the lecture notes will be devoted to:

- Instrumentation and methods to quantify typical components of the hydrological cycle, whilst considering the use of data
- Theory of propagation and sensing of errors
- Methods for interpolating in-situ observations
- Design of measuring networks

2

Theory of errors

2.1 Nature of errors

Errors of observation are usually grouped as random (or stochastic), systematic and spurious.

2.1.1 Random Errors

Random errors are sometimes referred to as experimental errors and the observations deviate from the mean in accordance with the laws of chance such that the distribution usually approaches a normal distribution. Repeating the measurements or extending the period of observation may reduce random errors. This will balance out the random effect and bring the result closer to an average value.

2.1.2 Systematic errors

Systematic errors are those which cannot be reduced by increasing the number of observations, if the instruments and equipment remain unchanged. In streamflow, the systematic errors may be present in the water level recorder, in the reference gauge or datum, and in the current meter. It is possible that the crest of a weir is leveled incorrectly to the station datum, so producing a systematic error in the head measurement, which might have a serious effect on low values of discharge.

2.1.3 Spurious errors

These are human errors or instrument malfunctions and cannot be statistically analyzed. The observations are recognized as out layers and must be discarded.

2.2 Measure for errors

The most used statistical term to estimate uncertainties in measurements is the standard deviation. Standard deviation is a measure of the dispersion or scatter of the observations about the arithmetic mean of the sample. It does account for the random errors. If a sample of

measurements fits a normal distribution, than by statistical inference the dispersion of the observations about the mean is measured in standard deviations. Then, on average, 68% of the observations will lie within one standard deviation of the mean, 95% will lie within two standard deviations of the mean, and almost all (actually 99%) will lie within three standard deviations of the mean. The same standard deviation from the mean obtained from a sample of measurements is used to determine the accuracy of a single measurement. In case of a single measurement, it can be argued that the true value (the true mean), on the average, lies with 68% probability within one standard deviation of the measurement. Equally true is that the true mean, on the average, lies with 95% probability within twice the standard deviation of the measurement.

Example: Measurement errors

Flow current meters are most accurately calibrated in flumes by moving the meter mounted on a carriage through stagnant water in a tank flume. Numerous measurements can be performed under equal conditions. The results of the current meter measurements will vary around a mean μ . The variation is expressed as the standard deviation σ from the mean. The relative standard deviation (called coefficient of variation) is defined as σ/μ , often expressed as a percentage. When doing a single measurement with this particular current meter, it is said that the error of the measurement equals the same value of $\sigma/\mu \cdot 100\%$. One step further is to say that the accuracy of the calibrated current meter is $\sigma/\mu \cdot 100\%$. Usually this is only valid within a certain range of measurements as a different accuracy might apply to extreme low or high current.

2.3 Error propagation from mathematical relations

Often a required parameter is derived from other measurable parameters. For example, average flow in a river (under stationary and uniform conditions) can be derived from measuring stage, slope and roughness. Then the question arises how an error in the measured parameters translates into the error of the wanted parameter. This would not only determine the total error but also, which of the parameters is most critical to the total error and hence should be measured with more care.

Relative simple equations can be derived at, giving the variance σ^2 of the wanted parameter expressed in terms of well known statistical terms (variance and co-variance) of the measured parameters. The co-variance determines whether or not measured parameters are statistical dependent.

Suppose that, in order to find a value for the function $q(x,y)$, we measure the two quantities x and y . The standard error of σ^2 becomes:

$$\sigma_q^2 = \left(\frac{\partial q}{\partial x}\right)^2 \sigma_x^2 + \left(\frac{\partial q}{\partial y}\right)^2 \sigma_y^2 + 2\frac{\partial q}{\partial x}\frac{\partial q}{\partial y}\sigma_{xy} \quad (2.1)$$

This gives the standard deviation σ_q , whether or not the measurement of x and y are independent, and whether or not they are normally distributed. If the measurements of x and y are independent the covariance σ_{xy} will approach zero. With σ_{xy} zero, the equation reduces to:

$$\sigma_q^2 = \left(\frac{\partial q}{\partial x}\right)^2 \sigma_x^2 + \left(\frac{\partial q}{\partial y}\right)^2 \sigma_y^2 \quad (2.2)$$

When the covariance σ_{xy} is not zero we say that the errors in x and y are correlated. In this situation the uncertainty σ_q in $q(x,y)$ is not the same as we would get from the formula for independent errors in x and y .

Equation 2.1 and 2.2 are the general rules for propagation of errors derived from mathematical relations. For a number of functions the relation for propagation of errors has been worked out below:

Example: Propagation errors 1

$$q(x) = ax + b \quad (2.3)$$

$$\sigma_q^2 = a^2 \cdot \sigma_x^2 \quad (2.4)$$

Example: Propagation errors 2

$$q(x, y) = a_1x + a_2y \quad (2.5)$$

For an independent relation between x and y :

$$\sigma_q^2 = a_1^2 \cdot \sigma_x^2 + a_2^2 \cdot \sigma_y^2 \quad (2.6)$$

For a dependent relation between x and y :

$$\sigma_q^2 = a_1^2 \cdot \sigma_x^2 + a_2^2 \cdot \sigma_y^2 + 2a_1a_2\sigma_{xy} \quad (2.7)$$

The maximum of the covariance σ_{xy} is obtained with maximum correlation $\rho = 1$. In that case $\sigma_{xy} = \sigma_x \cdot \sigma_y$. This will be further explained in section 2.4 under regression correlation analysis.

Example: Propagation errors 3

$$q(x, y) = a \cdot x^b \cdot y^c \quad (2.8)$$

For an independent relation between x and y :

$$\sigma_q^2 = \left(abx^{b-1}y^c\right)^2 \sigma_x^2 + \left(acx^by^{c-1}\right)^2 \sigma_y^2 \quad (2.9)$$

Through defining the relative errors as follows,

$$\frac{\sigma_q^2}{\bar{q}^2} = r_q^2 \quad \frac{\sigma_x^2}{\bar{x}^2} = r_x^2 \quad \frac{\sigma_y^2}{\bar{y}^2} = r_y^2 \quad (2.10)$$

this becomes:

$$r_q^2 = b^2r_x^2 + c^2r_y^2 \quad (2.11)$$

Example: Slope area method

The maximum discharge of a wide river after a flood is estimated by the slope area method applying Chezy's law. The formula reads:

$$Q = CBh^{3/2}i^{1/2} \quad (2.12)$$

The slope can be obtained from leveling two floodmarks (l_1, l_2) along the river a certain distance (L) apart. Floodmarks are for example formed by debris or mud lines. Assume a level $l_1=2.464\text{m}$ and $l_2=1.931\text{m}$ both relative to the same datum and a distance $L=987.35\text{m}$ apart. Floodmarks can easily be misjudged by a few centimetres, so assume $\sigma_l=0.02\text{m}$. The accuracy of L can also easily be misjudged by say $\sigma_L=1\text{m}$, as it should be measured according to the main channel of flow through the river during the flood, which in principle is unknown.

The slope is calculated as:

$$i = \frac{l_1 - l_2}{L} = (l_1 - l_2) \cdot L^{-1} = \Delta l \cdot L^{-1} \quad (2.13)$$

For the error in Δl one can write:

$$\sigma_{\Delta l}^2 = \sigma_{l_1}^2 + \sigma_{l_2}^2 = 2\sigma_l^2 \quad (2.14)$$

For the relative error in Δl one can write:

$$r_{\Delta l} = \frac{2\sigma_l^2}{\Delta l^2} = \frac{2 \cdot (0.02)^2}{0.533^2} = 0.0028 \quad \text{hence} \quad r_{\Delta l} = 5.3\% \quad (2.15)$$

The relative error in the distance L is:

$$r_L = \frac{1}{987.35} \cdot 100\% = 0.01\% \quad (2.16)$$

and the relative error in the slope :

$$r_i = \sqrt{(1)^2 r_{\Delta l}^2 + (-1)^2 r_L^2} = \sqrt{0.0028^2 + 0.000001} \approx r_{\Delta l} \quad (2.17)$$

This shows that the measurement of the levels is more critical in the relative error of the slope than the distance L .

According to the law of propagation of errors the relative error in Q is obtained from:

$$r_Q^2 = r_C^2 + r_B^2 + \left(\frac{3}{2}\right)^2 r_h^2 + \left(\frac{1}{2}\right)^2 r_i^2 \quad (2.18)$$

Similar reasoning as was done to obtain r_i can be performed to obtain and r_C , r_B and r_h . In the end this would indicate the largest contributor to the relative error of Q , and hence where improvements in measurements would be most effective.

2.3.1 Repetition of measurements

From the laws of propagation of errors, it can be demonstrated how the error reduces by repeating the measurement. Assume that a measurement is repeated n times ($x_1 \dots x_n$) and that the final result (y) is obtained as the average from these measurements:

$$y = \frac{x_1 + x_2 + \dots + x_n}{n} = \frac{x_1}{n} + \frac{x_2}{n} + \dots + \frac{x_n}{n} \quad (2.19)$$

For independent measurements, it writes:

$$\sigma_y^2 = \frac{1}{n^2}\sigma_{x_1}^2 + \dots + \frac{1}{n^2}\sigma_{x_n}^2 = n \cdot \frac{1}{n^2}\sigma_x^2 = \frac{1}{n}\sigma_x^2 \quad \text{or} \quad \sigma_y = \frac{1}{\sqrt{n}}\sigma_x \quad (2.20)$$

This shows that the error reduces inverse proportional to the square root of the number of measurements. In case the measurements are not independent the reduction is related to the degree of dependency between the measurements, for example expressed by a correlation coefficient. It can be shown that when repeating a measurement twice the equation (Eq. 2.20) changes into:

$$\sigma_y = \frac{\sqrt{1+\rho}}{\sqrt{2}}\sigma_x \quad (2.21)$$

where ρ is the correlation coefficient between the measurements, and $-1 \leq \rho \leq 1$.

2.4 Error propagation from bivariate regression and correlation

2.4.1 Bivariate linear regression

Statistical regression is an associative method that describes how two or more variables tend to change together. A distinction is made between a bivariate regression and multiple regression. In bivariate regression, a dependent variable is only related to one independent variable, while in multiple regression, relationship between a dependent variable and two or more independent variables is established.

The simplest regression model is the linear regression equation of two variables. This model considers the problem that the observed variable y should be estimated by means of a linear function of the variable x . The estimation equation is then,

$$\hat{y} = ax + b \quad (2.22)$$

where the coefficients a and b are the unknown regression coefficients which are determined by the methods of least squares. Geometrically, the problem is to find the equation of the straight line that is best fitted to n observed points (Fig. 2.1). The coefficient b is the intercept of the regression line with the y -axis and a is the slope of the regression line.

Mathematically, the regression problem is to find the values of a and b such that the following sum of squared differences is minimized:

$$S = \sum_{i=1}^n (y_i - \hat{y}_i)^2 \quad (2.23)$$

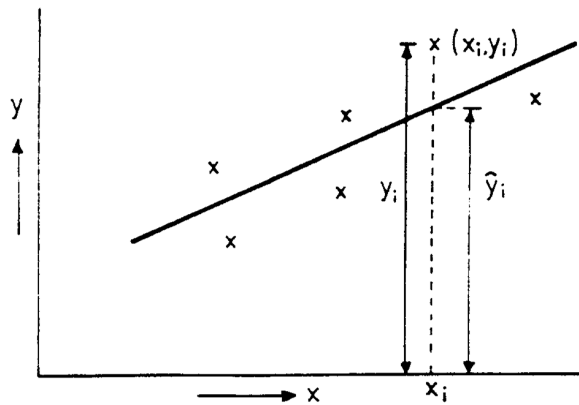


Fig. 2.1: Principle of regression

where n is the number of observations.

This yields:

$$S = \sum_{i=1}^n (y_i - \hat{y}_i)^2 = \sum_{i=1}^n (y_i - b - ax_i)^2 \quad (2.24)$$

S will be at a minimum only if the two partial derivatives of S with respect to a and b equal zero:

$$\frac{\partial S}{\partial a} = -2 \sum_{i=1}^n x_i (y_i - b - ax_i) = 0 \quad \frac{\partial S}{\partial b} = -2 \sum_{i=1}^n (y_i - b - ax_i) = 0 \quad (2.25)$$

This will lead to the two ‘normal equations’:

$$\sum_{i=1}^n (y_i - b - ax_i) = 0 \quad (2.26)$$

and

$$\sum_{i=1}^n x_i (y_i - b - ax_i) = 0 \quad (2.27)$$

with $i = 1, \dots, n$.

The simultaneous solution of Equation 2.26 and 2.27 yields:

$$a = \frac{\sum_{i=1}^n (x_i - \bar{x})(y_i - \bar{y})}{\sum_{i=1}^n (x_i - \bar{x})^2} \quad (2.28)$$

and

$$b = \bar{y} - a\bar{x} \quad (2.29)$$

With:

$$\bar{x} = n^{-1} \sum_{i=1}^n x_i \quad \text{and} \quad \bar{y} = n^{-1} \sum_{i=1}^n y_i$$

Sometimes the slope a is also expressed as:

$$a = \frac{s_{xy}}{s_x^2} \quad (2.30)$$

With:

$$s_{xy} = \frac{\sum^n (x_i - \bar{x})(y_i - \bar{y})}{(n-1)} \quad \text{and} \quad s_x^2 = \frac{\sum^n (x_i - \bar{x})^2}{(n-1)} \quad (2.31)$$

s_{xy} is the covariance from the data and s_x^2 the variance from the x -values.

2.4.2 Bivariate linear correlation

The regression line is a best fit to the data points, but does not indicate the deviation, or degree of association of the data points from the line. The correlation coefficient, r , is used to explain the degree of this association as a linear dependence. There are several types of correlation coefficients used in statistics. The most commonly used correlation coefficient, r , is defined between two variables x and y as:

$$r = \frac{\sum^n (x_i - \bar{x})(y_i - \bar{y})}{\sqrt{\sum^n (x_i - \bar{x})^2} \sqrt{\sum^n (y_i - \bar{y})^2}} \quad (2.32)$$

By using the definition of covariance and standard deviation, the equation can be rewritten as:

$$r = \frac{s_{xy}}{s_x s_y} \quad (2.33)$$

The value of correlation coefficient ranges between -1 and +1. If the correlation coefficient is larger than zero, two variables are said to be positively correlated. In this case the variable y tends to increase as x increases on a scatter plot. If the correlation coefficient is smaller than zero, two variables are said to be negatively correlated. In this case the variable y tends to decrease as x increases on a scatter plot. The correlation coefficient is actually a measure of how close the cloud of points lies near a straight line on a scatter plot. When the correlation coefficient equals -1 or +1, the scatter plot of points (x,y) will be a straight line with negative or positive slope. In that case the variables are completely dependent. The variables x and y are statistically uncorrelated if the correlation coefficient is zero.

Non linear relations

Independence doesn't simply mean that variables are independent since correlation coefficients measure only the degree of linear dependence. For example, the discharge formula for a V-notch reads

$$Q = mh^{5/2} \quad (2.34)$$

and has a correlation coefficient zero as there is no linear term.

Often relations between two hydrological variables are not linear. In these cases, nonlinear regression equations may be considered. For example, a rating curve where discharge is plotted against stage is usually a parabolic function. By applying a proper transformation the nonlinear relation can be reduced to a linear form. In this way, for example, the discharge formula for a V-notch turns into a linear equation by applying the logarithmic function to either side of the equation:

Tab. 2.1: Tables for calculating the correlation coefficient r

Year	Annual Rainfall [mm]	Annual Runoff [mm]
	x	y
1958	925	251,53
1959	760	273,35
1960	657	49,47
1961	876	188,12
1962	672	98,46
1963	1109	340,05
1964	542	36,35
1965	764	89,33
1966	841	64,11
1967	753	87,55
1968	486	17,01
1969	823	133,08
1970	753	64,70
1971	769	52,93
1972	965	195,41
1973	464	28,19
1974	1300	446,88
1975	1001	242,18

Year	Annual Rainfall [mm]	Annual Runoff [mm]
	x	y
1976	777	111,96
1977	954	251,69
1978	1237	387,53
1979	609	74,80
1980	768	97,27
1981	1126	385,69
1982	722	76,70
1983	558	28,57
1984	618	30,41
1985	975	171,97
1986	949	209,89
1987	488	56,55
1988	809	128,49
1989	831	134,22
1990	823	135,03
1991	562	55,95
1992	603	49,91
1993	785	71,29

x_{avg}	795,9
y_{avg}	142,1
s_x	204,5
s_x^2	41813,6
s_y	114
s_{xy}	21090

a	0,504
b	-259,3
r	0,904
r^2	0,8181

$$\log(Q) = \log(m) + \frac{5}{2} \log(H) \quad (2.35)$$

which is a linear equation when substituting $y = \log(Q)$ and $x = \log(H)$

Example: Linear regression

The relation between annual rainfall and annual runoff from the Manyame catchment in Zimbabwe (1850 km²) is analyzed through linear regression and correlation on the basis of 36 years of observations. The annual rainfall represents the independent variable (x), whilst the annual runoff (the dependent variable) is plotted on the y-axis, see Figure 2.2. Table 2.1 summarizes the relevant parameters derived from the data to perform the analysis. On the basis of the parameters the coefficients of the regression line and the correlation coefficient can be established. As the figure demonstrates often the so called r-squared (r^2) is used, instead of the correlation coefficient r .

Physical interpretations can be given to the regression line. The intersection of the regression line marks the approximated threshold value in terms of annual rainfall before significant runoff occurs. This is the x -value (annual rainfall) at which y (annual runoff) equals zero. Obviously this is for:

$$x = -\frac{b}{a} \quad \text{or} \quad x = -\frac{-259.3}{0.5044} = 514\text{mm} \quad (2.36)$$

The coefficient indicates that on the average 50% of the surplus rainfall above the threshold value will result in runoff.

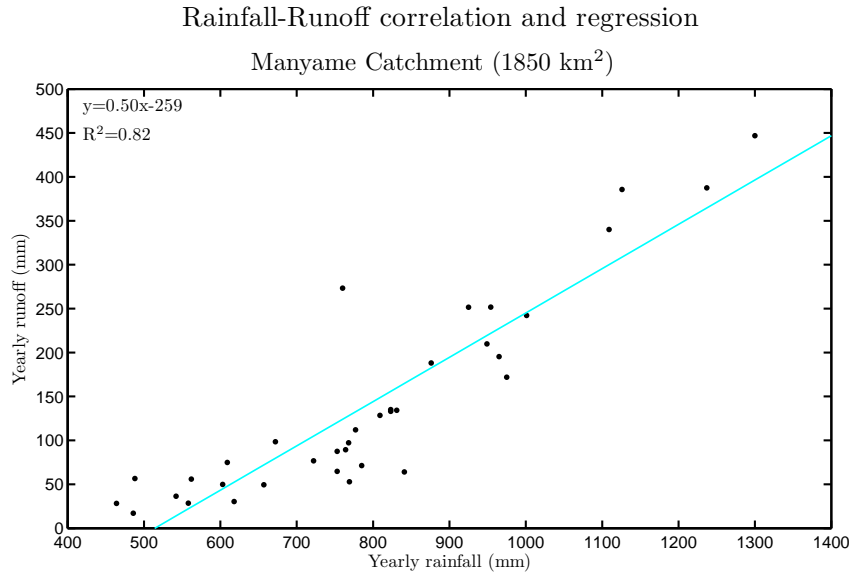


Fig. 2.2: Rainfall-runoff regression

Significance of the bivariate correlation coefficient

The correlation coefficient, r , based on a limited number of observations (n) will differ from the true correlation coefficient, ρ . It can be tested whether or not r significantly differs from $\rho=0$ with 95% accuracy. For this purpose r is transformed into z according to:

$$z = \frac{1}{2} \ln \frac{1+r}{1-r} \quad (2.37)$$

The properties of the transformation are that $\bar{z}=0$ and $\sigma_z=(n-3)^{-1/2}$. If $-2\sigma_z \leq z \leq 2\sigma_z$ applies, the null hypotheses $\rho=0$ is accepted with 95% accuracy, which indicates no significant correlation. On the contrary there is a significant correlation with 95% accuracy when:

$$\frac{1}{2} \ln \frac{1+|r|}{1-|r|} > \frac{2}{\sqrt{n-3}} \quad (2.38)$$

In this way significant correlation can be verified on the basis of n and r . Equation 2.37 is depicted in Figure 2.3.

Example: Determining the correlation coefficient

In the previous example, the correlation coefficient between annual rainfall and annual runoff was $r = 0.904$. This was based on 36 years of observations. Applying Equation 2.37 and 2.38 yields:

$$\frac{1}{2} \ln \frac{1+|r|}{1-|r|} = 1.4937 \quad \text{and} \quad \frac{2}{\sqrt{n-3}} = 0.3481 \quad (2.39)$$

On the basis of this result, it can be concluded that the correlation coefficient is significant with 95% accuracy.

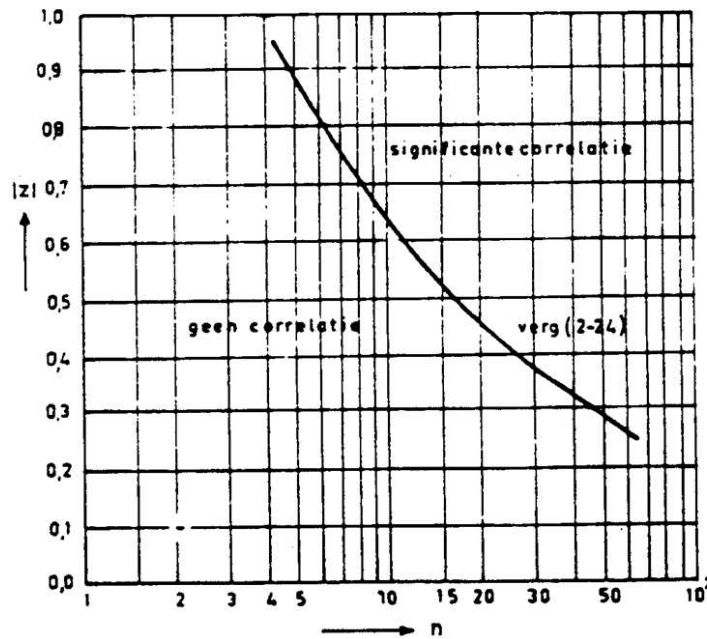


Fig. 2.3: Test for Correlation

Error propagation

Bivariate linear regression is, besides mathematical relations, another way to associate two variables. The dependent variable, y , is estimated from the independent variable, x . In case of a perfect linear relation the correlation coefficient is 1 or -1, and no error is introduced when estimating the dependent variable from the independent variable. If the correlation coefficient differs from 1 or -1, the match is not perfect and an error is introduced when estimating the dependent variable from the independent variable according to the regression line.

The error as a result of estimation can be defined as:

$$\epsilon = \hat{y} - y \quad (2.40)$$

Substitution of the regression line yields:

$$\epsilon = ax + b - y \quad (2.41)$$

According to the law of error propagation, the error variance writes:

$$\sigma_{\epsilon}^2 = a^2 \sigma_x^2 + \sigma_y^2 - 2a \sigma_{xy} \quad (2.42)$$

Using the relations $a = \frac{\sigma_{xy}}{\sigma_x^2}$ and $\rho = \frac{\sigma_{xy}}{\sigma_x \sigma_y}$ yields :

$$\sigma_{\epsilon}^2 = a^2 \left(\frac{1}{\rho^2} - 1 \right) \sigma_x^2 \quad (2.43)$$

The error variance is often referred to as the 'standard error of the y estimate'. It is a measure for the error in the estimated value according to the regression line.

Example: Error propagation

The relation between annual rainfall and annual runoff from the Manyame catchment in Zimbabwe (1850 km²) was examined in the previous example. This resulted in a regression line:

$$\hat{y} = ax - b \quad (2.44)$$

With:

- x annual rainfall (mm/y)
- \hat{y} estimated annual rainfall (mm/y)
- a 0.5044 (-)
- b -259.34 (-)

It was found that the correlation coefficient $r=0.904$ and $\sigma_x=204.5\text{mm/y}$. In 1957 the average annual rainfall for the same catchment was 908.5mm/y, but no annual runoff was observed. According to the regression line an estimate for the annual runoff would be 198.9mm/y. Substituting a , s_s and r in Equation 2.43 shows that $\sigma_\epsilon=48.6\text{mm/y}$. Under assumption that the error is normally distributed around the true value, follows that within 95% accuracy the true value is $198.9 \pm 2 \cdot 48.6\text{mm/y}$.

2.5 Error detection from measurements

So far in the previous chapters, the propagation of errors has been the subject of discussion. The topic in this chapter will be to discover irregularities in measurements, in particular from time series. Time series values from one location can be compared to the observed series to find spatial inhomogeneities, see section 2.5.1. Values from one and the same series at a specific site can also be scrutinized through statistic techniques. This is the topic using a split record technique in section 2.5.2.

2.5.1 Spatial inhomogeneities**Data estimation**

In this test, data of a base station is estimated based on data of surrounding stations. The procedure will be explained for rainfall based on monthly values, but would also apply to other periods of observation and other (rainfall) data with sufficient correlation.

In principle good correlation is expected between rainfall stations nearby. This is expressed by a negative exponential function:

$$\rho_i = \rho_0 \exp -\frac{r}{r_0} \quad (2.45)$$

With:

- ρ_i correlation at distance r
- ρ_0 correlation at distance 0
- r distance between stations (km)
- r_0 a length scale defining the rate at which the correlation decreases (km)

The constants $\rho_0=0.98$ and $r_0=1500\text{km}$ could be assumed for e.g. mixed convective, orographic, depression rainfall. Then the maximum distance r_{max} between the base station and neighboring station can be defined as the limit where correlation becomes insignificant.

To investigate the reliability of the monthly values, the measurements $P_{meas}(m,y)$ of one station from a certain month in a particular year is compared with an estimated $P_{est}(m,y)$ based on a weighted calculation using the rainfall at neighboring stations, from the same month in that particular year. A worked out example is provided in A.1. Only stations with a correlation distance smaller than r_{max} are considered. The weights are inversely proportional to some power of the distance between the base station and the neighboring stations. The estimated monthly value is calculated through:

$$P_{est}(m,y) = \frac{\sum P_i(m,y)/D_i^b}{\sum 1/D_i^b} \quad (2.46)$$

With:

- $P_{est}(m,y)$ estimated monthly value at base station for one certain month and year (mm/month)
- $P_i(m,y)$ measured rainfall at neighbor station(mm/month)
- D_i distance to neighboring station (km)
- b power of distance (usually $b=2$)

The difference between the observed value, $P_{meas}(m,y)$ and the estimated value, $P_{est}(m,y)$ is considered to be insignificant if the following conditions are met:

1. Absolute criterion

$$|P_{meas}(m,y) - P_{est}(m,y)| \leq X_{abs}$$

2. Relative criterion

$$|P_{meas}(m,y) - P_{est}(m,y)| \leq X_{rel} \cdot S_{P_{meas}}(m,y)$$

With:

- X_{abs} admissible absolute difference
- X_{rel} multiplier of standard deviation
- $S_{P_{meas}}(m,y)$ standard deviation of values of neighboring stations at time (t) within r_{max}

With a limited number of stations, calculation of $S_{P_{meas}}(t)$ is not found realistic and alternatively the relative criterion can be:

$$F_1 \leq \frac{P_{est}(m,y)}{P_{meas}(m,y)} \leq F_2 \quad (2.47)$$

With:

- F_i admissible relative difference coefficient

Double mass analysis

The principle of double mass analysis is to plot accumulated values of the station under investigation against accumulated values of another station or accumulated values of the average of other stations over the same period of time. Through a double mass curve inhomogeneities in

Tab. 2.2: Double mass analysis, completion of data and residual mass calculation

Year	P119 X _{meas} [mm]	P5 Y _{meas} [mm]	SUM X	SUM Y	Y/X	X _{missing}	Y _{missing}	X _{complete}	Y _{complete}	SUM X _{complete}	SUM Y _{complete}	RESIDUAL MASS
			0	0						0	0	0
51/52	127.6	63.5	127.6	63.5	0.50			127.6	63.5	127.6	63.5	-43.8
52/53	43.2		170.8	63.5			37.9	43.2	37.9	170.8	101.4	-42.2
53/54	76.3	88.9	247.1	152.4	1.17			76.3	88.9	247.1	190.3	-17.5
54/55	155.9	98.2	403	250.6	0.63			155.9	98.2	403.0	288.5	-50.3
55/56	193.9	163.2	596.9	413.8	0.84			193.9	163.2	596.9	451.7	-50.2
56/57	18	27.1	614.9	440.9	1.51			18.0	27.1	614.9	478.8	-38.2
57/58	132.4	130.9	747.3	571.8	0.99			132.4	130.9	747.3	609.7	-18.6
58/59	34.8	42.5	782.1	614.3	1.22			34.8	42.5	782.1	652.2	-5.4
59/60	85.2	33.3	867.3	647.6	0.39			85.2	33.3	867.3	685.5	-43.7
60/61	49.4	60.7	916.7	708.3	1.23			49.4	60.7	916.7	746.2	-24.5
61/62	140.3	141.3	1057	849.6	1.01			140.3	141.3	1057.0	887.5	-1.2
62/63	67.4	72.2	1124.4	921.8	1.07			67.4	72.2	1124.4	959.7	14.4
63/64	51.6	75.9	1176	997.7	1.47			51.6	75.9	1176.0	1035.6	46.9
64/65	107.4	111.5	1283.4	1109.2	1.04			107.4	111.5	1283.4	1147.1	68.1
65/66	48.7	59.6	1332.1	1168.8	1.22			48.7	59.6	1332.1	1206.7	86.7
66/67	75.8	39.7	1407.9	1208.5	0.52			75.8	39.7	1407.9	1246.4	62.7
67/68	89.3	66.7	1497.2	1275.2	0.75			89.3	66.7	1497.2	1313.1	54.3
68/69	33.1	45	1530.3	1320.2	1.36			33.1	45.0	1530.3	1358.1	71.5
69/70	236.4	180	1766.7	1500.2	0.76			236.4	180.0	1766.7	1538.1	52.8
70/71	89.3	91.6	1856	1591.8	1.03			89.3	91.6	1856.0	1629.7	69.3
71/72	96.3	108.9	1952.3	1700.7	1.13			96.3	108.9	1952.3	1738.6	97.2
72/73		89	1952.3	1789.7		101.5		101.5	89.0	2053.8	1827.6	100.8
73/74	85.5	62.3	2037.8	1852	0.73			85.5	62.3	2139.3	1889.9	91.3
74/75	44.6	22.4	2082.4	1874.4	0.50			44.6	22.4	2183.9	1912.3	76.2
75/76	35.8	32.2	2118.2	1906.6	0.90			35.8	32.2	2219.7	1944.5	78.3
76/77	42.3	0	2160.5	1906.6	0.00			42.3	0.0	2262.0	1944.5	42.7
77/78	34.8		2195.3	1906.6			30.5	34.8	30.5	2296.8	1975.0	44.0
78/79	85.1	60.4	2280.4	1967	0.71			85.1	60.4	2381.9	2035.4	32.8
79/80	51.6	6.1	2332	1973.1	0.12			51.6	6.1	2433.5	2041.5	-4.5
80/81	10.3		2342.3	1973.1			9.0	10.3	9.0	2443.8	2050.5	-4.1
81/82	115		2457.3	1973.1			100.8	115.0	100.8	2558.8	2151.3	0.0
					(Y/X) _{average}	0.88		Average	82.5	69.4		

the time series (in particular jumps) can be investigated, for example originating from change in observer, rain-gauge type, etc. This is indicated in the curve of a double mass plot, showing an inflection point in the straight line. The principle of double mass curve analysis will be demonstrated through plotting accumulated monthly rainfall for one certain month over the years of observation for station P119 against P5. Through the relation found in the (approximate) straight line a first attempt to data completion will be performed. A worked out example is provided in Table 2.2 and Figure 2.4.

Another way to look at results of double mass analysis is through plotting the residual mass of one station against the accumulated values of another station. When comparing two stations the residual mass is defined by:

$$M_i = \sum Y_i - \left(\frac{Y_{avg}}{X_{avg}} \right) \sum X_i \quad (2.48)$$

With:

- M_i Residual mass (mm/month)
- X_i, Y_i Monthly rainfall station X and Y (mm/month)
- X_{avg}, Y_{avg} Average monthly rainfall of station X and Y (mm/month)

In this definition the difference between the summed monthly rainfall values of station X and the average summed values (based on the measurements of station X and Y) is calculated. Plotting

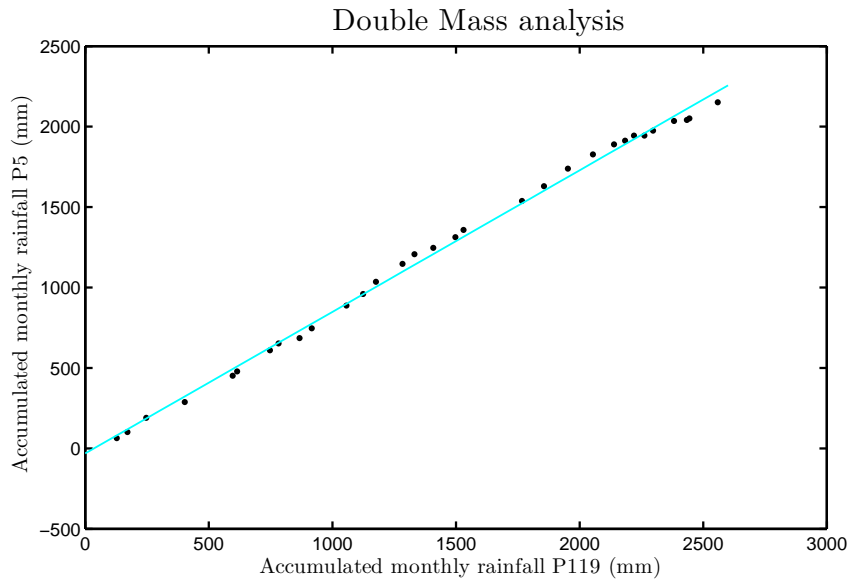


Fig. 2.4: Double Mass analysis fo monthly rainfall

M_i against $\sum X_i$ shows clearly any deviation of station Y from a constant relation between station Y and X (indicated as inflection points in the double mass analysis), see Figure 2.5. The curve can be interpreted as follows:

- an upward curve indicates relative high values of station Y
- a horizontal curve indicates an about constant relation between station X and Y
- a downward curve indicates relative low values of station Y

A residual mass curve can also be created from a single series to investigate trends (dry and wet periods). In that case the accumulated deviation from the mean is calculated as

$$M_i = \sum X_i - X_{avg} \quad (2.49)$$

- an upward curve indicates an above average sequence
- a horizontal curve indicates an about average sequence
- a downward curve indicates a below average sequence

2.5.2 Statistical time series analysis

In case one series is tested in itself, several series are generated from the original series by splitting the series or by some kind of mathematical operation. A certain parameter of the series will be analyzed. This can be the mean, variance or other parameters like a correlation coefficient. Another parameter is defined from the series as a basis for analysis. This parameter

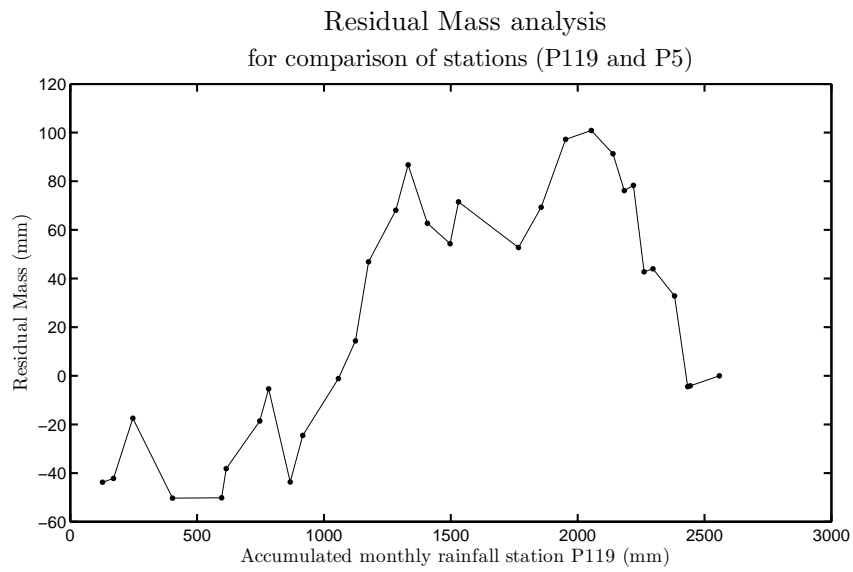


Fig. 2.5: Residual Mass Curve

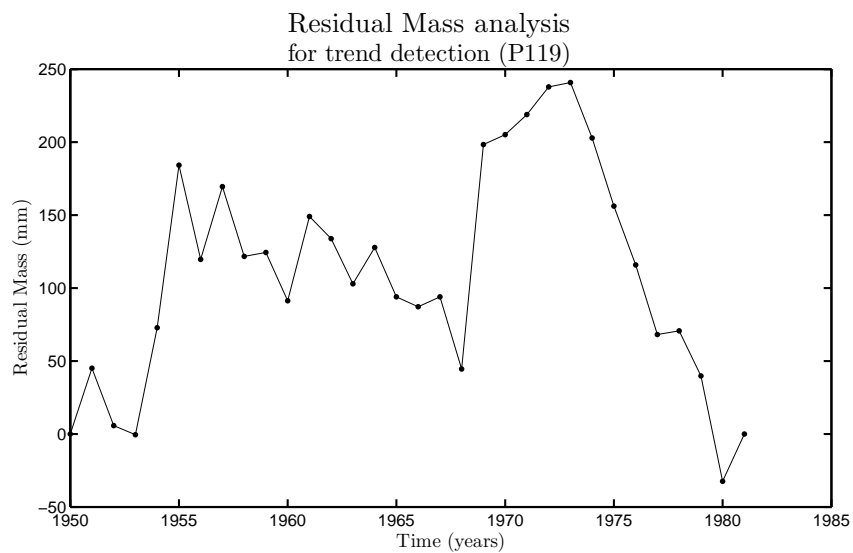


Fig. 2.6: Residual Mass curve for trend detection (P119)

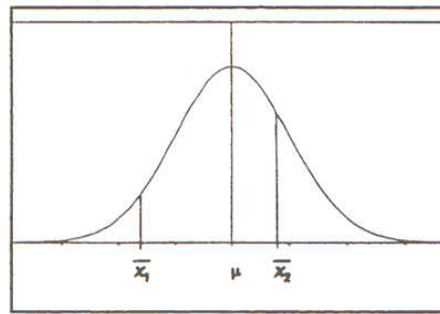


Fig. 2.7: Scatter of sample means around the true mean

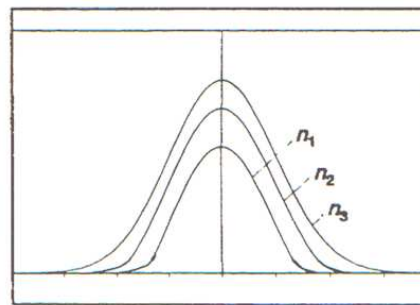


Fig. 2.8: Distributions as a function of the number of elements in a sample

is called the *test-statistic* and can be the mean or variance itself, a derivative of the mean or variance or another defined parameter.

When analyzing the values of test-statistics, the problem arises to qualify a comparison. For instance, for absence of trends in a time series we want to prove that the mean of the first 10 years of a series is not significantly different from the last 10 years. However, both values will never be equal. But what difference is accepted and what difference is not? Directly it is understood that the larger the series, the closer the two values of the mean will be. Both values will also come closer to the true mean (μ) when the number of years increases. In case one takes several samples (all with equal number of years) from the infinite time series (called the population), the mean values of these samples may differ in magnitude. It was found out that when a histogram of these values is made, the histogram can be represented by a smooth curve, defining the scatter of the values around the true mean ($=\mu$), see Figure 2.7.

The number of elements (n) in a sample has influence on the shape of the curve, see Figure 2.8. The curves are distributions, mathematically defined and often tabulated. Such a curve can be a normal distribution. Other distributions are Student's-t or Fisher-F distributions. Often we have a situation where the real mean (μ) is not known. From the sample, a mean (x) can be calculated. The only thing we can do, is assume a certain real mean (μ_0) and test on basis of our sample whether there is ground to reject the assumption. In statistical terms therefore two hypotheses are introduced, namely a null hypothesis H_0 and an alternative H_1 hypothesis.

$$H_0 \quad \mu = \mu_0$$

$$H_1 \quad \mu \neq \mu_0$$

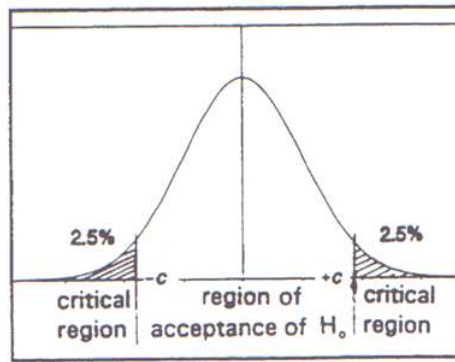


Fig. 2.9: Critical regions and the critical values (confidence level 95%)

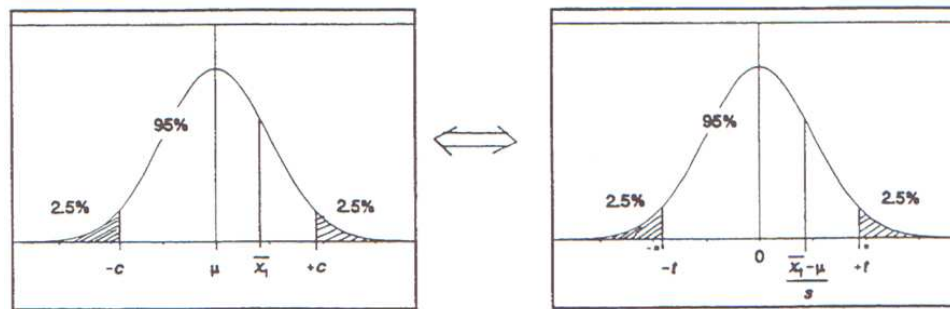


Fig. 2.10: Left: Normal distribution, Right: Standard normal distribution

On the basis of a sample, it never will be possible to prove with 100% certainty that H_0 nor H_1 is correct. One should realize that even when accepting one of the two hypotheses, there is a chance of making the error that it is still not the correct one. When H_0 is always stated in the way that it is the hypothesis we wish to prove, the worst that can happen is to accept H_0 , while it is not true (like the judge who is convicting an innocent suspect). In statistics this is called a type I error. This region representing the area of rejecting H_0 must be minimized to an acceptable level. This area is called the critical region, bordered by critical values, or confidence limits ($\pm c$), see Figure 2.9.

According to the distribution of x (for instance Normal, Students-t, Fisher-F) the critical values mark the probability of a type I error. The probability of a type I error is called the significance level α and $1-\alpha$ the confidence level. A confidence level of 95% is often applied ($\alpha=0.05$).

One can use the theory of a normal, distribution, in case it is valid, and its relation with the standard normal distribution to calculate the critical values (confidence limits $+c$ and $-c$), see Figure 2.10.

For a level of significance of 5%, confidence limits t from the standard normal distribution are $t=\pm 1.96$. This can be verified from a table of the standard normal distribution, see A.2. Confidence limits c for the real distribution are calculated using its relation with the standard normal distribution:

$$t = \frac{c - \mu}{\sigma} \quad (2.50)$$

With:

μ true mean of the population

σ true standard deviation of the population

for σ is known that,

$$\sigma = \frac{s}{\sqrt{n}} \quad (2.51)$$

With:

s standard deviation of the sample

n number of elements in the sample

Now we conclude that, in case μ is known, it can be verified whether a certain calculated mean is accepted as representing the population with a confidence level of 95%. In case μ is unknown we can verify an assumption $\mu=\mu_0$ with a certain confidence level.

What we did until now in fact was comparing one sample with its population, through the test statistic mean. However, in general the population parameters μ and σ are not known.

It is also possible to compare results of one sample with another. In case both are normal distributions, the difference of the means $d = x_1 - x_2$ also is a normal distribution with

$$\mu_d = \mu_1 - \mu_2 \quad (2.52)$$

and

$$s_d^2 = \frac{s_1^2}{n_1} + \frac{s_2^2}{n_2} \quad (2.53)$$

In case the two samples belong to the same population, $\mu_1=\mu_2$ and $\mu_d=0$. Again according to the principles of a standard normal distribution transformation from the normal distribution is by (also see Fig. 2.11):

$$d' = \frac{d - \mu_d}{s_d} \quad (2.54)$$

To test now whether the two samples are from the same population is testing $\mu_1=\mu_2$ (the null hypothesis H_0) against $\mu_1 \neq \mu_2$ (the alternative hypothesis H_1)

As indicated above, this is done by defining the confidence limits under assumption of H_0 , while not committing a type I error. Assuming H_0 , $\mu_d=0$ and hence

$$d' = \frac{d}{s_d} \quad (2.55)$$

For the confidence limits this means:

$$t = \pm \frac{c}{s_d} \quad (2.56)$$

In case $-t < d' < t$ it is accepted with a confidence level according the confidence limits that the average x_1 and x_2 originate from the same population and that there is no trend.

Note that the test statistic for the standard normal distribution is the variable

$$d' = \frac{d}{s_d} \quad (2.57)$$

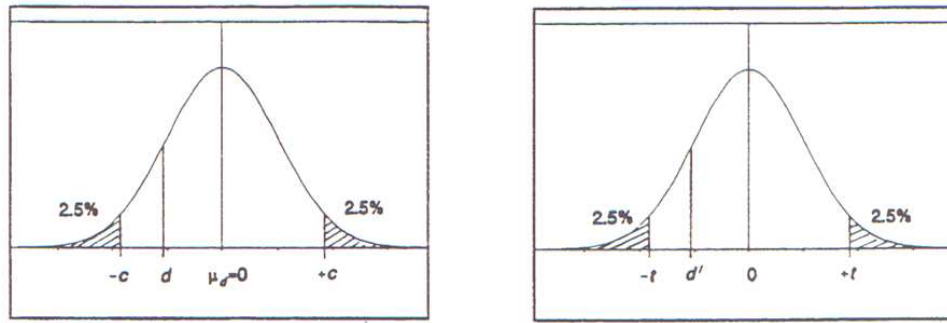


Fig. 2.11: Conversion from a Normal (left) to the Standard Normal (right) distribution

$$d' = \frac{x_1 - x_2}{\left(\frac{s_1^2}{n_1} + \frac{s_2^2}{n_2}\right)^{1/2}} \quad (2.58)$$

With small samples ($n < 30$) the standard normal distribution does not any longer give satisfactory results. Then one can better use the so called Students-t distribution. In case comparing means, the test statistic remains as given above.

Also for other parameters acceptance within predefined levels of significance can be defined. In all cases, a test statistic must be defined and its distribution. This distribution is not necessarily always a normal distribution or the Students-t distribution. For instance, for significance of variance the Fisher distribution is applied. In a Spearman rank test the significance of a correlation coefficient is tested through a Students-t test.

The spearman's rank test (for absence of trend)

The hypothesis is tested that there is no correlation between the order in which the data are observed and the increase (or decrease) in magnitude of those data. The test is usually performed on the whole data series but it is possible to select specific periods.

Two series are compared related to the rank of the data. K_{x_i} is the rank of the data as it was measured. K_{y_i} is the series of the rank of the same data in ascending or descending order.

The Spearman coefficient of rank correlation R_{sp} is then defined as:

$$R_{sp} = 1 - \frac{6 \sum D_i^2}{n(n^2 - 1)} \quad (2.59)$$

With:

$$D_i = K_{x_i} - K_{y_i}$$

When two or more observations have the same value, the average rank K_{y_i} is calculated. A test-statistic t_t is used to test the null hypothesis $H_0: R_{sp}=0$ against the alternative hypothesis $H_1: R_{sp} <> 0$. The test statistic is defined as:

$$t_t = R_{sp} \left(\frac{n - 2}{1 - R_{sp}^2} \right)^{1/2} \quad (2.60)$$

t_t has Student's t-distribution with $v=n-2$ degrees of freedom, where n is the number of elements in a sample. A.3 contains a table of the Student's-t distribution for a level of significance of 5% (two-tailed). The two sided critical region \cup of the test statistic t_t for a level of significance of 5% is bounded by:

$$\{-\infty, t(v, 2.5\%)\} \cup \{t(v, 97.5\%), +\infty\} \quad (2.61)$$

and the hypothesis H_0 is accepted when the computed t_t is not contained in the critical region. In other words, one concludes that there is no trend when:

$$t(v, 2.5\%) < t_t < t(v, 97.5\%) \quad (2.62)$$

A worked out example is provided in A.4.

F-test for the stability of the variance

The appropriate test statistics is the ratio of the variances of two non-overlapping sub-sets of series. The distribution of the variance ratio of samples from a normal distribution is known as the F-distribution or Fisher distribution. Even in absence of the normal distribution it is generally accepted that the F-test provides a useful indication for stability of the variance.

The number of data n in the test series should be equal to or greater than 10. The test statistics is thus:

$$F_t = \frac{\text{Var}_1}{\text{Var}_2} \quad (2.63)$$

The null hypothesis for the F-test is the equality of variances, $H_0: \text{Var}_1 = \text{Var}_2$ and the alternative hypothesis is $H_1: \text{Var}_1 <> \text{Var}_2$. The rejection region is bounded by:

$$\{0, F(v_1, v_2, 2.5\%)\} \cup \{F(v_1, v_2, 97.5\%), +\infty\} \quad (2.64)$$

where v_1 and v_2 are the respective numbers of degrees of freedom of the numerator and dominator. $v_1 = n_1 - 1$ and $v_2 = n_2 - 1$ where n_1 and n_2 are the number of observations in each sub-set.

In other words, the variability of the data is considered to be stable and the standard deviation s can be used as an estimate for the population standard deviation, when:

$$F(v_1, v_2, 2.5\%) < F_t < F(v_1, v_2, 97.5\%) \quad (2.65)$$

The F-distribution is not symmetrical for the number of degrees of freedom of the numerator and dominator. Tables should therefore be applied properly with usually v_1 horizontally and v_2 vertically. See A.5 for a condensed table of the F-distribution with a confidence level of 5%.

The procedure to apply the F-test on data series is to subdivide the series in two or three (approximately) equal non-overlapping sub-sets. The standard deviation is computed for each subset. The limits of a sub-set can also be selected in such a way that the set will cover a suspect period. Such a period is then compared with a non-suspect period or periods.

T-test for stability of the mean

The test for the stability of variance has to be performed before this test as statistically the variances of the sub-sets should not be different. The means of the same subsets can be compared to verify whether the mean is stable during the whole period of observations. A suitable test statistic for testing the null hypothesis $H_0: x_{avg,1}=x_{avg,2}$ against the alternative hypothesis is $H_1: x_{avg,1} <> x_{avg,2}$ is:

$$t_t = \frac{X_{avg,1} - X_{avg,2}}{\left(\frac{(n_1-1)var_1 + (n_2-1)var_2}{n_1+n_2-2} \cdot \left(\frac{1}{n_1} + \frac{1}{n_2} \right) \right)^{1/2}} \quad (2.66)$$

With:

n_i the number of data in the subset i

$x_{avg,i}$ the mean of the subset i

Var_i the variance of the subset i

The test statistics t_t has Student's-t distribution for a sample which is normally distributed. The test may also be applied for non-normal distributions, best for approximately equal lengths of subsets.

The two sided critical region \cup for the test statistic is defined as:

$$\{-\infty, t(v, 2.5\%)\} \cup \{t(v, 97.5\%), +\infty\} \quad (2.67)$$

and the number of degrees of freedom is $v=n_1 + n_2 - 2$

The null-hypothesis H_0 is accepted when the computed t_t is not contained in the critical region. In other words, one concludes that $x_{avg,1} = x_{avg,2}$ when:

$$t(v, 2.5\%) < t_t < t(v, 97.5\%) \quad (2.68)$$

A.6 contains a worked out example of the split record test on variance and the mean for yearly rainfall data of station P6 in Mozambique.

3

Precipitation

3.1 The precipitation mechanisms

The lifting of air is the most important mechanism that results into precipitation. Air masses are lifted and under adiabatic conditions the temperature drops to near its dew point. Five lifting mechanism can be distinguished, namely:

1. *Convection*, due to vertical instability of the air. Instability of the atmosphere usually results from the heating of the lower air layers by a hot earth surface and the cooling of the upper layers by outgoing radiation. Convective rainfall is common in tropical regions and it usually appears as a thunderstorm in temperate climates during the summer period. Rainfall intensities of convective storms can be very high locally; the duration, however, is generally short.
2. *Orographic lifting*. When air passes over a mountain it is forced to rise, which may cause rainfall on the windward slope. As a result of orographic lifting rainfall amounts are usually highest in the mountainous part of the river basins.
3. *Frontal lifting*. The existence of an area with low pressure causes surrounding air to move into the depression, displacing low pressure air upwards, which may then be cooled to dew point. If cold air is replaced by warm air (warm front) the frontal zone is usually large and the rainfall of low intensity and long duration. A cold front shows a much steeper slope of the interface of warm and cold air usually resulting in rainfall of shorter duration and higher intensity, see Figure 3.1. Some depressions are died-out cyclones.
4. *Cyclones*, tropical depressions, typhoons or hurricanes. These are active depressions which gain energy when moving over warm ocean water and which dissipate energy while moving over land or cold water. They may cause torrential rains and heavy storms. Typical characteristics of these tropical depressions are high intensity rainfall of long duration (several days).
5. *Convergence*. The Inter Tropical Convergence Zone (ITCZ) is the tropical region where the air masses originating from the tropics of Cancer and Capricorn converge and lift.

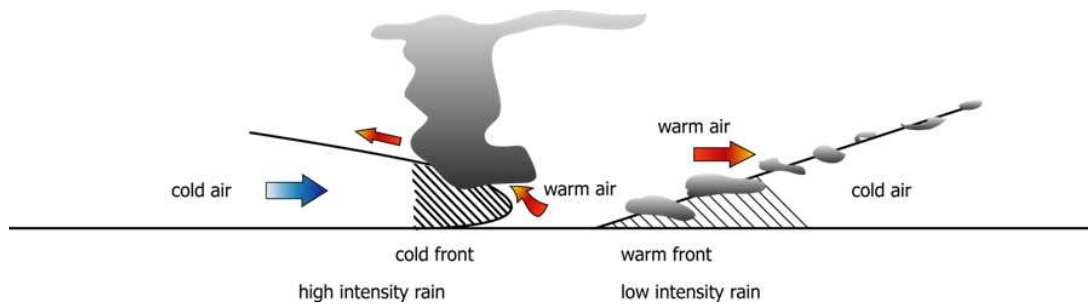


Fig. 3.1: Frontal lifting mechanism

In the tropics, the position of the ITCZ governs the occurrence of wet and dry seasons. This convergence zone moves with the seasons. In July, the ITCZ lies to the North of the equator and in January it lies to the South. In the tropics the position of the ITCZ determines the main rain-bringing mechanism. In certain places near the equator the ITCZ passes twice per year, causing two wet seasons. Near the Tropics of Cancer and Capricorn, however there is only one dry and wet season.

3.2 Measuring rainfall

From all the components of the hydrological cycle, the elements of precipitation, particularly rain and snow, are the most commonly measured. It would appear to be a straightforward procedure to catch rain as it falls and measure the depth of snow lying. However, climatologists and water engineers appreciate that making an acceptable precipitation measurement is not as easy as it may appear. It is not physically possible to catch all the rainfall or snowfall over a drainage basin.

The traditionally way is to sample the precipitation over the area by rain gauges (Section 3.2.1). The measurements are made at several selected points representative of the area and values of total volume (m^3) or equivalent areal depth (mm) over the catchment are calculated later. The measurements have to be done proper and standardized and therefore rules have evolved on equipment and placement of gauges.

Nowadays, more and more radar and remote sensing products become available which provide spatial patterns of rainfall. Nevertheless these products rely on verification on the ground. These products and why ground verification is necessary will be explained in Section 3.2.2.

3.2.1 Point observations of rainfall

Funnel

The most common way to capture and collect precipitation is by means of a funnel. The surface area at the orifice is the catching surface area. Obviously a large surface area reduces the measurement error. The opening surface area is usually standardized to an acceptable level of error. A common size for the aperture is 200 cm^2 . The rims of the funnel are sharp to avoid turbulence, and the drop in the funnel is such as to minimize losses from out splash in heavy

rain.

The next step is to record the captured precipitation. The required time interval of recording can be related to the use of the data:

- For the assessment of water resources, monthly totals may suffice. To avoid loss of the catch over a full month through evaporation, the required data is usually compiled from daily readings. Daily data might well be detailed enough for flood analysis in the larger catchments as well. Daily readings are also practical when an observer manually operates a station.
- For evaluating flood peaks in urban areas, rainfall intensities over an hour or even minutes could be required and continuous or near-continuous recording rain gauges are used. Numerous automatic recording instruments have been invented, usually built by enthusiasts of mechanical devices. Two main types have endured, the tilting-siphon rain recorder, and the tipping bucket gauge.

Tipping bucket rain recorder

Nowadays most used are tipping buckets (Figure 3.2.1). Rain is led down a funnel into a wedge-shaped bucket of fixed capacity. When full, the bucket tips to empty and a twin adjoining bucket begins to fill. At each tip, a magnet attached to the connecting pivot closes circuit and the ensuing pulse is recorded on a counter or electronically. This makes the tipping bucket suitable for electronic logging and/or telemetry. The capacity of the bucket is designed as to represent e.g., 0.2 mm, 0.5 mm or 1 mm of rainfall depth. What is registered electronically is the time of tipping, knowing that each tip represents accumulated rain equal to the capacity of the bucket since the last tipping. It has to be noticed that the tipping bucket does not properly register (low intensity) rainfall less than the bucket capacity and that there is a limit to high intensity rain that it can register accurately. It is also advised to arrange for water to be collected below the buckets for verification, so that totals can be measured if the recording fails.



Fig. 3.2: Tipping Bucket

Placement / Siting

The height of the aperture of the rainfall recorder above the ground surface has a significant effect on the catch of actual rainfall. Wind around the measuring device causes turbulence and hence lowers the catch. Generally, wind speeds increase with height above the ground. As

a result, the catch reduces with increasing heights. At 1.50m above the ground surface the measured rainfall can be $84\% - 96\%$ from the actual rainfall at ground level. The wind effect can be diminished through levelling the air flow at gauge height by means of an aerodynamic screen, e.g. the Alter wind shield or Nipher screen (Fig. 3.3).

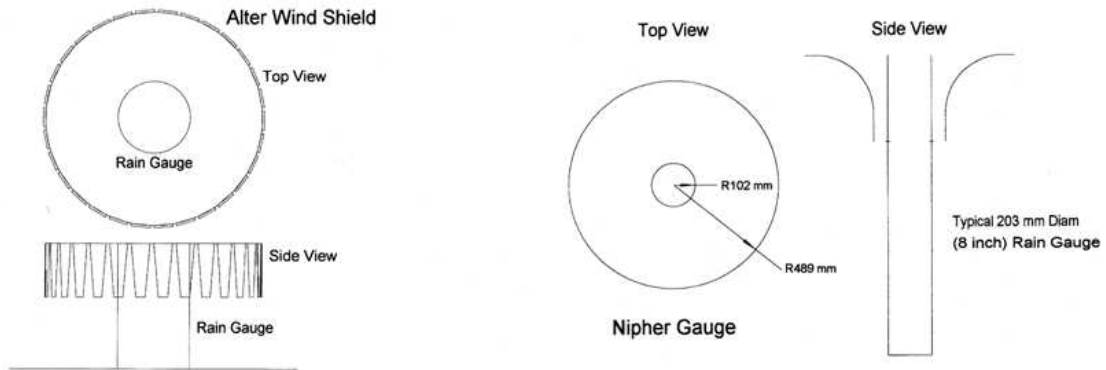


Fig. 3.3: Alter wind shield and Nipher screen

On the other hand, rain gauges are placed at a standard height above the ground level as to avoid water splashing in from the direct surrounding. In this way also interference by animals is avoided.

Some rain gauge sites do have the aperture of the gauge at ground level, with the recorder dug in and the gauge surrounded by a screen or brush. In this way splashing in is avoided and the wind effect is minimized. At other sites a circular turf wall of 3m diameter, and as high as the aperture of the gauge, has been constructed to obtain the same effect, see Figure 3.4.



Fig. 3.4: Turf wall photo KNMI (P.J. van Eif)

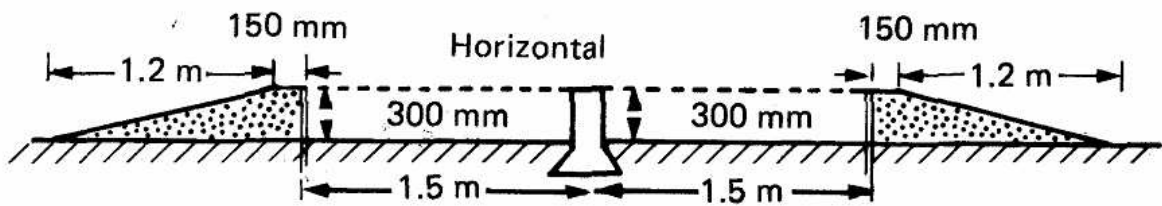


Fig. 3.5: Turf wall around rain gauge

Measurements of rainfall on or near the ground will also be effected by wind disturbances caused by obstacles nearby. As a rule of thumb it can be said that no obstacles should be present nearer than about 5 times the obstacle height, since at shorter distance the rainfall in the gauge will be influenced by air flow deflections around the obstacles. Observers should be encouraged to report any major changes regarding structures or vegetation in the near vicinity of the gauge that may change the wind patterns and hence cause in-homogeneity in the rainfall records.

Tilting-siphon rain recorder

Nowadays, the tilting-siphon rain recorder is not often used anymore; however, in developing countries it is sometimes still used. The rain falling into the funnel is led down to a collecting chamber containing a float. A pen attached to the top of the plastic float marks a chart on a revolving drum. When there is no rain falling, the pen draws a continuous horizontal line on the chart; during rainfall, the float rises and the pen trace on the chart slopes upwards, according to the intensity of the rainfall. When the chamber is full the siphon is activated and empties the chamber within seconds. At that moment the pen drops back to the bottom of the chart. A larger container can be installed to accumulate the releases and provide a means to verify the results.

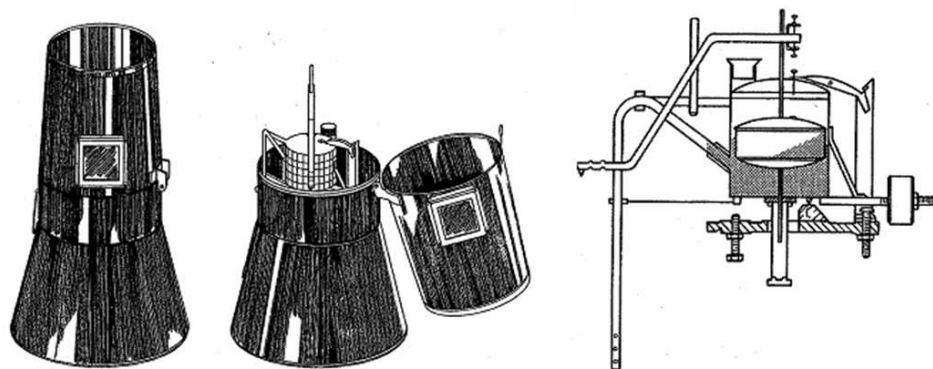


Fig. 3.6: Tilton siphon rain recorder

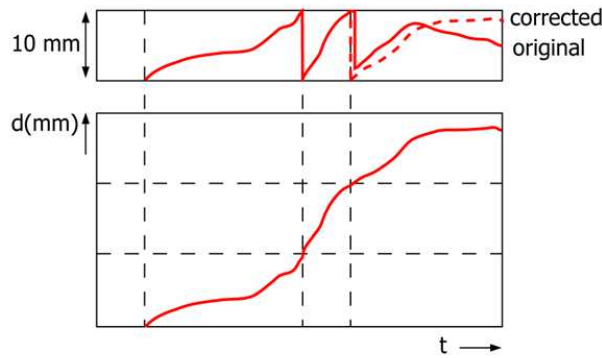


Fig. 3.7: Pluviograph of a tilting siphon recorder

Disdrometers

Disdrometers measure rain by counting drops. There are various underlying principles for disdrometers: video disdrometers, laser disdrometers, acoustic disdrometers, to name a few. Compared to other type of rain gauges, disdrometers have the advantage that, in addition to rain rates, they also measure drop size from which drop size distributions can be derived. Also, by measuring ‘every’ drop, disdrometers have a higher resolution. A drawback of disdrometers is that they usually do not measure rainfall directly, so they have to be calibrated. Because of the nature of disdrometers, this is not something easily done in the field.

Figure 3.8 demonstrates an optical disdrometer, the ORG-700 Series Optical Rain Gauge that measures rainfall intensity by means of infrared red light. Errors due to evaporation and splashing in this way are avoided. The measurable intensities range from as little as 0.1 mm/hr to 3000 mm/hr. This makes the equipment suitable for recording extreme rainfall conditions.

3.2.2 Areal observations of rainfall

Although traditionally precipitation over the area is sampled by rain gauges, modern techniques have been applied to obtain areal distributed information on precipitation. Nowadays, more and more products become available (often for free) to give areal estimates for rainfall. The most common are radar and satellites. Although one might think that these areal products replace the necessity of point observations, radar and satellite data are always calibrated and validated with ground observations. Hence point observations remain important.

Radar

A well known method to measure rainfall is a weather radar. Radar is an acronym for **R**adio **D**etection and **R**anging and measures the reflectivity of radio waves. An antenna (see Figure 3.9a) transmits a pulse, which bounces off on any object resulting in an echo. Clouds without rain do not produce an echo, but clouds with rain reflect the pulse. The higher the reflectivity, the higher the rain intensity. By comparing the radar images (see Figure 3.9b) in time, the

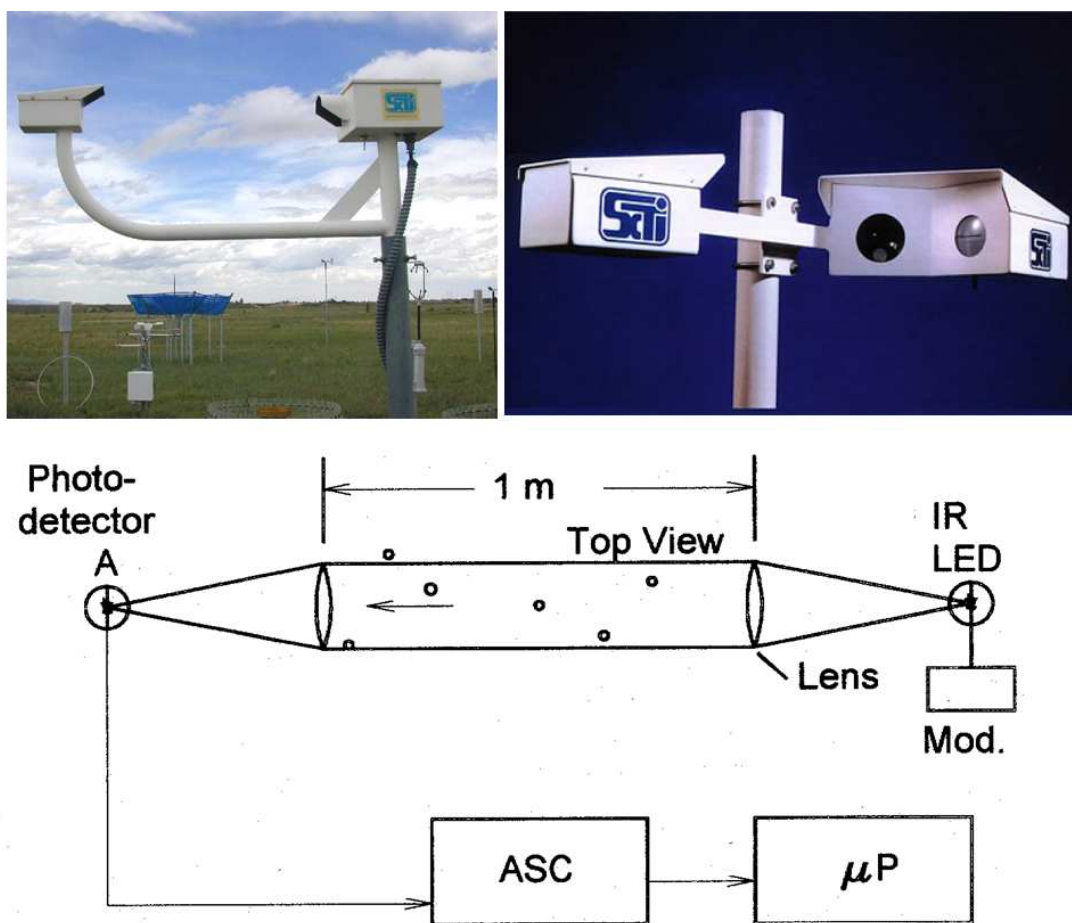


Fig. 3.8: ORG Series optical raingauges

direction of the shower can be derived. Modern radar systems do this by making use of the Doppler effect. These new systems also give information on the wind speeds inside the storm. The temporal resolution of radar data can be as small as 5 minutes. Theoretically, the radar can produce rainfall estimates for a circle with a radius of 300 km from the antenna. However, in practice this is limited to a radius of 180-200 km, because of the curvature of the earth. Due to this curvature, the pulse is traveling through higher elevations with increasing distance from the antenna. Since rainfall clouds are usually present in the lower 5 km of the atmosphere, the radar can not observe showers anymore when the pulse is higher than that 5 km. Another problem with radars occurs when large showers block all radio waves, so showers behind the large shower can not be observed anymore.

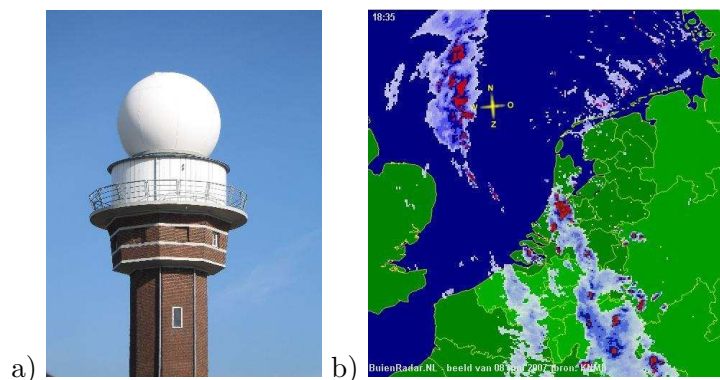


Fig. 3.9: a) Radar of the KNMI in De Bilt, the Netherlands. b) Example of a radar image.

Rainfall from satellites¹

Remote sensing data becomes more and more important to estimate rainfall. One of the first empirical relations used was the relation between cloud top temperatures (measured with a thermal band) and rainfall, also called cold cloud duration. It is now widely used with geostationary satellite imagery from Meteosat, Meteosat Second Generation (MSG) and Geostationary Operational Environmental Satellite (GOES). For instance the GOES Precipitation Index (GPI, Arkin and Meisner [1987]) is a precipitation algorithm based on this relation. Cold cloud tops are caused by release of latent heat to the atmosphere during convective rain storms and it is assumed that when a temperature threshold is underspent, a certain rain rate will occur. Estimating daily rainfall is therefore a matter of counting the number of times that underspending of this temperature occurred. This approach is therefore especially suitable for tropical areas, where most of the rainfall is of a convective nature.

Microwave imagers (e.g., Special Sensor Microwave/Imager (SSM/I), Advanced Microwave Soundings Unit (AMSU-B), TRMM Microwave Imager (TMI) and Advanced Microwave Scanning Radiometer - EOS (AMSR-E)) may also be used to retrieve precipitation fields. Two types of algorithms are developed: one based on scattering and one on emission (e.g., Ferraro and Marks [1995]; Zhao and Weng [2002]). The algorithm based on scattering is where the amount

¹ From Winsemius, H. C., 2009. Satellite data as complementary information for hydrological models. Ph.D. thesis, Delft University of Technology Winsemius [2009]

of scatter of the microwave signal is dependent on the quantity and size of ice particles and the algorithm based on emission is where the variations in brightness temperature are an indication of present water vapour and rainfall. Problems with the first type of algorithms occur where the rainfall is relatively warm such as oceanic rainfall events due to orographic lifting or shallow convective storms, because there are no or only little ice particles present. For both algorithms, there are some problems with scale. The range or footprint of a SSM/I sensor is in general too large to detect small convective events, since the algorithms are based on footprint-averaged exceeding of thresholds. TRMM is the first mission that carries a Precipitation Radar (PR) to estimate 3-dimensional cloud properties and concurrent rainfall.

The difference between rainfall estimates from some different algorithms is given in Figure 3.10. It becomes clear that microwave algorithms see different rainfall properties than cold cloud duration. Therefore, the best results are expected when different estimates are merged. In general, end user rainfall products are combinations of independent estimates, where the weight of the independent estimate is usually somehow based on local groundtruth rainfall. Examples of two popular rainfall estimates are FEWS RFE 2.0 and TRMM.

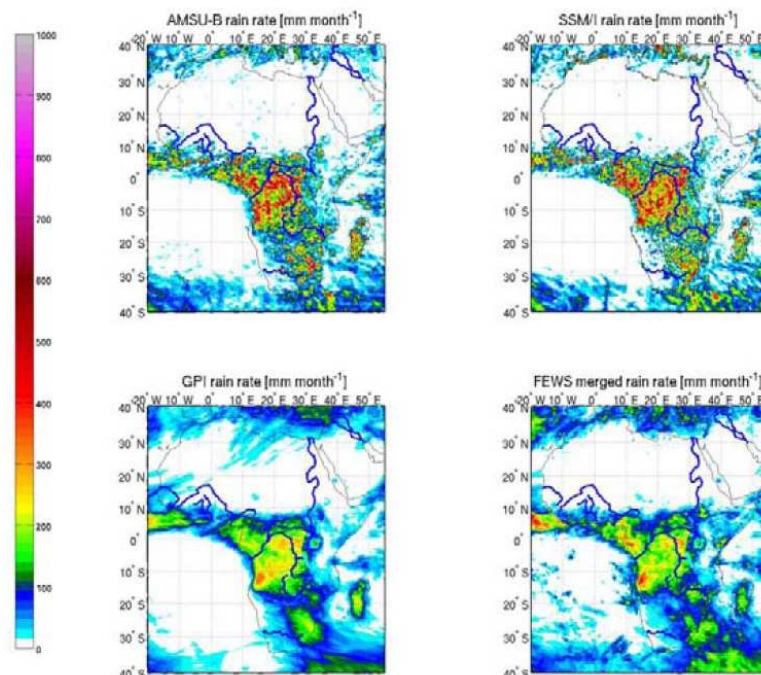


Fig. 3.10: Three independent accumulated rainfall estimates and station data based estimates for a 30-day time window (November 1st until 30th 2007) over Africa. From left to right: AMSU-B microwave, SSM/I microwave, Meteosat GPI, and a merged estimate. The merged estimate shows the impact of rain gauges, especially over the Atlantic Ocean.

3.3 The correlation function

When observation stations are closely together, data from these stations may show a good correlation. The further these stations lay apart, the smaller the chances of coincidence become. For

a given period of observation, the correlation between two stations is defined by the correlation coefficient ρ ($-1 < \rho < 1$). If there is no correlation ρ is close to zero, if there is perfect correlation $\rho = 1$ or $\rho = -1$. For the definition of correlation see Chapter 2.4.2. Negative correlation exists when the depth in one station is persistently high when the depth in the other station is small and vice versa. With rainfall data this will not occur. The correlation coefficient, ρ , will always be between 0 and 1. It can be concluded that ρ is a function of the distance, r , between stations. From worldwide observations it was found that most frequently this function is a negative exponential expression:

$$\rho = \rho_0 \cdot \exp\left(-\frac{r}{r_0}\right) \quad (3.1)$$

This formula has been developed by Kagan. The relation is a curved line, see Figure 3.11. It is also observed that the correlation and hence the shape of the curve is further influenced the precipitating mechanism and by the period of observation.

Depending on the precipitation mechanism the dying of the exponential correlation curve is more or less pronounced. E.g. for convective storms, which are of limited areal extent, the curvature is very pronounced. For storms of large areal extent, e.g. frontal systems, the curvature is much smaller, see Figure 3.11.

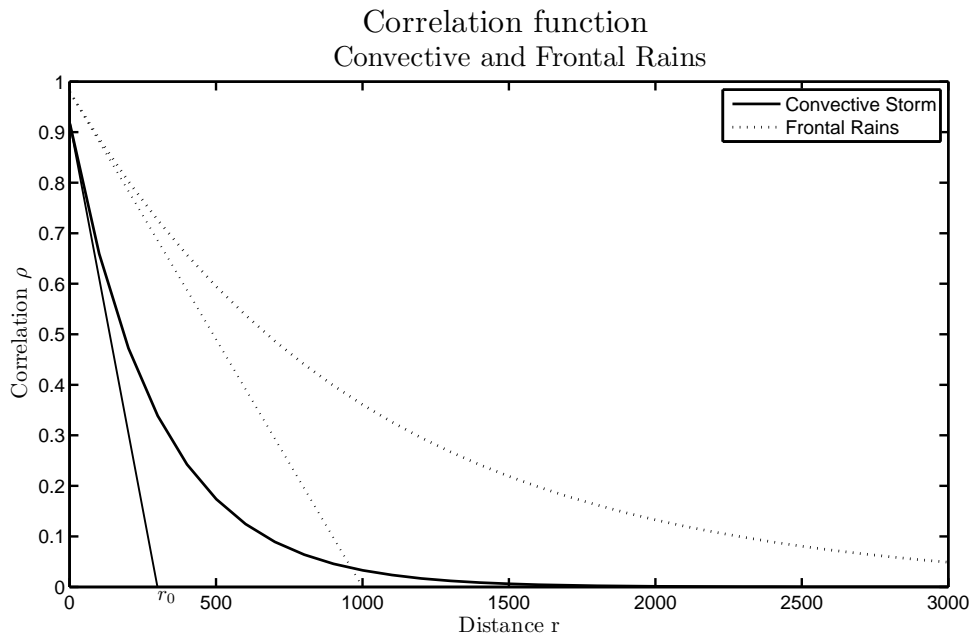


Fig. 3.11: The correlation function compared for convective storms and frontal rains

It is also observed that the correlation is better when the period of observation is larger. For rainfall depths of short periods, e.g. hours or days, the curvature will be appreciable, whereas for longer periods like weeks, months and years the curvature will be smaller again (Fig. 3.12). This is true for any type of rain.

The curvature of the correlation function for rainfall is defined by r_0 . The larger r_0 , the less pronounced is the curvature. The correlation coefficient, ρ_0 , is the correlation at range $r = 0$. It

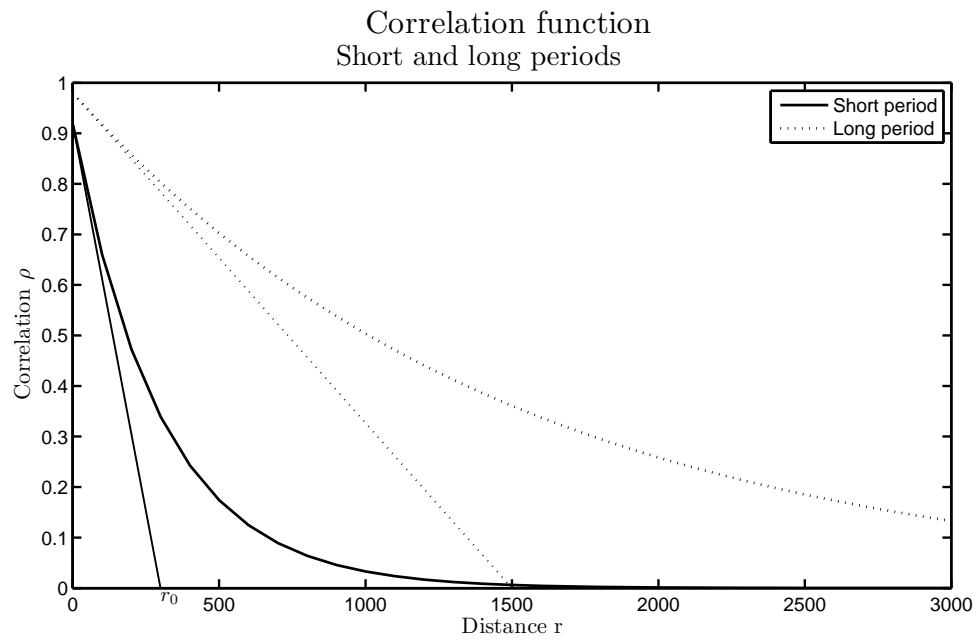


Fig. 3.12: The correlation function compared for short and long periods

caters for the randomness of the event. Hence it can be expected that ρ_0 is smaller for convective storms compared to frontal rains, and is again smaller for hourly observations compared to monthly observations. In a table this can indicatively be represented as follows:

Tab. 3.1: Differences in parameter values for types of rains and time scales

	1 hour	1 hour	1 day	1 day	1 month	1 month
Rain type	r_0 [km]	ρ_0	r_0 [km]	ρ_0	r_0 [km]	ρ_0
Local convective	5	0.80	10	0.88	50	0.95
Convective, orographic	20	0.85	50	0.92	1500	0.98
Frontal depression	100	0.95	1000	0.98	5000	0.99

3.3.1 Example: Rainfall correlation in the Netherlands

Ten days totals from 36 rainfall stations in the Netherlands over the period 1966-1972 were processed by De Bruin (1975). The results for 14 selected stations and all 36 stations is presented in Table 3.2:

Tab. 3.2: Example

	14 selected stations	14 selected stations	All 36 stations	All 36 stations
Period	r_0 [KM]	ρ_0	r_0 [KM]	ρ_0
Nov-March	1000	.99	1000	.95
Sep,Oct,Apr,May	270	.99	270	.98
July-Aug.	190	.99	190	.99

It is seen from the table that a seasonal effect exists: in winter, r_0 has a maximum and in summer a minimum value. This is explained by mainly frontal (that is large scale) precipitation in winter, whereas in summer also convective storms (small-scale precipitation) are likely to occur.

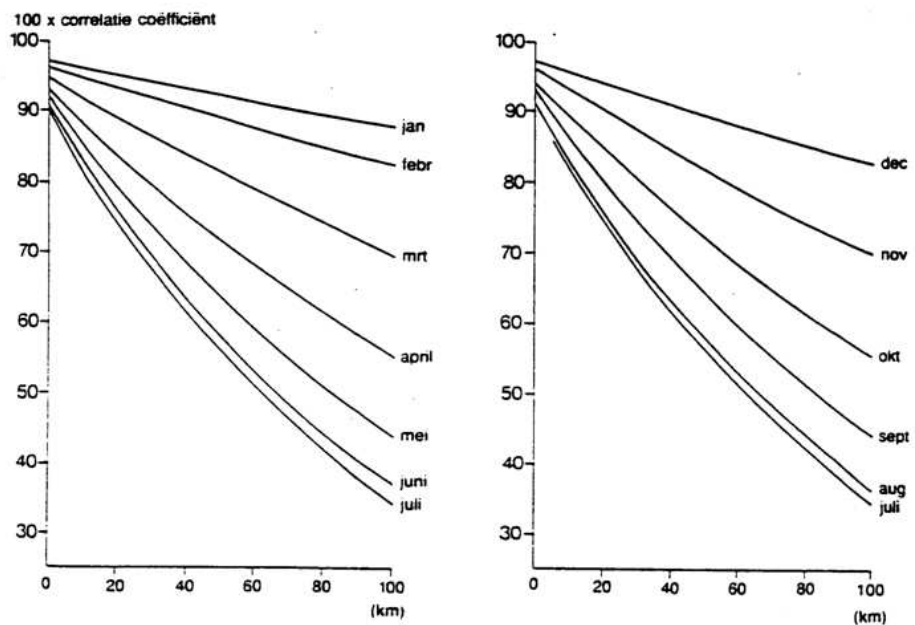


Fig. 3.13: The correlation coefficient ρ , as a function of the distance r for each month in the Netherlands (daily totals $>0.5\text{mm}$)

Tab. 3.3: Correlation coefficient ρ as a function of the distance r for each month in the Netherlands

Month	ρ_0	r_0 [km]
1	.97	962
2	.96	630
3	.95	320
4	.94	190
5	.93	135
6	.91	111
7	.91	104
8	.92	110
9	.93	133
10	.95	186
11	.96	309
12	.97	609

4

Evaporation

4.1 Types of evaporation and definitions

Evaporation is the transfer of water from liquid state into gaseous state. Within the spacial framework of the hydrological processes it normally means the average vertical vapour transport over an area. Evaporation can occur by direct evaporation of water and by transpiration.

- Direct evaporation:
 - Open water evaporation, E_o [L/T]. This is the amount of vaporized water within a certain time from an open water surface. The availability of the water is hereby not restricted.
 - Soil evaporation, E_s [L/T]. The water that is vaporized is soil moisture. When the moisture content is limited, the evaporation is more constrained.
 - Interception evaporation, E_i [L/T]; Evaporation from the wet surface after rainfall. This is more than just interception by leaves, it contains evaporation from all wet surfaces; vegetation, paved surfaces, dropped leaves, bare soil, etc.
 - Snow or ice evaporation, also called sublimation, E_{sub} [L/T]. In cold climates where there is snow or ice sublimation can be considerable. From the solid state water molecules transform into a vapor state.
- Transpiration (E_t [L/T]): The transfer of water vapor into the atmosphere through the stomata of living plants. Just a very small amount of the water absorbed by plants from the soil remains inside the plant itself. The major part vaporizes from the leaves. Because of the influence of solar radiation, transpiration occurs primarily during daytime. At night the pores close and little water leaves the plant. An exception is for instance the cactus (the stomata only open at night).

Summarizing, direct evaporation is the transfer of liquid into vapour by molecules which escape the water surface; transpiration is a physiological process of water molecules transferring by gas exchange in the stomata from the vegetation into the atmosphere.

The sum of all occurrences of evaporation is called ‘actual evaporation’, E_a [L/T]. This is the total amount of vapour that is fed back to the atmosphere and is the flux of interest in the water balance equation. So the total or actual evaporation is a combination of all previous forms:

$$E_a = E_o + E_s + E_i + E_{sub} + E_t \quad (4.1)$$

The open water evaporation is important to add to the summation especially for swamps and rice paddies. Sublimation is only important for areas where snow and ice are dominantly present. Hence actual evaporation is the flux we need for our water balance, but unfortunately it is often very difficult to determine (as shown later) because it is constrained by the availability of water. Therefore, the ‘potential evaporation’, E_p , is often used. The potential evaporation is the same as the total or actual evaporation, but then without the constraint of available water. Resulting in the fact that actual evaporation is thus always lower or equal to the potential evaporation. The potential evaporation indicates the upper boundary of the possible evaporation.

4.2 The process of evaporation

Evaporation, the transfer of water from liquid state into gaseous state, uses energy. The reversed process produces the same amount of energy. This energy is known as the latent heat of vaporization; λ . The latent heat λ for a set temperature is defined as the amount of Joule which is used at that temperature to transfer 1 gram of water from liquid state into water vapor. The dependence of λ on temperature proves to be minor. That is why λ is in practice taken as a constant: $\lambda = 2.45 \cdot 10^6$ J/kg = 2.45 MJ/kg. The latent heat of vaporization per cubic meter becomes $\rho\lambda = 2.45$ GJ/m³.

The energy for evaporation is, directly or indirectly, provided by solar radiation. The amount of radiation which is available to evaporation depends on the latitude, the time of the year, atmospheric conditions like the cloudiness, reflection by the earth’s surface, atmospheric absorption and storage capacity of the ground or the water. To keep the process of evaporation going, the water vapour has to be removed from the evaporating surface (e.g., by wind). This is a process of diffusion and turbulent transport which is affected by the humidity and temperature of the air, the roughness of the surface and the wind speed.

The resistance to flow of water inside the plant and the percentage of the soil covered by crop play an important role in the process of transpiration.

Summarizing, the (potential) evaporation is affected by factors which are determined by:

A Evaporation surface

A.1 Reflection coefficient (albedo)

A.2 Roughness of the surface

A.3 Fraction covered

A.4 Crop resistance (resistance to flow of water inside the plant itself)

B Atmospheric conditions

Surface	Albedo (r)
Free water surface	0.06
Grass	0.24
Bare soil	0.10 - 0.30
Fresh snow	0.90

Tab. 4.1: Albedo (r) for different surfaces.

B.1 Wind velocity

B.2 Relative humidity

B.3 Temperature

B.4 Solar radiation

In the following section these factors will be further elaborated and explained how to measure them.

4.2.1 Factors influencing evaporation

A.1. Reflection coefficient (albedo); Typical values for the reflection of solar radiation reaching the earth's surface are given in Table 4.1. For the influence of reflection on evaporation see the paragraph about solar radiation.

A.2. Roughness of the surface; The turbulent transport of water vapor from the evaporating surface into the atmosphere is largely determined by the roughness (e.g., crop height) of the surface. The resistance to this transport is called the aerodynamic resistance and may for a specific surface (roughness) be written as a function of the wind speed, see the paragraph about wind velocity.

A.3. Heat storage capacity; In climates with a distinct summer and winter period, part of the energy that becomes available in spring is used to warm up the surface. This energy is released during the next autumn and winter. A deep lake or wet soil has a large heat storage capacity. Hence, the evaporating surface will remain relatively cold during spring which affects the evaporation. The subsequent release of heat during the autumn and the winter causes a phase shift in the evaporation cycle of deep lakes as compared to shallow lakes.

A.4. Fraction covered; The fraction of soil that is covered by the crop directly affects the transpiration of the area.

A.5. Crop resistance; Transpiration of a cropped surface is usually less than the evaporation of an open water surface due to the additional resistance of water transport in the plant and the transfer of water vapor through the stomata. For tall crops, however, the increased turbulence lowers the aerodynamic resistance which may result in higher values for the

transpiration as compared to open water evaporation. The crop resistance is often taken from literature.

The atmospheric conditions affecting evaporation comprise:

B.1. Wind velocity; The aerodynamic resistance to water vapour transport r_a (d/m) is a function of the wind speed. Wind speed is measured with anemometers and is a function of the height above the surface. Values which apply for a height of 2m are generally used to estimate evaporation. The wind speed at other heights can by approximation be converted to wind speed at 2m. The aerodynamic resistance in (d/m) to water vapour transport is computed with the formula:

$$r_a = \frac{245}{0.5u_2 + 0.5} \frac{1}{86400} \quad (4.2)$$

with u_2 as the wind speed (m/s) at a height of two meters measured with an anemometer (Fig. 4.1).



Fig. 4.1: Anemometer

Stagnant air in contact with the water surface will eventually approach the (saturation) vapour pressure at the surface and evaporation will cease.

B.2. Relative humidity; Evaporation is very sensitive to the humidity of the air at constant temperature. That is why the actual humidity relative to the saturated state is important. The actual humidity is expressed as the actual vapor pressure e_a and is often the parameter for computing the evaporation. Vapour pressure is the pressure of water particles in the atmosphere. This can be determined in different ways, for example with a psychrometer or by measuring the relative humidity. Before going into details, the saturation vapor pressure has to be explained. The saturation vapor pressure $e_s(T)$ is the maximum vapor pressure of water particles before condensation. Saturation vapor pressure (kPa) is a function of the temperature T and is expressed in the formula:

$$e_s(T) = 0.61 \exp\left(\frac{17.3T}{237 + T}\right) \quad (4.3)$$

where T is the temperature in $^{\circ}\text{C}$.

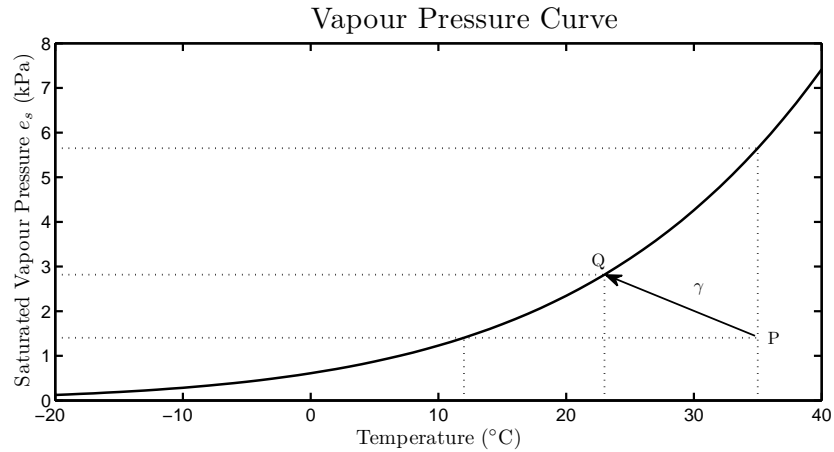


Fig. 4.2: Saturation vapour pressure as a function of the air temperature

In Figure 4.2 we see the equation as a graph. Each specific point P in the temperature-vapour pressure space has an actual temperature T_a and an actual vapour pressure e_a . The saturation vapour pressure is reached when the temperature drops to the dew temperature T_d and fog, dew or condensate evolves.

For some computations the slope of the saturation vapour pressure curve ($s = de_a/dt$) is important. This is easily determined by the derivative of Equation 4.4 in [kPa/ $^{\circ}\text{C}$]:

$$s = \frac{4100e_s}{(237 + T)^2} \quad (4.4)$$

There are two ways to determine the actual vapour pressure e_a :

- a. *Determining the actual vapour pressure by the relative humidity;* In case of direct measurement of the relative humidity (h (-)), e.g. by a hygrometer the actual humidity e_a is determined by the relation:

$$h = \frac{e_a(T_a)}{e_s(T_a)} \quad (4.5)$$

where $e_s(T_a)$ is the saturation vapour pressure at the current air temperature T_a according to Equation 4.3.

- b. *Determining the actual vapour pressure by a psychrometer;* A psychrometer consists of two thermometers, a dry one and one in a wet state. By means of for example a fan, an air flow is forced past the thermometers. This results in a lower temperature of the wet thermometer than of the dry one due to the extraction of energy of latent heat for the evaporation of water from the wet thermometer. The actual vapour pressure [kPa] is computed with the formula:

$$e_a(T_a) = e_s(T_w) + \gamma(T_a - T_w) \quad (4.6)$$

With:

- $e_s(T_w)$ computed with Equation 4.3 9kPa)
- T_a temperature ‘dry’ thermometer ($^{\circ}\text{C}$)
- T_w temperature ‘wet’ thermometer ($^{\circ}\text{C}$)
- γ psychrometer constant (0.066 kPa/ $^{\circ}\text{C}$)

In Figure 4.2 the line PQ indicates the situation of a humid medium (e.g., a wet patch) cooling down under the influence of ventilation from the actual temperature T_a to ‘wet’ temperature T_w . The evaporation involved in this process causes a drop in temperature until a new equilibrium is reached in point Q. At this point the vapour pressure is increased to the saturation vapour pressure of a wet medium $e_s(T_w)$. Note that $-\gamma$ gives the slope of the line PQ.

B.3. Temperature; To measure the temperature properly, only air temperature has to be measured, hence the energy should be supplied by convection and not by radiation, condensation or conduction. For that the thermometer needs to be naturally ventilated and sheltered from sun and rain. This can be done according the WMO standard in a ‘Stevenson shelter’ (Fig. 4.3).



Fig. 4.3: Stevenson Shelter

B.4. Solar radiation; The latent heat of vaporization is, direct or indirect, provided by solar energy; the latent heat for evaporation λ for water is 2.45MJ/kg. Solar radiation is therefore the most dominant factor for the determination of evaporation.

The net radiation, R_n , is important for the estimation of the evaporation. This is the difference between the net short wave radiation ($R_{s,n}$) and the net long wave radiation ($R_{l,n}$). The net short wave radiation is the difference between the incoming short wave radiation $R_{s,in}$ and the fraction that is reflected $rR_{s,in}$ (r is the albedo). The net long wave radiation is the difference between the emitted radiation from the surface ($R_{l,out}$) and the long wave radiation that is scattered back by e.g., clouds ($R_{l,in}$).

The net radiation energy is defined as [$\text{J d}^{-1}\text{m}^{-2}$]:

$$R_n = (R_{s,in} - R_{s,out}) - (R_{l,out} - R_{l,in}) = R_{s,in} - rR_{s,in} - R_{l,n} = (1 - r)R_{s,in} - R_{l,n} \quad (4.7)$$

The net radiation can be measured with a radiometer (see Fig. 4.5). Values of R_n obtained

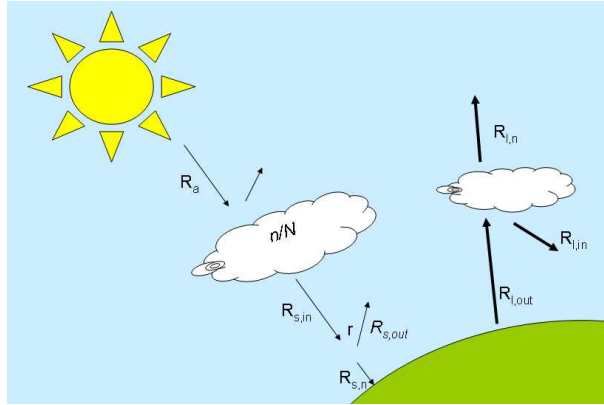


Fig. 4.4: Radiation balance.

above a surface covered with grass differ from those obtained above for example an open water surface due to differences in albedo and emissivity.



Fig. 4.5: Radiometer

In the absence of radiation measurements R_n is to be estimated from standard meteorological data using empirical formulae. The procedure is the following. The short wave radiation energy (wave lengths $0.3 - 3 \mu\text{m}$) R_a that is received at the outer limits of the atmosphere, may be read from tables for a given latitude and time of the year. R_a ($\text{J d}^{-1}\text{m}^{-2}$) divided by the latent heat of vaporization λ (J kg^{-1}) yields equivalent evaporation values R_a/λ in ($\text{kg d}^{-1} \text{m}^{-2}$), which is with a density of 1000kg/m^3 equal to mm/d (Tab. 4.2).

$R_{s,in}$ is the short wave radiation that is received at the earth's surface. Its value depends on the local atmospheric conditions (e.g., smog) and the cloudiness n/N . Where n is the number of actual hours of sunshine and N is the number of possible hours of sunshine. The actual hours of sunshine are easily measured with a Cambell-Stokes sunshine recorder (see Fig. 4.6). The possible hours of sunshine are read in Table 4.3.

In Table 4.4 examples of empirical expressions for $R_{s,in}$ as a function of R_a and the proportion n/N are read.

The net short wave radiation is equal to $(1 - r)R_{s,in}$. To determine the net radiation R_n the net outgoing long wave radiation has to be known. The net outgoing long wave

	Lat	Jan	Feb	Mar	Apr	May	Jun	Jul	Aug	Sept	Oct	Nov	Dec
NORTHERN HEMISPHERE													
Equator	60	1.4	3.6	7.0	11.1	14.6	16.4	15.6	12.6	8.5	4.7	2.0	0.9
	52	3.2	5.5	8.8	12.5	15.4	16.6	16.0	13.6	10.2	6.7	3.9	2.6
	50	3.7	6.0	9.2	12.7	15.5	16.6	16.1	13.7	10.4	7.1	4.4	3.1
	40	6.2	8.4	11.1	13.8	15.9	16.7	16.3	14.7	12.1	9.3	6.8	5.6
	30	8.1	10.5	12.8	14.7	16.1	16.5	16.2	15.2	13.5	11.2	9.1	7.9
	20	10.8	12.4	14.0	15.2	15.7	15.8	15.8	15.4	14.4	12.9	11.3	10.4
	10	12.8	13.9	14.8	15.2	15.0	14.8	14.9	15.0	14.8	14.2	13.1	12.5
	0	14.6	15.0	15.2	14.7	13.9	13.4	13.6	14.3	14.9	15.0	14.6	14.3
	10	15.9	15.7	15.1	13.9	12.5	11.7	12.0	13.1	14.4	15.4	15.7	15.8
	20	16.8	16.0	14.5	12.5	10.7	9.7	10.1	11.6	13.6	15.3	16.4	16.9
	30	17.2	15.8	13.5	10.9	8.6	7.5	7.9	9.7	12.3	14.8	16.7	17.5
	40	17.3	15.1	12.2	8.9	6.4	5.2	5.6	7.6	10.7	13.8	16.5	17.8
	50	16.9	14.1	10.4	6.7	4.1	2.9	3.4	5.4	8.7	12.5	16.0	17.6
60	16.5	12.6	8.3	4.3	1.8	0.9	1.3	3.1	6.5	10.8	15.1	17.5	
SOUTHERN HEMISPHERE													

Tab. 4.2: Short wave radiation expressed in equivalent evaporation; R_a/λ ($\text{kg m}^{-2}\text{d}^{-1}$)



Fig. 4.6: Campbell-Stokes sunshine recorder.

Tab. 4.3: Mean daily duration of maximum possible sunshine hours N

North Lats. South Lats.	Jan July	Feb. Aug.	Mar. Sept	Apr. Oct.	May Nov.	June Dec.	July Jan.	Aug. Feb.	Sept Mar.	Oct. Apr.	Nov. May	Dec. June
60	6.7	9.0	11.7	14.5	17.1	18.6	17.9	15.5	12.9	10.1	7.5	5.9
58	7.2	9.3	11.7	14.3	16.6	17.9	17.3	15.3	12.8	10.3	7.9	6.5
56	7.6	9.5	11.7	14.1	16.2	17.4	16.9	15.0	12.7	10.4	8.3	7.0
54	7.9	9.7	11.7	13.9	15.9	16.9	16.5	14.8	12.7	10.5	8.5	7.4
52	8.3	9.9	11.8	13.8	15.6	16.5	16.1	14.6	12.7	10.6	8.8	7.8
50	8.5	10.0	11.8	13.7	15.3	16.3	15.9	14.4	12.6	10.7	9.0	8.1
48	8.8	10.2	11.8	13.6	15.2	16.0	15.6	14.3	12.6	10.9	9.3	8.3
46	9.1	10.4	11.9	13.5	14.9	15.7	15.4	14.2	12.6	10.9	9.5	8.7
44	9.3	10.5	11.9	13.4	14.7	15.4	15.2	14.0	12.6	11.0	9.7	8.9
42	9.4	10.6	11.9	13.4	14.6	15.2	14.9	13.9	12.6	11.1	9.8	9.1
40	9.6	10.7	11.9	13.3	14.4	15.0	14.7	13.7	12.4	11.2	10.0	9.3
35	10.1	11.0	11.9	13.1	14.0	14.5	14.3	13.5	12.4	11.9	10.3	9.8
30	10.4	11.1	12.0	12.9	13.6	14.0	13.9	13.2	12.4	12.0	10.6	10.8
25	10.7	11.3	12.0	12.7	13.3	13.7	13.5	13.0	12.3	12.0	10.9	10.6
20	11.0	11.5	12.0	12.6	13.1	13.3	13.2	12.8	12.3	12.0	11.2	10.9
15	11.3	11.6	12.0	12.5	12.8	13.0	12.9	12.6	12.2	12.0	11.4	11.2
10	11.6	11.8	12.0	12.3	12.6	12.7	12.6	12.4	12.1	12.0	11.6	11.5
5	11.8	11.9	12.0	12.2	12.3	12.4	12.3	12.3	12.1	12.0	11.9	11.8
Equator	0	12.0	12.0	12.0	12.0	12.0	12.0	12.0	12.0	12.0	12.0	12.0

Tab. 4.4: Empirical relations for $R_{s,in}$

The Netherlands	$R_{s,in} = (0.20 + 0.48 n/N)R_a$
Average climate	$R_{s,in} = (0.25 + 0.50 n/N)R_a$
New Delhi	$R_{s,in} = (0.31 + 0.60 n/N)R_a$
Singapore	$R_{s,in} = (0.21 + 0.48 n/N)R_a$

radiation $R_{l,n}$ ($\text{J d}^{-1} \text{m}^{-2}$) may be estimated from the following empirical formula:

$$R_{l,n} = \sigma(273 + t_a)^4(0.47 - 0.21\sqrt{e_a})(0.2 + 0.8\frac{n}{N}) \quad (4.8)$$

Where σ is the Stefan-Boltzmann constant ($\sigma = 4.9 \cdot 10^{-3} \text{ J d}^{-1} \text{m}^{-2} \text{K}^{-4}$), T_a is the temperature of the air in $^{\circ}\text{C}$ and e_a is the actual vapour pressure of the air in kPa.

4.3 Measuring evaporation

There exist several ways to measure evaporation directly or more often indirectly. In Table 4.5 an overview of some of the techniques are shown. It is important to realize what kind of evaporation is measured. Does the method gives you an estimate for the potential evaporation or for the actual evaporation. And what type of evaporation is measured? Evaporation by open water (E_o), transpiration (E_t), soil (E_s), or evaporation of intercepted water (E_i)?

In the following sections the different techniques will be explained.

4.3.1 Penman Equation

The most well known method to calculate open water evaporation E_o is the method of Penman (Penman [1948]), which has found world-wide application because it has a strong physical basis. This formula, which may be used for estimating the potential evaporation E_p , is written as:

$$E_p \approx E_o = \frac{\frac{sR_n}{\rho\lambda} + \frac{c_p\rho a}{\rho\lambda} \frac{(e_s - e_a)}{r_a}}{s + \gamma} \quad (4.9)$$

Tab. 4.5: Overview of methods to measure evaporation.

	Potential		Actual			
	E_o	E_t	E_o	E_t	E_s	E_i
Penman	x		x			
Penman-Monteith		x				
Pan evaporation	x	x				
Lysimeter				x ¹	x ²	x ¹
Sapflow				x		
Bowen ratio			x	x	x	x
Eddy correlation			x	x	x	x
Scintillometer			x	x	x	x
Energy balance			x	x	x	x

¹ If vegetation in lysimeter.

² If soil layer in lysimeter.

With:

- R_n net radiation on the earth's surface ($\text{J d}^{-1} \text{m}^{-2}$)
- λ latent heat of vaporization (J/kg) (2.45 MJ/kg)
- s slope of the saturation vapour pressure-temperature curve ($\text{kPa}/^\circ\text{C}$) (see Eq.4.4)
- c_p specific heat of air at constant pressure ($\text{J kg}^{-1} \text{K}^{-1}$) ($1004 \text{ J kg}^{-1} \text{K}^{-1}$)
- ρ_a density of air (kg/m^3) (1.205 kg/m^3)
- ρ density of water (kg/m^3) (1000 kg/m^3)
- e_a actual vapour pressure in the air at 2m height (kPa)
- e_s saturation vapour pressure for the air at 2m height (kPa)
- γ psychrometer constant ($\text{kPa}/^\circ\text{C}$) ($0.066 \text{ kPa}/^\circ\text{C}$)
- r_a aerodynamic resistance (d/m)

Notice that all pressures are expressed in kPa and that the final evaporation is computed in m/d. If the net radiation energy R_n is divided by $\rho\lambda$, this term has also the unit of m/d. If this term is expressed in mm/d (by multiplying it with 1000) and the aerodynamic resistance is expressed in d/mm (by dividing it with 1000), then the calculated evaporation has also the unit of mm/d. This is a more common unit to express evaporation.

The method described above only needs four standard meteorological parameters:

- Net radiation (or at least sunshine hours)
- Wind velocity
- Relative humidity
- Air temperature

The required data of the meteorological observations are 24 hour means at a height of 2 meters above the soil surface.

4.3.2 Penman-Monteith Equation

The formula of Penman for open water evaporation is also used as a reference to estimate the potential transpiration ($E_{p,t}$) of a crop; therefore the crop resistance is introduced (Monteith [1965]):

$$E_{p,t} = \frac{\frac{sR_n}{\rho\lambda} + \frac{c_p\rho a}{\rho\lambda} \frac{(e_s - e_a)}{r_a}}{s + \gamma\left(1 + \frac{r_c}{r_a}\right)} \quad (4.10)$$

where r_c (d/m) is the crop resistance. The crop resistance depends on the availability of soil moisture. If a crop is supplied with an abundant amount of water, the crop resistance reaches a minimum level; the transpiration is equal to the potential transpiration $E_{p,t}$.

The relation between crop resistance and soil moisture availability is crop dependent and difficult to evaluate. To come to the total evaporation, the evaporation of interception water and the direct evaporation of water on the ground still has to be taken into account.

To compute the water requirements for irrigation purposes the maximum (potential) transpiration of a crop T_p is normative. It is not always possible to use Equation 4.10 because some e.g., meteorological values are missing or r_c can not be estimated. In that case it is common practice to use the reference evaporation E_{ref} . The reference evaporation is defined as the evaporation from an idealized grass crop with a fixed crop height of 0.12m, an albedo of 0.23 and a $r_c=70$ s/m:

$$E_{p,t} = k_c E_{ref} \quad (4.11)$$

where k_c is the crop factor. The crop factor expresses the factors that are related with the evaporation surface, for instance the type of crop and the stage of growth the crop is in, so k_c is actually time dependent.

More information on the Penman-Monteith equation and calculation examples can be found in the FAO manual (Allen et al. [1998]).

4.3.3 Pan evaporation

The most straightforward method to measure open water evaporation directly is with a pan (Fig. 4.7). The pan is filled with water and every time interval (e.g., daily) the water level is measured. The drop in the water level divided by the time interval gives the rate of open water evaporation. Of course, the water level difference should be compensated for rainfall. Therefore, next to the pan a rain gauge should be installed.

Various types of pans are in use, such as the sunken pan, floating pan, and surface pan. The use of the surface pan is most widely spread, despite its shortcomings. The most common is the U.S. Weather Bureau Class A-pan, with a diameter of 4ft and depth of 10 inch. The water level is maintained 2-3 inches below the rim (Fig. 4.7).

Although the Class A-pan is a direct method, one should be careful with assuming that the pan evaporation is an estimate for the open water evaporation. Often the pan evaporation is higher than the open water evaporation due to warming of the sides by the sun. To reduce this effect the pan can be installed on floats in a lake or one can make use of correction factors (see e.g., Grismer et al. [2002] for an overview).



Fig. 4.7: Class A-pan

4.3.4 Lysimeters

[will be discussed in the lectures]

4.3.5 Sapflow

[will be discussed in the lectures]

4.3.6 Bowen ratio

Another way to determine the evaporation is by using the energy balance and the Bowen ratio. The Bowen ratio gives the ratio between the sensible heat flux and the latent heat flux. The Bowen ratio can be determined with temperatures and vapour pressures at different heights.

The energy balance can be written as:

$$R_N = \rho\lambda E + H + G \quad (4.12)$$

With:

- R_N Netto solar radiation (W/m^2)
- $\rho\lambda E$ latent heat flux (W/m^2)
- ρ density of water (kg/m^3)
- λ latent heat of vaporization (J/kg)
- E evaporation (m/d)
- H sensible heat flux (W/m^2)
- G ground heat flux (W/m^2)

The Bowen ratio can be written as:

$$\beta = \frac{H}{\rho\lambda E} = \gamma \frac{T_2 - T_1}{e_{a,2} - e_{a,1}} \quad (4.13)$$

With:

- β Bowen ratio (-)
 γ psychrometric constant (kPa/°C)
 T_1 temperature at height z_1 (°C)
 T_2 temperature at height z_2 (°C)
 e_1 vapor pressure at height z_1 (kPa)
 e_2 vapor pressure at height z_2 (kPa)

Often the ground heat flux can be neglected, so the evaporation can be written as:

$$E = \frac{R_N}{\rho\lambda(1 + \beta)} \quad (4.14)$$

To determine the evaporation in this way, it is necessary to measure the temperature and humidity at least 2 heights. Three measurements will give a more precise result. z_1 should be 30 cm above the vegetation, z_2 2 meters above z_1 and z_3 2-4 meters above z_2 .

Example bowen ratio

The following data are averaged over one hour on a certain day:

	T (°C)	e_a (kPa)
z_1 (0.5 m)	20	0.88
z_2 (2.5 m)	18	0.82
z_3 (6.5 m)	16	0.75

The average net radiation during this hour is $R_N=200$ W/m²

The Bowen ratio can now be determined by plotting the vapour pressure to the temperature (Figure 4.8).

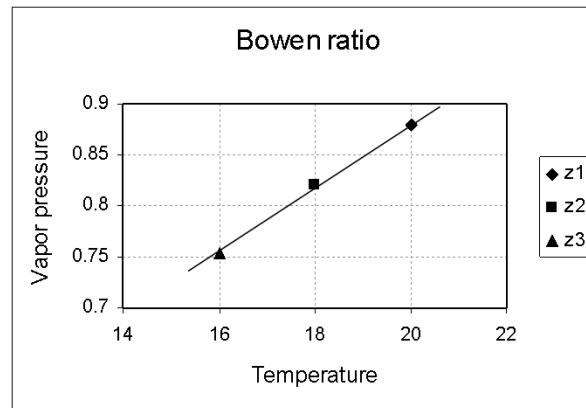


Fig. 4.8: Values for vapour pressure and temperature

From the trend line in Figure 4.8 the Bowen ratio can be derived:

$$\beta = \gamma \frac{\Delta T}{\Delta e_a} = 0.066 * \frac{4}{0.11} = 2.4 \quad (4.15)$$

From the Bowen ratio the evaporation can be determined:

$$E = \frac{R_N}{\rho\lambda(1 + \beta)} = \frac{200 \cdot 3600}{1000 \cdot 2.45 \cdot 10^6 * (1 + 2.4)} = 8.6 \cdot 10^{-5} \text{m/hour} = 0.086 \text{mm/hour} \quad (4.16)$$

When this evaporation would be constant during 12 hours a day, this would lead to evaporation of 1.03 mm/day.

Note: In this case it seems a bit unnecessary to plot a trend line because the line fits perfect to all the data point. Of course in the field this won't be the case, so it will be necessary to make a plot with a trend line.

4.3.7 Eddy correlation

[will be discussed in the lectures]

4.3.8 Scintillometer

[will be discussed in the lectures]

4.3.9 Energy balance

[will be discussed in the lectures]

5

Soil water

Soil water is the water that is stored in the unsaturated zone. Thus the zone between the surface and the ground water table, where the pores in the soil are partly filled with water and partly with air. The unsaturated zone (or vadose zone) is the buffer between infiltrated water and percolated water to the ground water and is mainly important for plants.

The water content in the soil can be measured directly by the gravimetric method, whereby a soil sample is taken from the field and taken to a lab. The sample is successively weighted in the ‘wet’ state (M_{sample}) and afterwards completely saturated and again weighted (M_{sat}). Next, the sample is dried in an oven and weighted for the last time (M_{dry}). The volumetric soil moisture content θ ($0 < \theta < 1$) is then expressed as:

$$\theta = \frac{M_{sample} - M_{dry}}{M_{sat} - M_{dry}} = \frac{V_w}{V_t} \quad (5.1)$$

Although this method is cheap and straightforward, it has the disadvantages that it is destructive and that it can not be used for continuous measurements, which is often required. The indirect methods are more appropriate for this purpose.

There are several ways to measure soil moisture indirectly. In Vereecken et al. [2008] and Robinson et al. [2008] a good overview is given. The most common methods are those that make use of the dielectric permittivity (Capacitance Probe, Time Domain Reflectometry (TDR), and Frequency Domain Reflectometry (FDR)) or the thermal conductivity (Heat Pulse Sensors). Furthermore, also remote sensing techniques become more important for soil moisture measurements.

5.1 Capacitance Probe

The capacitance probe uses the capacitance to measure the dielectric permittivity of the surrounding soil, which is a function of soil water. The probe measures the charge time of a capacitor which uses the soil and water as a dielectric. The charge time is related to capacitance, which is again a function of dielectric permittivity. The dielectric permittivity of water is 80, while soil has a dielectric permittivity in the order of 2-5. Hence when the soil contains more water the dielectric permittivity will increase. This relation is used to measure the soil moisture content.

The dielectric permittivity is measured with a so-called capacitor sensor, which consists of a number of electrodes: either two circular rings or an array of parallel metal spikes (Figure 5.1). The rings or spikes form the plates of the capacitor with the soil in between acting as the dielectric.



Fig. 5.1: Capacitance probe (*10HS Soil Moisture Sensor - Decagon*)

5.2 Time Domain Reflectometry (TDR)

A TDR probe consists of a device with two or three pins attached to it (Figure 5.2). The device transmits a high frequency electromagnetic wave and measures the travel time between transmitting and the reflected signal. The shorter the travel time, the lower the dielectric permittivity, and thus the lower the water content.

TDR probes are relatively expensive, but highly accurate if properly calibrated. Compared to the capacitance probes, the TDR probes are less sensitive for salinity and temperature.



Fig. 5.2: Time Domain Reflectometry (*Trime Data Pilot System - IMKO*)

5.3 Frequency Domain Reflectometry (FDR)

The FDR-method (Figure 5.3) uses a similar principle as the TDR; however, while the TDR measures the travel time of an electromagnetic pulse, the FDR-method uses the difference in

transmitted and reflected frequency of radio waves. The advantages of the FDR in comparison to the TDR are the price and the sensitivity to temperature and salinity.



Fig. 5.3: Frequency Domain Reflectometry (*PR2 Profile Probe - Delta-T Devices*)

5.4 Heat Pulse Sensors

Heat pulse sensors are relatively a new methodology to measure soil moisture. Campbell et al. [1991] introduced the method where two needles are inserted into the soil. One of the needles is heated with a short heat pulse and the temperature response at the second sensor is measured. In this way the soil's volumetric heat capacity can be determined, which is a function of soil moisture. Campbell et al. [1991] used two needles, but current heat pulse sensors have more needles to improve the accuracy of the measurement and are often also combined with dielectric measurements.

5.5 Remote Sensing

Nowadays, soil moisture is more and more measured by remote sensing techniques, like passive microwave radiometers, synthetic aperture radars, scatterometers or thermal methods (Wagner et al. [2007] and Drusch et al. [2004]). Although remote sensing data is promising for the future, currently it suffers from problems with spatial averaging and the small penetration depth. The spatial resolution of the satellite is so large that the measurements do not reflect the heterogeneity of the soil moisture which is important. Furthermore, the satellite is only able to detect the moisture in the top layer of the soil, while measurements of the moist in the root zone are much more important.

5.5.1 Further readings

Njoku, E. G., a. E. D., 1996. Passive microwave remote sensing of soil moisture. *Journal of Hydrology* 184, 101–129

Wagner, W., Scipal, K., 2000. Large-scale soil moisture mapping in Western Africa using the ERS scatterometer. *IEEE Transactions on Geoscience and Remote Sensing* 38, 1777–1782

Kerr, Y. H., Waldteufel, P., Wigneron, J. P. ., Martinuzzi, J. M., Font, J., Berger, M., 2001. Soil moisture retrieval from space: The soil moisture and ocean salinity (SMOS) mission. *IEEE Transactions on Geoscience and Remote Sensing* 39, 1729–1735

de Jeu, R. A. M., Wagner, W., Holmes, T. R. H., Dolman, A. J., van de Giesen, N. C., Friesen, J., 2008. Global soil moisture patterns observed by space borne microwave radiometers and scatterometers. *Surveys in Geophysics* 29, 399–420

Entekhabi, D., Njoku, E. G., O'Neill, P. E., Kellogg, K. H., Crow, W. T., Edelstein, W. N., Entin, J. K., Goodman, S. D., Jackson, T. J., Johnson, J., Kimball, J., Piepmeier, J. R., Koster, R. D., Martin, N. McDonald, K. C., Moghaddam, M., Moran, S., Reichle, R., Shi, J. C., Spencer, M. W., Thurman, S. W., Tsang, L., Van Zyl, J., 2010. The soil moisture active passive (SMAP) mission. *Proceedings of the IEEE* 98, 704–716

6

Measurements of stage

6.1 Introduction

The stage of a river is the height of the water surface above an established reference plane. Stages are relatively easy measurable, even though the requirements for the accuracy of the measurement can differ for each different purpose. The highest accuracy is required when the slope of the water surface for a relatively short reach of the river needs to be determined. Stages are frequently used to determine stage-discharge curves or to estimate a discharge at a particular moment with the help of a discharge-curve (See also Jansen et al. [1979, reprint 1994], p. 174 and further).

6.2 Selection of Location

Before starting with the actual measurements a suitable location has to be selected. The choice of the location depends on:

- Purpose of the measurement
- Hydrological and hydraulic properties of the location
- Costs of installation and sustenance
- Accessibility and distance to public road
- Availability of mains voltage

Besides these points of decision the watercourse, at the point of measurement, has to fulfill certain requirements for the usefulness of the measurement. The requirements for the watercourse are:

- The watercourse has to be straight for at least 100m upstream and downstream from the point
- measurement for a regular velocity distribution in the water
- No inundation (flooding) when extreme high water occurs (1 time per 50 years)

- No backwater
- Close to the point of measurement, measurements of velocity have to be possible so stage-discharge curves can be compiled
- No big changes in resistance (think of plant growth or lack of such in wintertime, this for instance occurs with discharge measurement stations in the Swiss Rhine).

6.3 Equipment pre-considerations

The accuracy of the discharge data is determined by the accuracy with which the stages can be measured. It is essential that the measurement equipment fulfills the necessary accuracy. The choice of measurement equipment depends on:

1. Local field situation
2. Purpose of the measurement
3. Possibility of data processing
4. Available manpower
5. Costs of installation and maintenance
6. Availability of mains voltage

ad 1

Depending on the local situation stage-discharge relations are more or less sensitive to water level changes. A wide but shallow control section needs more accurate water level measurements than a deep narrow section. Turbulent flow needs a proper stilling well.

ad 2

When the stage is the only point of interest, accuracy of 1 to 5 cm normally will do, depending on the purpose of the measurement. When the discharge is also of interest a 10 times more accurate measurement is necessary.

ad 3

For the choice of the layout of the measurement station the way of processing and analyzing the measurement data needs to be taken into account. Many institutions begin measuring with often-sophisticated equipment without having the possibility of processing the data. Measurement data needs to be processed shortly after the arrival of the data. Shortcomings in observation equipment can often still be corrected and/or improved, because the observer is still familiar with the special circumstances.

ad 4

Normally the equipment chosen has to be as simple as possible. When the equipment gets more sophisticated, higher demands are being asked from the observer. A simple float-operated water level recorder is little interference sensitive, easily understandable and repairs can mostly be self performed. When advanced equipment is being used, highly qualified field personal is needed.

ad 5

Between the different measurement equipment prices, differences exist. The costs attached to the layout of the measurement station can often be earned back by low maintenance costs and long lifespan of the measurement systems.

ad 6

In case of no present main voltage or no mains voltage available for a reasonable price, measurement equipment with low energy consumption can be necessary, but there are alternatives to mains voltage. Solar panels are becoming more and more popular and can supply measuring stations with sufficient power throughout the year. Unfortunately they are vulnerable to vandalism: complex fencing won't prevent this, explaining the need for measurements does. Nowadays some equipment has such a low power requirements that special batteries can last for 10 to 15 years.

6.4 Principles of measurement equipment

With measurements of stage one should differentiate between direct and indirect measuring systems. Direct systems measure the stage directly, while indirect systems measure not the stage, but another parameter (e.g. water pressure) which is being converted into a stage.

Available direct systems are:

- Staff gauges
- Float gauges

Available indirect systems are:

- Bubble-type pneumatic gauges
- Ultrasonic water level gauges
- Electronic pressure transducers

The above mentioned measuring equipment will be discussed in the remainder of this paragraph.



Fig. 6.1: Left: Vertical staff gauge, right: inclined staff gauge

6.4.1 Staff gauges

The easiest way to measure a stage is with a staff gauge, normally either a vertical staff gauge (see Fig. 6.1 (left)) or an inclined staff gauge (see Fig. 6.1 (right)). The latter is less vulnerable for ships and floating ice. The zero line of the scale has to be fixed to a reference plane by means of a leveling instrument. The smallest subdivision of the scale is 10 mm. The reading accuracy is 3 mm.

Advantages of staff gauges:

- Easily installed
- Direct reading

Disadvantages of staff gauges:

- Difficult reading when waves occur
- Not suitable for automatic data processing
- Chance of inaccurate reading. Staff gauges usually show only intervals of decimetres and centimetres, this has often showed to be a recipe for reading the improper meter indication.

6.4.2 Float gauges

The float gauge is the oldest and most commonly used equipment for measurements of stage. It is the only direct system, which can measure the water stage continuously and automatically. The float gauge is used mainly as an inside stilling well reference gauge for a water level recorder

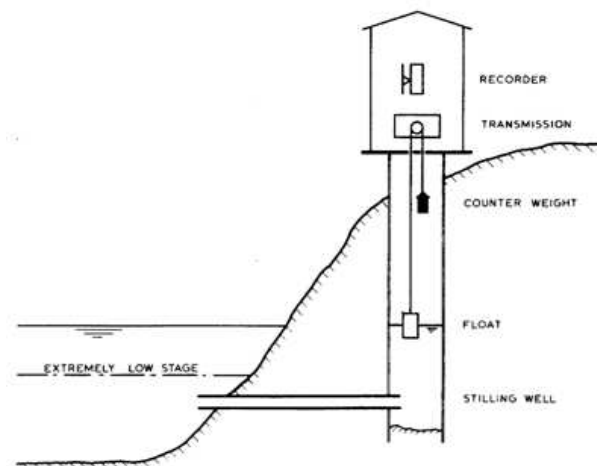


Fig. 6.2: Float gauge

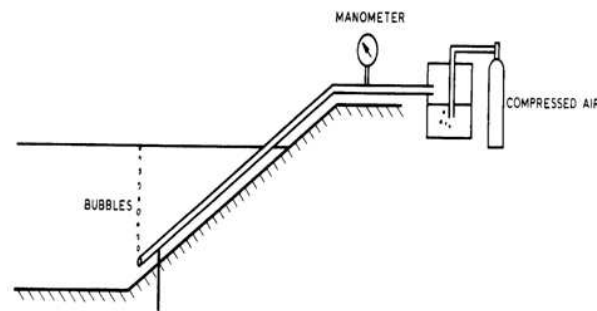


Fig. 6.3: Bubble-type pneumatic gauge

and consists of a float attached to a counterweight by means of a cable or a stainless steel tape. The cable or tape passes over a pulley of the recording device (see Fig. 6.2) (for stilling well see section 6.5). The recording device continuously records the stage (for recording device see section 6.6)

6.4.3 Bubble-type pneumatic gauge

The bubble-type pneumatic gauge is based on measurement of the pressure needed to produce bubbles against the water pressure (see Fig. 6.3). A gas, mostly nitrogen or air, is blown through a tube into the water. The pressure needed to overcome the water pressure at the end of the tube is an indication for the water head above the end of the tube.

The bubble-type pneumatic gauge is mainly used when the location is not suitable for a float gauge; e.g. conditions for a tower and stilling well are unfavorable. On the other hand, for the bubble-type pneumatic gauge an airtight tube has to be laid, which is potentially cumbersome and vulnerable.

Extreme temperature variations of the gas in the purge system will cause pressure fluctuation. An increase of the temperature will cause an overestimate of the real stage.

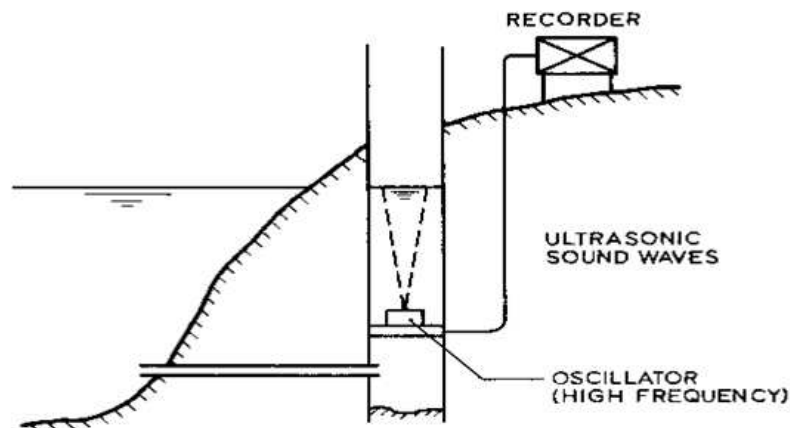


Fig. 6.4: Ultrasonic water level gauge with sensor below the water surface

6.4.4 Ultrasonic water level gauges

The ultrasonic water level gauge has a sensor located at either a fixed point above the water surface or a fixed point below the water surface (see Fig. 6.4). This sensor sends, with high frequency, sonic waves to the water surface, the sonic waves are reflected by the water surface and received again by the sensor. The time interval between transmission and reception is measured, from knowledge of the velocity of sound in air or water, as the case may be, this can be converted into a stage. The main advantage of the ultrasonic water level gauge with a sensor located at a fixed point above the water surface is that the sensor doesn't have contact with the water. This is especially useful for measurements in polluted water; the ultrasonic water level gauge is for this reason often used by purification plants. The velocity of sound in air or water changes with density. Hence temperature and humidity affect the accuracy of the method. Most systems correct their measurements automatically for temperature and humidity, but this is only a partial correction. The accuracy of this sensor is about the same as the accuracy of the diaphragm-type pneumatic gauge. The ultrasonic water level gauge is used mainly within a stilling well (for stilling well see section 6.5).

6.4.5 Electronic pressure transducers

An electrical pressure transducer has two main components: the force summing device, which responds to the pressure (caused by the water head above the device), and the sensor which converts the output of the force summing device into an electrical signal. There are several designs for each component part (see Fig. 6.5).

The transducer may contain signal processing electronics, which change the low-level sensor output into a form suitable for transmission over long distances. In all transducers, water pressure + atmospheric pressure are measured with respect to a reference. This reference gives the transducer a classification:

1. Vented transducer - reference to atmospheric pressure
2. Sealed transducer - reference to a fixed known pressure

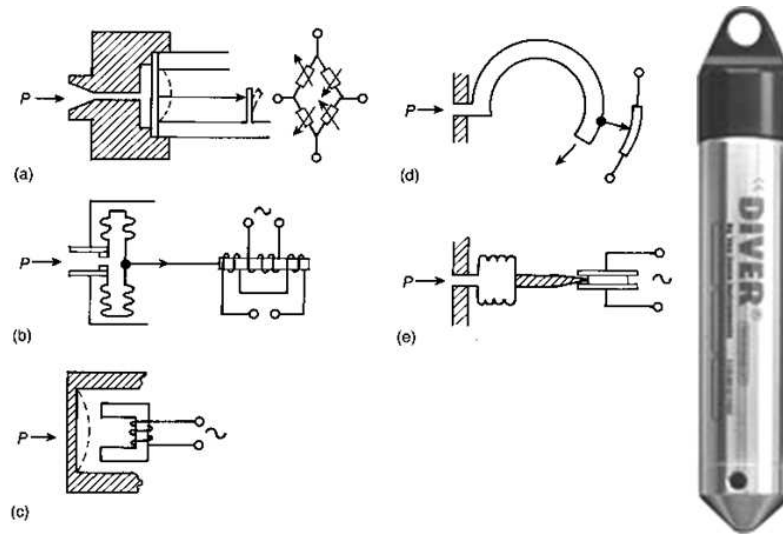


Fig. 6.5: Left: possible electric pressure transducers for measurements of stage, right: sealed pressure transducer (van Essen diver)

Since all open channel flows are subject to atmospheric pressure, the vented gauge type is the most suitable for application to measurements of stage. The vented gauge incorporates a vent pipe. Disadvantage is that for instance condensation water in the vent pipe, can cause the transducer to become inaccurate. Sealed transducers need additional measurement of atmospheric pressure.

For all measuring systems a regular check of equipment on the measuring site is necessary. Suspicions about correctness of the data are never superfluous. Regular calibration (in the field) is highly recommend.

6.5 Stilling well and intake

Measuring systems can be used within a stilling well. A stilling well is used to damp out natural oscillations in the water surface, waves and turbulence among other things. The function of the stilling well is to provide within the well an accurate representation of the mean water level. The stilling well is in contact with the stream via the intake. The function of the intake is to allow water to enter or leave the stilling well so that the water in the well is maintained at the same elevation as that in the stream under all conditions of flow. The system has to be designed in such a way that significant variations in stage also occur within the stilling well.

The error of the water level in the stilling well (S_h (m)) can be described with Equation 6.1:

$$S_h = \frac{\xi}{2g} \left(\frac{A_p}{A_b} \right)^2 \left(\frac{dh}{dt} \right)^2 \quad (6.1)$$

With:

A_p (horizontal) cross-section of the stilling well (m^2)

A_b cross-section of the intake (m^2)

dh/dt variations in stage (m)

ξ loss-coefficient; consists of entry-loss, friction-loss and exit loss in the intake pipe (-)

Recommended is:

$$\xi = \xi_{in} + \xi_w + \xi_{out} = \frac{1}{2} + \frac{fL}{D} + 1$$

With:

L length (m)

D diameter (m)

f Darcy-Weisbach coefficient (-)

Sediment flowing through the intake can cause the intake to get fully or partially jammed, this is why regular checks are necessary. Flushing of the intake pipes for removal of sediment has to be possible.

Stilling wells are often used with wire gauges, float gauges and ultrasonic water level gauges, but can also be used with other stage measuring systems.

6.6 Water level recording devices

Water level recording devices are used to record the measured stage. Water level recording discussed in this paragraph encompasses:

- Manual recording
- Autographic recorders
- Solid-state recorders
- Others

6.6.1 Manual recording

A person reads the water stage from the measuring device and records this by means of writing the measured stage or by typing it into a computer.

6.6.2 Autographic recorders

The autographic recorder is used to record the stage measured by a float gauge. There are two basic mechanisms used:

- The moving float, looped over a geared pulley with a counterweight, activates a pen marking the level on a chart driven round on a vertical clockwork drum (see Fig. 6.6(right))
- The float, with its geared pulley and counterweight, turns the charted drum set horizontally and the pen arm is moved across the chart by clockwork (see Fig. 6.6(left)).

The time scale of the charts is fixed and can be e.g. a day, a week or a month.

Many instruments have been designed to overcome the shortcomings of the two simple mechanisms described. Additional gearing to the pen arm and a trip device can reverse the trace on the vertical chart and thereby record excessive peak levels as a mirror image in the top of the

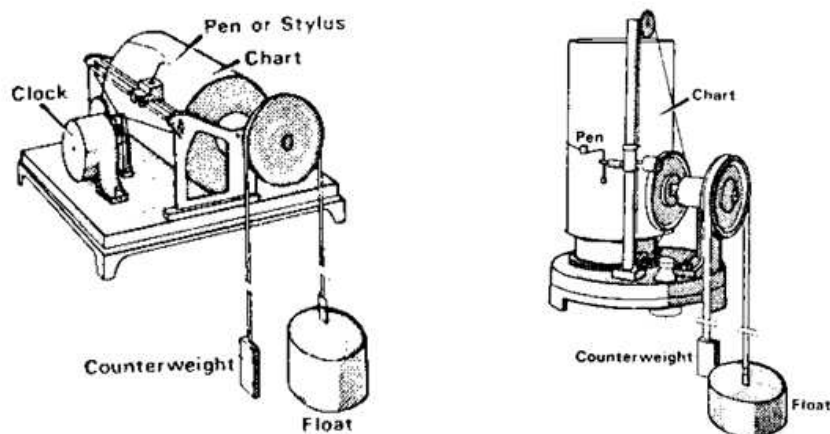


Fig. 6.6: Left:Horizontal autographic recorder, Right:Vertical autographic recorder

chart. Other devices do not record on a chart on a revolving drum but on a chart that moves from one roll to another, in this way extending the record period significantly.

6.6.3 Solid-state recorders

A different generation of recording devices is available capable of accepting and storing data within an entirely solid-state system. The recorder stores the data in a solid-state memory. Being a digital device the solid-state recorder accepts suitable signals of a digital form; analogue signals require appropriate conditioning. Solid-state recorders have a facility for putting in suitable test data in order to check the correct functioning of the equipment. The stored data in the solid-state memory has to be returned to a processing centre, which can be done with several alternative methods:

- The complete logger is returned to the processing centre for data extraction.
- A separate data storage unit is taken to the logger and data is downloaded on to the unit, the separate data storage unit is returned to the processing centre for data extraction.
- The storage device (cartridge) itself is extracted from the logger and returned, while it is replaced by an unused memory.
- Via telemetry

6.6.4 Others

Another recording device is the punched-tape recorder. This is used to record the stage measured with a float gauge. The float attached to its counterweight is geared to move two calibrated discs. At regular intervals the freely moving discs lock and the level measurement is punched in binary code on the paper tape.

7

Stage-discharge relation

7.1 Introduction

Determination of the discharge of a river by direct measurement is either laborious and time consuming or expensive. It is therefore common practice to establish a relationship (rating curve) between the stage at a particular gauging station and the discharge. A continuous record of discharge can then be obtained from a continuous record of stage. The relationship is based on the correlation between discharge and stage. This chapter deals with discharge curves at natural control sections, i.e. undisturbed reaches of a river or canal. Rating curves for structures e.g. weirs, flumes etc. can be derived from the characteristics of the structure.

7.2 Site selection

Often the use of the discharge data roughly determines the location of the gauging station. Nevertheless, one must take river properties into account in order to establish a reliable and stable relation.

If the channel is stable, relatively a few measurements may be required although very few rivers have completely stable characteristics. The calibration therefore cannot be carried out once and for all, but has to be repeated as frequently as required by the rate of change in the stage-discharge relation. In order to define the relation in sand-bed channels, for example, several discharge measurements a month might be required. In particular, surveys are required after flood flows, when not only the cross-sectional area might have changed, but even the course of the river. This indicates that selecting a stable site e.g. on rock bottom and between rock outcrops is preferred. A stable section where the stage-discharge relation does not change with time is called permanent. When it does change with time it is referred to as a shifting control. Furthermore, a stage-discharge relationship has to be as unique as possible. Therefore, e.g. a varying backwater curve from downstream effects has to be avoided. This might be the case when downstream of the gauging station a tributary with variable flow confluent with the main river (see section 7.4). In this respect a control section upstream of a waterfall or rapids, where critical flow occurs, is preferred.

Ideally, the site is selected at a location where the flow is uniform. A guideline is to select a 100m straight reach, with little turbulence, in such a way that the stage is representative for the entire section. This is in contrast, e.g., to a section where the channel bends. In a uniform flow section also the discharge can be established with larger accuracy, as the velocity profile will be according to expectations.

7.3 Composition of Rating curves

A rating curve gives the relation between discharges and gauge readings (also referred to as stages or water level readings) in a certain cross section of a river at a fixed geographical location (gauging station). The rating curve can be approximated by the formula:

$$Q = a (h - h_0)^b \quad (7.1)$$

With:

- Q discharge (m^3/s)
- h stage reading (m)
- h_0 stage reading at zero flow (m)
- a coefficient (m^2/s)
- b coefficient (-)

For a channel control this equation is compatible with the Chézy formula, where the cross sectional area A and the hydraulic radius R are functions of $(h-h_0)$. Assuming a wide river, where approximately $A=B*(h-h_0)$ and $R=(h-h_0)$ applies to, it can be shown that:

$$Q = CB (h - h_0)^{3/2} i_b^{1/2} \quad (7.2)$$

With:

- i_b slope of the energy level (-)
- C the Chézy roughness ($\text{m}^{1/2}/\text{s}$)

The coefficient b has a value of 1.59 in a rectangular channel, a value of 1.69 in a trapezoidal channel with side slopes 1:1 and a value of 2.67 in a triangular channel. When the coefficients a and b are fixed, plotting Q against $(h-h_0)$ produces a straight line on double logarithmic paper, as can be seen from the transformed equation of the rating curve:

$$\log(Q) = \log(a) + b \log(h - h_0) \quad (7.3)$$

In reality a cross section of a river bed is a composite of sections. Consequently, a rating curve on double logarithmic paper also can be a composite of several straight lines, each with its own values for a and b . Often one distinguishes between conditions under normal flow and bankfull flow. In rivers with movable beds, h_0 fluctuates considerably and therefore should be updated regularly, preferably after each significant flood.

Applying linear regression is a suitable way to obtain the coefficients a and b . Then the logarithmic values of the discharge and the corresponding observed water depth above zero flow

$(h - h_0)$ are plotted. A first estimate of the stage at zero flow, h_0 , can be obtained by plotting non-transformed values of discharge Q against stage h . It is possible to try to get a better fit by slightly changing h_0 . The best fit will have the highest correlation coefficient.

Example: Composition of rating curve at Boane 1991/1992

During the hydrological year 1991/92, twenty-four discharge measurements were carried out at 'Boane' station in the Umbuluzi River in Mozambique. The results have been plotted in Figure 7.1.

Drawing a regression line through the values of lower discharges reveals a first estimate of $h_0=0.8\text{m}$. Plotting $\log(Q)$ against $\log(h-0.8)$, with $h_0=0.8\text{m}$ results in a correlation coefficient $r^2=0.9467$, see Figure 7.2 (left). By trial and error this was improved till $h_0=0.5\text{m}$ with $r^2=0.9547$, see Figure 7.2 (right).

In general, sufficient measurements with low or moderate flow are available, but little from flood events. However, to a large extent these extreme events define the rating curve. Therefore the results of historic discharge measurements at high flows can be added.

When plotting all the values in one graph, Figure 7.3 (left), it can be concluded that the rating curve could be better represented by a composite of two lines, Figure 7.3 (right). The profile of the cross section (not provided) hints that floodplains start to be inundated at $h=4.5\text{m}$. Therefore, the inflection point can be selected at $h=4.5\text{m}$, or $\log(h-h_0)=0.602$.

Tab. 7.1: Discharge and waterlevel data at Boane

Discharge measurements 1991/92				Discharges Historic floods					
H	Q	H	Q	Date	H	Q	Date	H	Q
1.47	7.652	1.67	12.338	18-feb-75	7.38	513.44	26-feb-75	4.18	71.934
4.67	88.339	1.37	8.175	11-feb-77	6.77	485.986	10-feb-55	3.63	70.95
3.35	35.599	1.77	14.857	22-mrt-72	6.66	355.859	9-feb-55	3.96	69.743
2.77	27.45	1.79	15.879	22-dec-73	6.76	328.384	25-feb-55	3.45	57.52
2.43	23.536	1.4	6.539	13-feb-85	3.95	316	16-mrt-78	3.61	47.497
2.28	26.916	1.28	6.617	1-feb-74	5.9	244.743	28-nov-69	3.67	46.111
3.16	37.279	1.33	7.231	6-dec-89	4.74	208	12-dec-69	3.5	45.574
2.49	26.302	1.22	5.344	21-feb-67	5.72	207.928	12-jan-78	3.5	45.218
1.69	10.865	1.2	4.853	10-jan-66	5.05	189.027	26-feb-55	3.18	44.656
1.64	12.505	1.08	3.931	28-feb-67	5.48	169.81	14-jan-72	3.79	44.637
1.44	8.7	1.1	5.479	6-feb-55	5.28	168.15	3-jan-74	3.38	39.462
1.43	8.383	2.8	62.297	4-feb-55	4.73	146.396	21-feb-55	3.05	34.938
				15-feb-55	4.7	137.749	12-jan-55	2.02	30.728
				28-dec-73	4.65	137.482	5-feb-58	2.2	30.022
				12-feb-55	4.37	121.037	15-apr-55	2.21	27.756
				8-feb-55	4.5	118.335	22-nov-76	2.88	27.488
				18-dec-80	4.61	109	17-mrt-81	2.77	27.45
				3-mrt-75	4.72	105.974	27-mrt-81	2.28	26.916
				10-feb-81	4.67	88.339	8-jan-59	1.92	26.797
				18-feb-67	4.67	79.589	3-apr-81	2.49	26.302
				21-okt-69	4.73	77.608			

The coefficients of the regression lines for the logarithmic transformation of the rating curve and the exponential rating curve are summarized below (Table 7.2).

Hence the rating curve reads:

For $h < 0.5\text{m}$

$$Q = 0 \quad (7.4)$$

For $0.5\text{m} < h < 4.5\text{m}$

$$Q = 9.7297 (h - 0.5)^{1.5952} \quad (7.5)$$

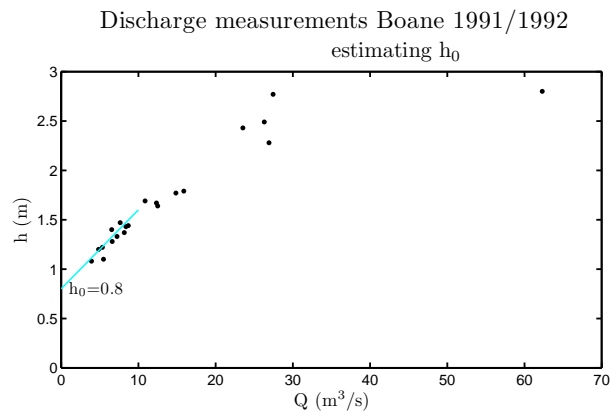


Fig. 7.1: Discharges and waterlevels Boane 1991/1992

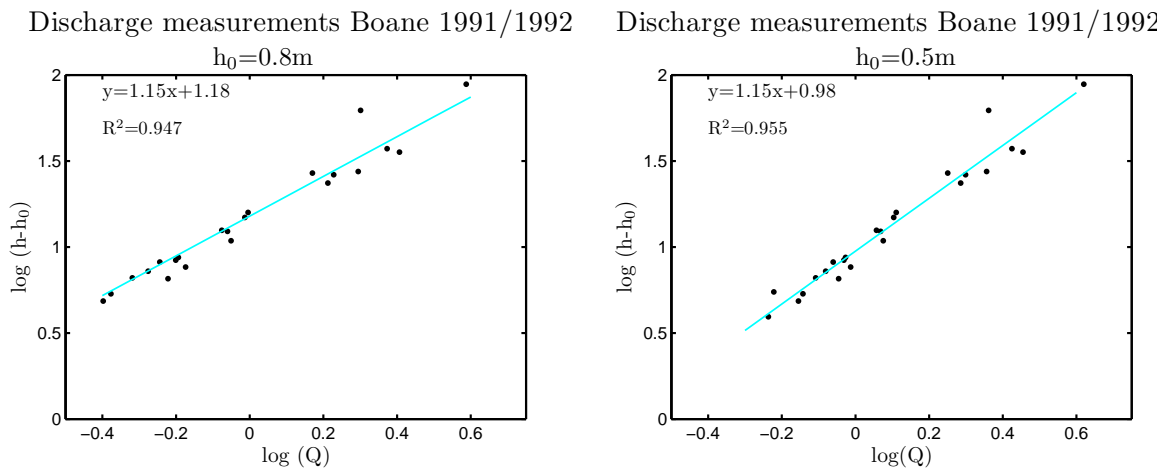
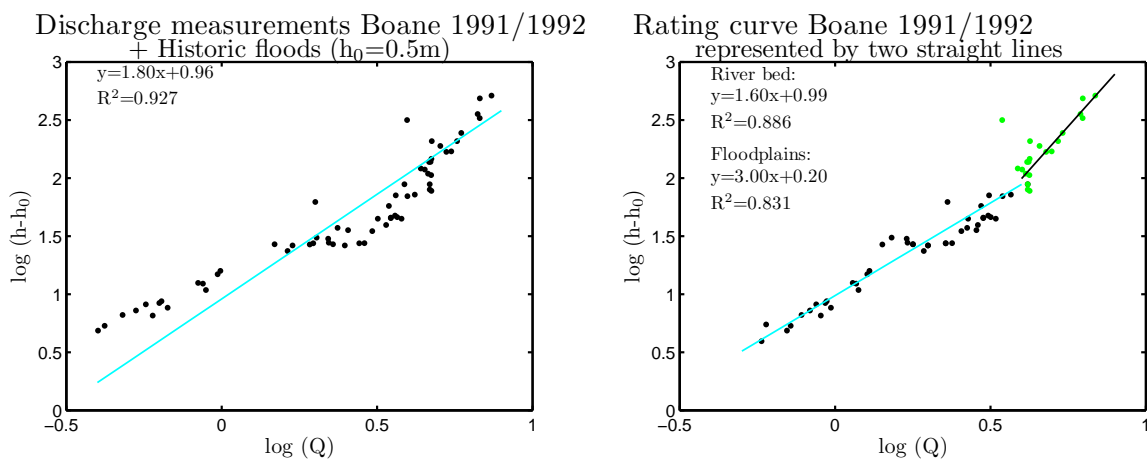
Fig. 7.2: Determining h_0 

Fig. 7.3: Constructing rating curve

Tab. 7.2: Coefficients of the regression lines for logarithmic transformation

	$0.5\text{m} < h < 4.5\text{m}$	$h > 4.5\text{m}$
$\log(a)$	0.9881	0.1958
A	9.7297	1.5696
B	1.5952	2.9987
h_0	0.5	0.5

and for $h > 4.5\text{m}$

$$Q = 1.5696 (h - 0.5)^{2.9987} \quad (7.6)$$

The stage discharge relation on linear scales is depicted in Figure 7.4

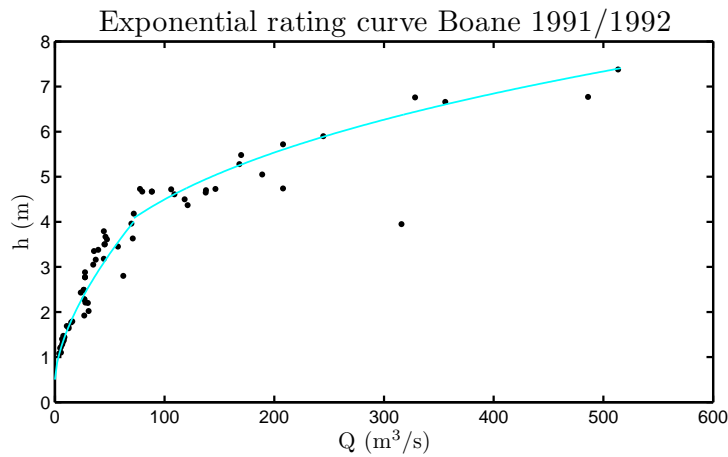


Fig. 7.4: Rating curve Boane

7.3.1 Rating Curve Accuracy

Composition of a confidence level

Through linear regression a line as a relation between two variables, y and x can be composed. The line can be used to estimate values of \hat{y} for x values that were not measured. Then the question arises how accurate the estimated values of \hat{y} are. The estimated value \tilde{y} (Eq. 7.7) is a stochastic variable as a and b are stochastic variables as well. The value of a and b follows from the linear regression theory and are shown in Equation 7.8

$$\tilde{y} = a + b(x - \bar{x}) \quad (7.7)$$

$$a = \frac{1}{n} \sum y_i \quad \text{and} \quad b = \frac{\sum y_i(x - x_i)}{\sum (x_i - \bar{x})^2} \quad (7.8)$$

With:

- x_i, y_i pairs of measured variables
- n number of measured pairs

Under assumption of a normal distribution for \hat{y} with every x , a and b are normal distributions with a standard deviation for a of s_a (Eq. 7.9) and a standard deviation for b s_b (Eq. 7.9).

$$s_a = \frac{\sigma_\epsilon}{\sqrt{n}} \quad \text{and} \quad s_b = \frac{\sigma_\epsilon}{\sqrt{\sum (x_i - \bar{x})^2}} \quad (7.9)$$

Note that σ_ϵ is derived from the differences between the estimated and the measured values of y through:

$$\sigma_\epsilon = \sqrt{\frac{\sum (y_i - a - b(x_i - \bar{x}))^2}{n - 2}} \quad (7.10)$$

For normal distributions and independent variables, it holds in general that when $y = a_1x_1 + a_2x_2 + \dots + a_nx_n$

$$s_y = \sqrt{a_1^2\sigma^2(x_2) + \dots + a_n^2\sigma^2(x_n)} \quad (7.11)$$

Under the assumption that a and b are independent and normal distributed, follows that

$$s_y = \sigma_\epsilon \sqrt{\frac{1}{n} + \frac{(x - \bar{x})^2}{\sum (x_i - \bar{x})^2}} \quad (7.12)$$

Notice that s_y has become a function of x .

The 95% confidence interval for a particular estimate of \hat{y} becomes: $\tilde{y} - t_{0.975}^{n-2} s_y < \tilde{y} < \tilde{y} + t_{0.975}^{n-2} s_y$ and hence is a function of x as well.

Confidence lines for rating curves

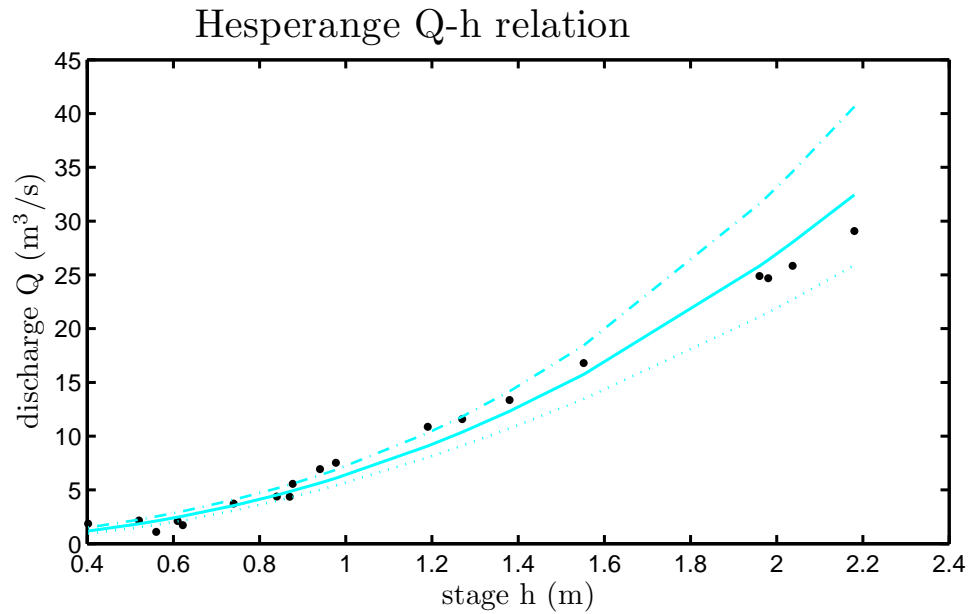
As earlier presented rating curves can be approximated by Equation 7.1. Confidence lines can be defined on the basis of a linear regression. Therefore the rating relation is linearized through a logarithmic transformation (Eq. 7.3).

The procedure as described in the previous chapter is now performed on the values of the logarithms of discharge and stage with $x = \log(h - h_0)$ and $y = \log(Q)$. The confidence interval for each estimated value $\hat{y} = \log(Q)$ is obtained through this procedure. The confidence interval of a particular Q is obtained through the inverse function of the logarithm as follows.

$$10^{\tilde{y} - t_{0.975}^{n-2} s_y} < Q < 10^{\tilde{y} + t_{0.975}^{n-2} s_y} \quad (7.13)$$

Example: Confidence lines for a rating curve

On the basis of discharge measurements a rating curve was established for the Alzette river at Hesperange (Luxembourg). Discharge measurements, stage and results of calculation are provided in the table. Linear regression on the logarithm of discharge Q and logarithm of stage $h - h_0$ gave an optimum correlation for $h_0 = -15\text{cm}$. For the Q - h Relation, please refer to Figure 7.5.



b	-0,94	n	19,00
log(a)	2,30	$t_{0,975}^{n-2}$	2,09
h_0	-15	σ_ε	0,1075
log(h-h ₀) _{avg}	2,0683		

Date	h	Q	x=log(h-h ₀)	y=log(Q)	y=log(Q)	Q	Q _{min}	Q _{max}
	[cm]	[l/s]		measured	estimated	estimated	minimum	maximum
95% confidence limit								
1-10-1981	40,2	1861	1,74	3,27	3,07	1179,50	927,65	1499,73
27-4-1982	52	2159	1,83	3,33	3,27	1842,17	1515,46	2239,30
15-7-1982	56	1090	1,85	3,04	3,32	2105,16	1753,65	2527,14
26-10-1982	61	2112	1,88	3,32	3,39	2462,09	2079,73	2914,75
15-9-1981	62,2	1715	1,89	3,23	3,41	2552,48	2162,70	3012,51
19-11-1981	74	3729	1,95	3,57	3,55	3541,00	3075,29	4077,25
13-1-1983	84	4382	2,00	3,64	3,66	4524,34	3982,71	5139,63
20-4-1983	87	4372	2,01	3,64	3,69	4846,10	4277,84	5489,84
28-10-1981	87,7	5562	2,01	3,75	3,69	4922,98	4348,18	5573,77
12-10-1982	94	6926	2,04	3,84	3,75	5645,90	5005,63	6368,08
13-10-1981	97,7	7519	2,05	3,88	3,79	6096,74	5411,66	6868,55
21-10-1981	119	10875	2,13	4,04	3,96	9080,69	8017,19	10285,27
1-12-1981	127	11580	2,15	4,06	4,02	10377,11	9109,00	11821,76
12-4-1983	138	13357	2,18	4,13	4,09	12321,08	10709,63	14175,01
1-12-1981	155,2	16791	2,23	4,23	4,20	15744,55	13444,77	18437,72
28-1-1988	196	24894	2,32	4,40	4,41	25816,87	21088,30	31605,73
15-10-1981	198	24685	2,33	4,39	4,42	26383,52	21505,35	32368,25
16-10-1981	203,7	25840	2,34	4,41	4,45	28036,77	22715,83	34604,09
16-10-1981	218	29075	2,37	4,46	4,51	32436,42	25895,70	40629,19

Fig. 7.5: Hesperange Q-h relation with the 95% confidence limits indicated

7.4 Non-steady and non-uniform flow

The effect of non-steady and non-uniform flow on the stage-discharge curve will be discussed in this paragraph. Examples of hydraulic conditions with non-steady and/or non-uniform flow which have an effect on the uniqueness of a rating curve:

- Scour and fill in an unstable channel
- Growth and decay of aquatic (weed) growth
- Formation of ice on the river
- Variable backwater in a uniform channel
- Rapidly changing discharge (for example when flood wave occurs)

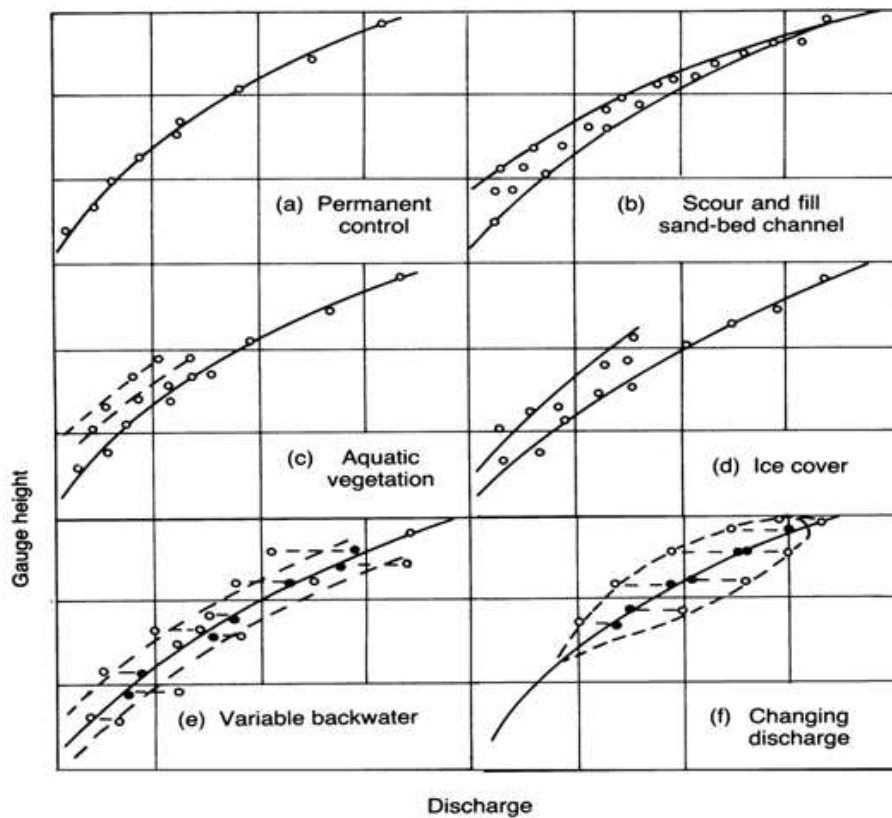


Fig. 7.6: Stage-discharge relation for different hydraulic conditions

Corresponding stage-discharge curves for the above hydraulic conditions are given in Figure 7.6, a brief discussion of each follows.

Permanent control (Fig. 7.6a)

A control is permanent if the stage-discharge relation it defines does not change with time. The relation can be defined as a simple exponential relation.

Sand-bed channel (Fig. 7.6b)

The movement of fluvial sediment affects the conveyance, the hydraulic roughness, the channel sinuosity and the energy slope. This makes the determination of a stage discharge relation difficult.

Aquatic vegetation (Fig. 7.6c)

The growth of weed decreases the conveyance of the channel and changes the roughness with result that the stage for a given discharge is increased.

Ice cover (Fig. 7.6d)

Ice in the measuring section increases the hydraulic radius and the roughness and decreases the cross sectional area. The stage for a given discharge is increased.

Variable backwater (Fig. 7.6e)

If the control reach for a gauging station has within it a weir or a dam, a diversion or a confluent tributary which can increase or decrease the energy gradient for a given discharge, variable backwater is produced.

Rapidly changing discharge (Fig. 7.6f)

At some stations, generally those of low energy slope, the stage discharge relation is affected by the rate of change of the discharge. If the discharge is increasing rapidly, it will be greater than that for zero rate of change and, conversely, if it is rapidly decreasing it will be less..

The consequences of a flood wave and backwater on the rating curve will further be discussed in the remainder of this paragraph.

7.4.1 The flood wave

The 1-dimensional equation of momentum (the width assumed to be constant) is called the Saint Venant equation and consists of:

$$\frac{\partial u}{\partial t} + u \frac{\partial u}{\partial x} + g \frac{\partial h}{\partial x} = g i_b - \frac{gq|q|}{C^2 h^3} \quad (7.14)$$

For floods in rivers that last at least a day $\partial u/\partial t$ and $\partial u/\partial x$ are relatively small compared to the other terms; when $\partial u/\partial t$ and $\partial u/\partial x$ are neglected, the Saint Venant equation turns into:

$$\frac{\partial h}{\partial x} = i_b - \frac{q|q|}{C^2 h^3} \quad (7.15)$$

Equation 7.15 rewritten gives:

$$q = C h^{3/2} \sqrt{i_b - \partial h/\partial x} \quad (7.16)$$

This is the famous Chézy equation for steady and uniform flow in a river with slope i_b , but with the term $\partial h/\partial x$ added to compensate for the surface slope as a consequence of the flood wave.

As we are rather interested in the relation of q and h at a fixed location the term $\partial h/\partial x$ can be transformed into $\partial h/\partial t$ by locally applying the kinematic wave equation (locally applying the kinematic wave equation is nothing more than assuming a none distorting wave):

$$\frac{\partial h}{\partial t} + c \frac{\partial h}{\partial x} = 0 \quad (7.17)$$

With:

$c = dq/dh$, being the velocity of the flood wave

Combining Equation 7.16 and 7.17 gives the Jones equation (see for instance Henderson [1963]).

$$q = q_e \sqrt{1 + \frac{1}{c i_b} \frac{\partial h}{\partial t}} \quad (7.18)$$

With:

$$q_e = C h^{3/2} i_b^{1/2} \quad (7.19)$$

As a result of the non-steady character ($\partial h/\partial t \neq 0$) an error $q = q - q_e$ has been made. First order Taylor applied on Equation 7.18 gives an impression of the relative error q/q_e :

$$\frac{\delta q}{q_e} = \frac{1}{2} \left(\frac{1}{c \cdot i_b} \right) \frac{\partial h}{\partial t} \quad (7.20)$$

When $c \approx \frac{3}{2}u$ Equation 7.20 becomes ($c \approx \frac{3}{2}u$ is the case when the channel is rectangular of shape):

$$\frac{\delta q}{q_e} = \frac{1}{3} \left(\frac{1}{u \cdot i_b} \right) \frac{\partial h}{\partial t} \quad (7.21)$$

If during the occurrence of a high water wave the discharge is being determined from a stage-discharge curve with steady flow, applies

- In the front of the wave ($\partial h/\partial t > 0$) the discharge q is bigger then the discharge obtained from the stage-discharge curve (see Fig. 7.7).
- In the rear of the wave ($\partial h/\partial t < 0$) the discharge q is smaller then the discharge obtained from the stage-discharge curve (see Fig. 7.7).

This would give the opportunity to correct the measured discharge for a discharge under steady flow (q_e) and hence plot the proper values on the stage-discharge curve.

Alternatively the Jones formula is used to obtain the real discharge on basis of the stage-discharge curve for steady flow. In that case one has to establish the rate of change of the stage in time ($\partial h/\partial t$), e.g. by observing the stage as a function of time.

7.4.2 Backwater curves

In this section an example will be given of the influence of backwater, caused by a downstream tributary, on the discharge in a river, see Figure 7.8.

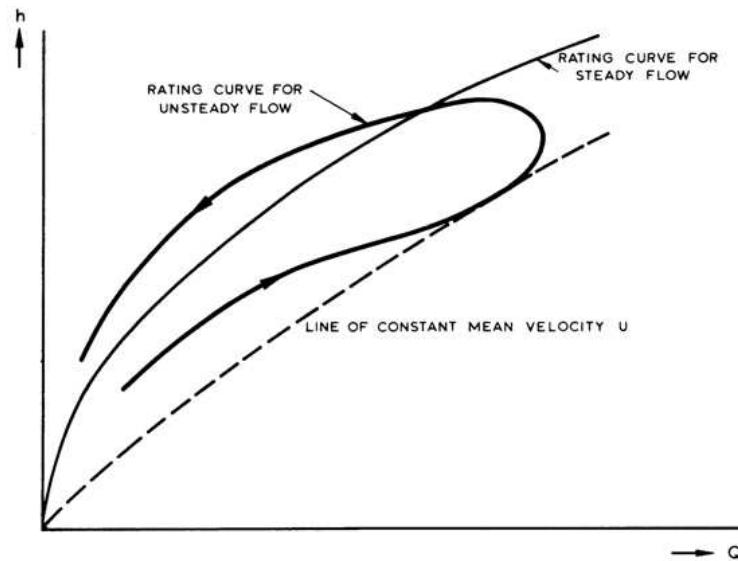


Fig. 7.7: Loop in rating curve for flood wave

For known river properties (B , i_b and C) there is an equilibrium depth h_e that can be derived from the Chézy equation:

$$h_e = \sqrt[3]{\frac{Q^2}{C^2 i_b B^2}} \quad (7.22)$$

At the point of confluence, the equilibrium depth according to the properties and discharge of the joint rivers is valid. In general, this is not the equilibrium depth of each of the two branches. This disturbance propagates upstream in each of the two branches only a certain distance L from the confluence. The effect slowly fades out and can be described by the equation of a backwater curve.

In Figure 7.8 a river is depicted with a confluence at $x = 0$. It is questioned whether the variable discharge ΔQ from the tributary through backwater will affect the stage at $x = L$.

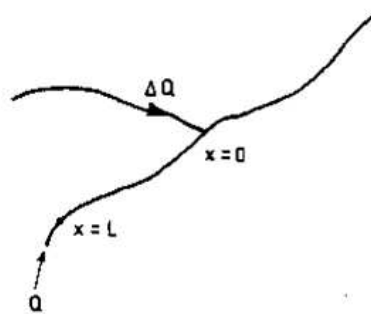


Fig. 7.8: River and tributary

The general equation for a backwater curve can be presented as:

$$\frac{\partial h}{\partial x} = i_b \frac{h^3 - h_e^3}{h^3 - h_c^3} \quad (7.23)$$

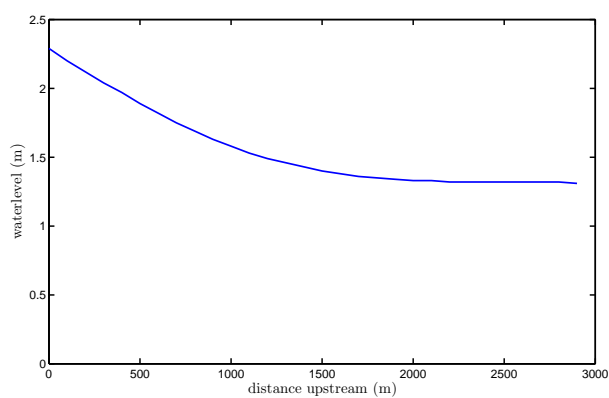
With:

$$h_e = \left(\frac{Q|Q|}{C^2 B^2 i_b} \right)^{1/3} \quad \text{and} \quad h_c = \left(\frac{Q^2}{g B_s^2} \right)^{1/3} \quad (7.24)$$

- h water depth (m)
- h_e stationary flow depth (m)
- h_c critical flow depth (m)
- i_b bottom slope (-)
- Q discharge (m³/s)
- C Chezy roughness coefficient (m^{1/2}/s)
- B width of a river (m)
- x distance in upstream direction (m)

At the point of a river confluence, assuming there are no further obstructions downstream, the water level h_0 is according to the stationary flow in the downstream part. The water level h_0 is usually above h_e for each of the individual branches. As a consequence, a backwater curve can occur in each of the branches. The point is that in the region of these backwater curves the relation between discharge Q and waterlevel h is not uniquely defined. It is affected by the discharge in the other branch.

A gauging station in the tributaries is best located out of the influence of the backwater curve. This should be based on the range of discharge combinations of the tributaries for which the rating discharge relations will be applied.



		SMALL TRIBUTARY	LARGE TRIBUTARY	JOINT RIVER
Discharge	Q	2	33	35
Width	B	4	30	30
Chezy	C	20	20	20
Bottom Slope	ib	0,001	0,001	0,001
Critical depth	hc	0,29	0,50	0,52
Equilibrium depth	he	0,86	1,45	1,50

Fig. 7.9: Backwater curve for a small tributary

Streamflow measurements

8.1 Introduction

Streamflow measurement is a way to obtain information about the discharge of a river; various methods can be applied. Often it is hard to measure discharge itself and therefore it is derived from measuring other parameters. Examples are: combining measurements of velocity and cross-sectional area into discharge, changes in electro-magnetic properties of the stream as a function of discharge, or change in concentration of a substance that is released into the stream.

Good water management is founded on reliable streamflow information and the final reliability of the information depends on the initial field measurements. The hydrologist making these measurements has therefore the responsibility of ensuring that raw data of acceptable quality is collected. The successful processing and publication of the data depend largely on the quality of the field measurements.

There are many different uses of streamflow data within the broad context of water management, such as water supply, pollution control, irrigation, flood control, energy generation and industrial water use. The importance placed on any one of these purposes may vary from country to country. In India and China, for example, emphasis may be placed upon irrigation and flood control whereas in the United Kingdom water supply may be given priority; the emphasis for anyone may also change over short or longer periods of time. Basically the streamflow data is either required as infinite integration over time (= runoff) or as instantaneous values for e.g. design purposes.

Continuous measurements of streamflow are often derived from continuous stage measurements, as stage is easier to measure than flow. The streamflow in that case is obtained through a stage discharge relationship (=the rating curve) based on occasional measurements. Nevertheless some methods exist which under specific condition are capable of continuously measuring streamflow. Various ways exist to measure discharge instantaneously. Both, continuous measurements and instantaneous measurements will be discussed in this chapter.

8.2 Velocity Area Method

8.2.1 Principles

The velocity area method is a method to obtain a near instantaneous value of the discharge of a river. The discharge Q of a river is being measured by means of measuring velocities (u_i), representative for the part A_i of the area (A), in a suitable cross-section. The method of approach is:

$$Q = \int^A u dA \approx \sum^n u_i \cdot \Delta A_i \quad (8.1)$$

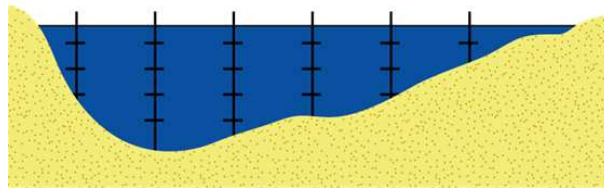


Fig. 8.1: Example 'velocity-area-method'

A common approach is to select a number of verticals within the cross-section. In each of these verticals the velocity is being measured at a pre-determined depth (see Fig. 8.1). There are various methods to determine the discharge from the measured geometry and velocity measurements. It should be realized that the cross-sections are usually more stretched ($B \gg h$) than shown in Figure 8.1. An elaborate study in ISO-connection has shown that it is preferred to have many verticals in the cross-section rather than many measuring points in each vertical. This goes for regular velocity profiles, not for tidal rivers, even if no density flows occur in the tidal river. For a tidal river, the time interval during which one vertical is being measured is not negligible compared to the tide period. In this case options are:

- When no density flows occur the moving-boat method with flow at a fixed depth could be applied (see subsection 8.2.6)
- When density flows do occur the moving-boat method with an acoustic doppler flow instrument (ADCP), applying measurement over the vertical, could be applied (see subsection 8.2.3)
- Use of a reference vertical. By means of elaborate measuring, a correlation between the velocity in the vertical and the mean velocity in the whole cross-section is established.

An example of using the reference vertical method

For the Mekong River the secretariat of the Interim Mekong committee has worked out the reference vertical method (referred to as 'the velocity index method') for a couple of cross-sections. In Figure 8.2 an example is given of the correlation between the mean velocity in the index vertical (= reference vertical) and the mean velocity in the cross-section.

In this case the choice of measuring method has a political background. The Mekong is a border river between Thailand and Laos. A measurement over the whole cross-section, approved by both countries, requires a lot of diplomatic preparations. The data obtained by measurements over the whole cross-section are being used to make routine measurements possible without having to cross the border. Given the fact that the Mekong secretariat is established in Bangkok, it is not a surprise that the reference vertical in Figure 8.2 is situated in Thailand. Nonetheless, it is still necessary to check the validity of the correlation from time to time. After all, morphological changes in the considered reach can occur.

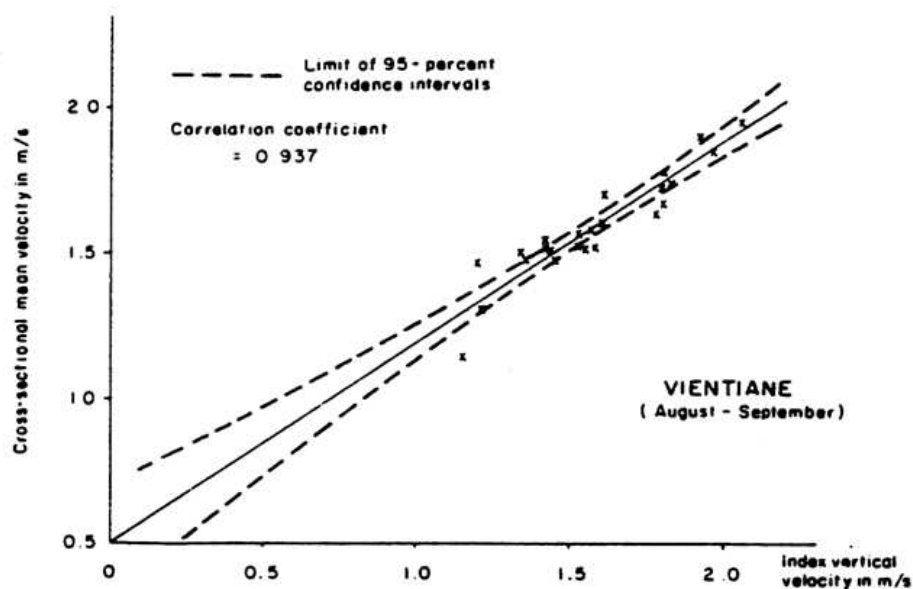


Fig. 8.2: The use of reference vertical by Vientiane

In general three main sources of errors associated with the velocity area method, as depicted in Figure 8.1, can be distinguished. Assumed is the use of a propeller current meter (OTT) to determine the velocities.

Error I: The error in the determination of the velocity u_i . This error is small when for more than a minute the velocity is being measured.

Error II: The error as a result of the limited number of measuring points in a vertical. The local discharge per unit width holds an error.

Error III: The error as a result of the limited number of verticals. This gives a great contribution to the error made in the discharge as a result in the approach of the integral given in Equation 8.1.

Elaborate measurements of various rivers have been analyzed. In Figure 8.3 and 8.4 the results are summarized.

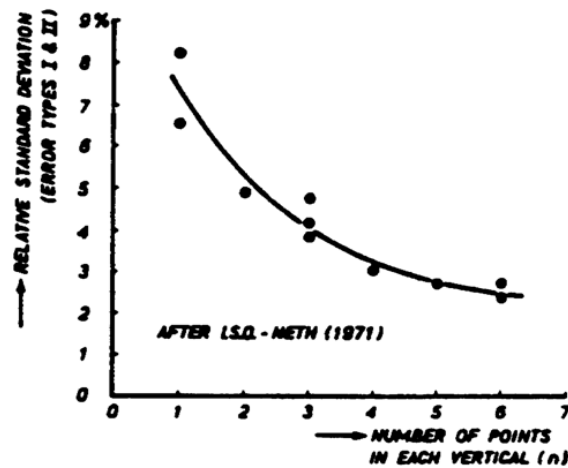


Fig. 8.3: Influence number of points in the vertical

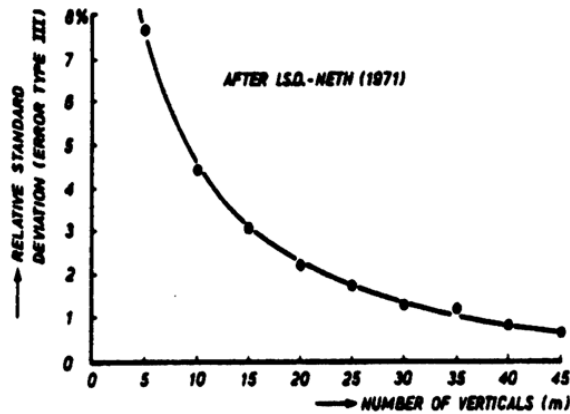


Fig. 8.4: Influence number of verticals in the cross-section

Notes

- The results as depicted in Figure 8.4 depend on the applied interval between the verticals. The easiest way is to choose the distance between the verticals equally. More accurate is to choose the distance between the verticals in such a way that every vertical equally contributes to Q , hence $Q(y) = q(y)\Delta y$ is constant.
- Especially for small watercourses it is usual to limit the number of measuring points in the vertical.
 - Three point measurement (measured away from the water surface):

$$\bar{u} = \frac{1}{3}(u_{0.2} + u_{0.6} + u_{0.8}) \quad (8.2)$$

or

$$\bar{u} = \frac{1}{4}(u_{0.2} + 2u_{0.6} + u_{0.8}) \quad (8.3)$$

- One point measurement: Measured velocity on half of the water depth multiplied by 0.95.
3. In watercourses with high velocities it is often difficult to measure below the water surface. Thus the mean velocity in a vertical can not be determined accurately. It is therefore advisable to multiply the measured velocities at the surface by a factor 0.84 à 0.90 to obtain the mean velocity in the vertical.

8.2.2 Site selection

As discharge potentially varies along the reach of a river or canal the location is generally defined by the site where the discharge is required. Nevertheless, on a smaller scale the variation of discharge might well be negligible. In that case a reach or cross section is preferred having the following characteristics.

- A straight reach with the threads of velocity parallel to each other.
- A stable streambed free of large rocks, weeds or other obstacles that create turbulence
- A flat streambed profile to eliminate vertical components of velocity.

8.2.3 Instruments to measure point velocity

The velocity area method uses point information of flow velocity in the considered cross-section. Various instruments have been designed to obtain these velocities. The following instruments will be discussed:

- Pendulum
- Cub current meter
- Propeller current meter
- Electromagnetic current meter
- Doppler current meter
- Float

The pendulum

The pendulum current meter, developed by the Delft Hydraulics Laboratory, consists of a resistance body suspended on a cable. When lowered in flowing water the 'pendulum' experiences a horizontal force due to the flow pressure. This causes the suspension cable to deviate from the vertical and the magnitude of the deviation is a measure of the flow velocity at the location of the pendulum. The velocity is measured, by means of the resistance force being a function of the velocity, namely

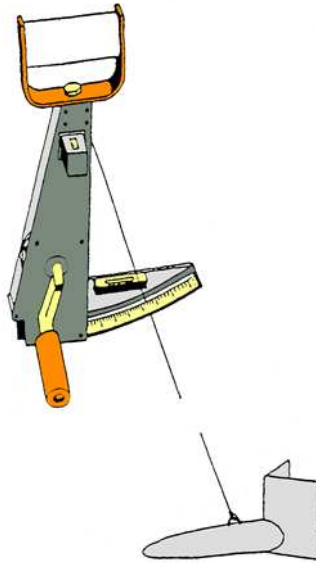


Fig. 8.5: Pendulum

$$F_N = C_N * \frac{1}{2} \rho u^2 A \quad (8.4)$$

The structure for suspending the resistance body can be fixed to a rail of a boat, the parapet of a bridge, to a trolley, or can be held by hand in the case of the smaller types. Generally, the cable to which the body is attached can be reeled by a winch provided with an indicator showing the length of cable released. Obviously the bending of the submerged part of the cable due to flow pressure has to be taken into account. At every measuring point, the resistance body should be given time to become adjusted to the flow before the reading is taken. The instrument will also facilitate reading of the flow direction with respect to a fixed orientation in the horizontal plane. This may be of importance when the flow direction changes with depth. To cover a wide velocity range, the pendulum current-meter is provided with a series of resistance bodies. By a careful choice of body, velocities ranging from 0.05m/s to 3.5m/s can be measured. The choice of resistance bodies should be such that the readings can be made with maximum accuracy. To this end, the angle with the vertical should not become too small and it may sometimes be necessary to change resistance bodies during a series of measurements in the vertical.

In order to determine velocities and corresponding depths from the field data, a number of diagrams are needed. They are based on the equation:

$$\bar{u}^2 = \text{coefficient} * \tan(\phi_{body}) \quad (8.5)$$

The coefficient as well as the correction for bending of the submerged part of the cable depends on the characteristics of the resistance bodies, the drag coefficient and the diameter of the cable. They have to be determined by calibration. The manufacturer of the instruments usually supplies the diagrams.

Cub- and propeller- type current meters

Both cub- and propeller- types of current meters have the same basic principle, which is the proportionality between the local flow velocity and the resulting angular velocity of the rotor of the instrument. An electrical circuit closed intermittently by contact points measures the number of the revolutions of the rotor. The interruptions are transmitted to an acoustic or electric counter.

The cub current meter can be held in the stream either by a rigid rod or by suspension from a cable. Rigid rod suspension enables placement of the meter at exactly the required point of measurement. In deep streams, however, cable suspension has to be used. A suitably shaped counterweight is then attached to ensure that the cable deviates from the vertical as little as possible. The counterweights must be interchangeable so they can be adapted to the flow velocity. They vary from 25 kg where flow velocities are lower than 1 m/s to 100 kg for flow velocities exceeding 1.5m/s.

Calibration of these types of current meters is carried out by experimental determination of the curves representing the relationship between the velocity of flow and the propeller or rotor speed, usually expressed in revolutions per second. Current meters may be calibrated individually or a group rating may be supplied by the manufacturer for a particular type of meter. A calibration curve, a formula, or a rating table is supplied by the manufacturer and the actual limits of validity are also indicated. Usually a current meter is calibrated by moving the complete current meter, at accurately known speeds, through stagnant water in a flume of adequate dimensions. Although it remains questionable whether this is identical with the reverse situation where the water moves and the meter is at rest, this method of calibration is generally accepted.

Cub current meter The cub current meter has a vertical axis; attached to the axis are a number of cubs. The water flows into one cub pushing the cub backward and thus turning the axis round. Now the opening of another cub is pointing towards the side from which the water is flowing, the water flows into this cub pushing this cub backward turning the axis further round. The rotors of the cubs are replaceable in the field without affecting the rating. The cub current meter operates at lower velocities than the propeller-type meter. A single rotor serves for the entire range of velocities. Due to its shape, a cub current meter should not move in a vertical direction during the measurements, because the flow at a cub can be disturbed by the turbulence from the other cubs. Therefore, this type cannot be used for an integration method. Compared to the propeller current meter (see below) the cub current meter is more sensitive to vertical components in the velocity and to the bobbling of a boat.

Propeller current meter The propeller current meter (OTT) has a horizontal axis to which a propeller is attached. The flow makes the propeller turn and thus the axis. The propeller is less likely to become entangled with debris than the cub current meter. Propeller current meters are not so susceptible to vertical currents as cub current meters and therefore give better results when used for measurements from boats.



Fig. 8.6: Cub current meter

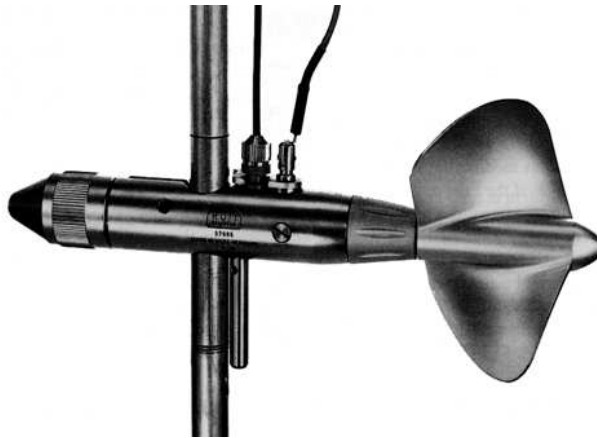


Fig. 8.7: Propellor current meter

Electromagnetic current meter

The electromagnetic current meter employs the Faraday principle of electromagnetic induction whereby a magnetic field (in the velocity sensor) induces an electropotential in a moving conductor (the water). An alternating current is passed through a coil in the velocity probe, which in turn sets up an alternating field in the probe head and surrounding water. Movement of water past the probe causes an electric potential in the water, which is detected by two electrodes in the probe. This potential is then amplified and transmitted through the connecting cable to the display unit where the velocity signal is digitized and displayed in meters per second at preset intervals in the range 2-60 seconds as required. Maintenance of the meter is minimal and consists of keeping the velocity probe's electrodes clean at all times. Because of the principle of electromagnetic induction the meter will not operate successfully in very low conductivity solutions.



Fig. 8.8: Electromagnetic current meter

Doppler current meter

An instrument, that measures the flow velocity by means of the Doppler effect, is the Acoustic Doppler Current Profiler or ADCP. ADCP's are used to measure discharges in open channels, according to the velocity-area method. There are either downward looking ADCP's, measuring velocity profiles from near the water surface to the bed, or upward looking ADCP's, installed on the bed. An example of a downward looking installation is the vessel mounted ADCP, which is in use since the mid-1980's.

The Doppler effect is a change in the observed sound pitch that results from relative motion. Doppler shift is the changed frequency observed from a moving sound source, compared to the stagnant situation.

$$F_d = F_s \frac{v}{c} \quad (8.6)$$

With:

F_d is the Doppler shift frequency (Hz)

F_s is the frequency of the sound under stagnant condition(Hz)

v is the relative velocity between the sound source and the sound receiver (m/s)

c is the speed of sound (m/s)

ADCP's use the Doppler effect by transmitting sound at a fixed frequency and listening to echoes returning from sound scatters in the water. These sound scatters are small particles (suspended load) that reflect the sound back to the ADCP. Scatters are everywhere in rivers. They float in the water and on average they move at the same horizontal velocity as the water (Note that this is a key assumption!). Sound scatters in all directions form scatters. Most of the sound goes forward, unaffected by the scatters. The small amount that reflects back is Doppler shifted.

When sound scatters move away from the ADCP, the sound you hear is Doppler shifted to a lower frequency proportional to the relative velocity between the ADCP and the scatter. When the sound reaches the sound scatters the sound is Doppler shifted, then the sound reflects back towards the ADCP, so when it reaches the ADCP the Doppler shift is double, changing to:

$$F_d = 2F_s \frac{v}{c} \quad (8.7)$$

Finally the Doppler shift only works when sound sources and receivers get closer to or further from one another, this is radial motion. Limiting the Doppler shift to the radial component gives

$$F_d = 2F_s \frac{v}{c} \cos(A) \quad (8.8)$$

The ADCP measures only the velocity component parallel to the acoustic beams. The angle A is the angle between the beam and the direction of flow (see Fig. 8.9).

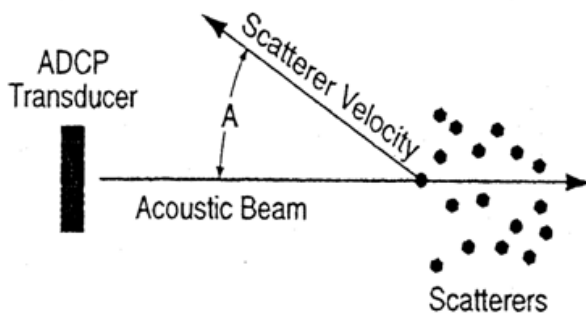


Fig. 8.9: Relative velocity vector

Acoustic Doppler Current Profiler is an accurate description of how the instrument determines flow velocities in a vertical profile:

1. Acoustic, as it uses sound waves to sense flow velocities;
2. Doppler, because it uses Doppler effect which is directly proportional to the flow velocity;
3. Current. The ADCP needs three beams to determine the three vector components of water flow. The four-beam configuration provides two vertical vectors that the ADCP uses to check data integrity;
4. Profiler. The instrument measures flow velocities in a large number of points (depth cells) in the vertical by 'range-gating' the back scattered signal in time.

The ADCP makes a velocity profile for many depth cells, which can be from 5 cm in height or more (depending on the frequency). Figure 8.10 shows a four beam configuration measuring in 14 cells. Each depth cell is comparable to a single current meter. Therefore an ADCP velocity profile is like a string of current meters uniformly spaced. Thus, we can make the following definitions by analogy:

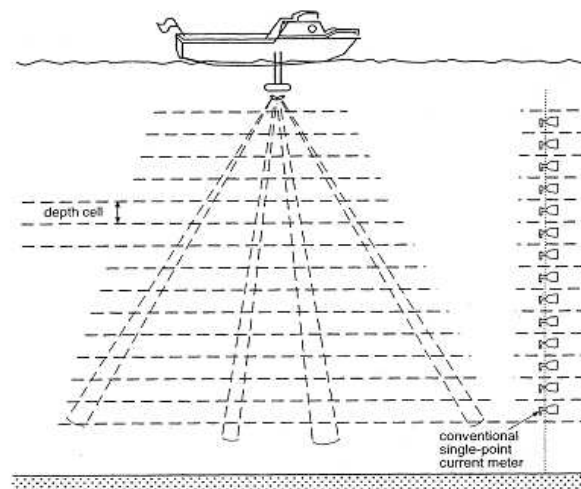


Fig. 8.10: ADCP current profiler

- Depth cell size = distance between current meters
- Number of depth cells = number of current meters

There are two important differences between the string of current meters and an ADCP velocity profile. The first difference is that the depth cells in an ADCP profile are always uniformly spaced, while current meters can be spaced at irregular intervals. The second is that the ADCP measures average velocity over the depth range of each depth cell while the current meter measures current only at one discrete point in space.

Use of the instrument The ADCP is able to determine flow-velocity magnitude and direction at selected depths in the vertical. It is also able to determine the relative location of the instrument and to measure water depths. The transducer head is normally mounted about 0.2m to 0.5m below the water surface. The transducer should be mounted to minimize pitch, roll and wave bobbling of the head. The head should also be mounted so that cavitation will not occur around the transducers. The vessel is positioned a measurable distance from the edge of the stream in the water that is deep enough for the instrument to operate. The instrument is turned on, and the vessel on which the instrument is mounted traverses the channel. Depending on the design and the software, the instrument can provide continuous values of water depth, velocity magnitude and direction and vessel position. Estimates of distances to the channel edges from the closest point at which the instrument can measure are made by the operator and entered into the program. Algorithms can be used to estimate velocities and flow in the unmeasured areas near the top, bottom and sides of the channel so that the total measured discharge in the channel is available when the traverse of the channel is complete.

The vessel on which the transducer head is mounted must be moved slowly enough during a measurement so that cavitation does not occur around the transducer head. The uncertainty of any set of velocity measurements is directly related to the speed of the vessel moving across the channel and the measurement rate of the instrument. Despite vessel speed limitations, it is

possible to obtain an accurate discharge measurement in a 200 meter-wide channel in about 5 to 10 minutes.

The vessel is not required to move in a straight line across the channel or to move perpendicular to the flow direction. It is only necessary to traverse the cross-section from one bank to the other. The instrument can be moved in a very irregular path across the channel and can finish at a point some distance upstream or downstream from the starting point. The instrument is able to compensate for these irregularities in the traverse of the channel because of its ability to determine continuously vessel position.

Measurement characteristics and limitations Some parts of the channel cross-section cannot be measured with the ADCP instrument. One area void of measurement is near the surface. The transducer head must be mounted slightly below the water surface, and there is also a minimum distance required for the instrument to respond to returned acoustic signals. This depth in which no measurements are obtained can be 0.5m or more. When the acoustic signal is transmitted, the signal produces unwanted side-lobes. Some of these side-lobes travel in a vertical direction, while the primary signal is travelling at a set angle to the vertical. The side-lobe signal, therefore, reaches the channel-bed before the primary signal. The reflected side-lobe signals thus return to the transducer from the bed before the near-bed primary signal and are much stronger than those returned from sediment particles in the water, thus overshadowing return signals from the primary signal before it completes its top-to-bottom excursion. The percentage of the depth at the bottom of the channel that cannot be measured, D_p , is therefore, approximately equal to:

$$D_p = 100(1 - \cos\phi) \quad (8.9)$$

where ϕ is the angle of the acoustic beam from the vertical.

Thus, for an angle of the acoustic beam to the vertical of 30° , approximately 13% of the depth at the bottom of the channel cannot be measured. For an angle of 20° , this decreases to about 6%.

Depths near the banks are commonly too shallow for the instrument to operate properly or for the vessel on which the instrument is mounted. Therefore, part of the flow near the banks cannot be measured, and must be estimated. In large, deep channels, unmeasured flows are relatively small. Unmeasured flows are important in small streams, however where a large percentage of the flow may have to be estimated.

Instruments are currently capable of measuring velocities in depths as shallow as about 5m. For best results, the transmitted signal frequency for shallow water should be relatively high while measurements made in deeper water should be made using lower frequencies. High-frequency (short-wavelength) transmissions provide for detailed velocity definition throughout the water column but do not penetrate as far through a water column as a low-frequency (long wavelength) transmission. Common frequencies range from 300 to 2400 kilohertz.

Velocities can be measured in depth cells as small as 0.1m. The uncertainty of the measurement increases with decreasing depths, velocities and depth cell size. Velocities as slow as 0.05m/s can be measured but the uncertainty tends to increase for these slow velocities. A number of

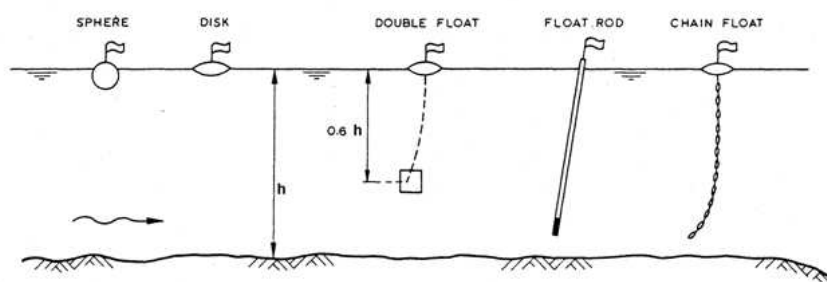


Fig. 8.11: Floats

comparisons have been made between measurements using the ADCP and measurements using vertical-axis or acoustic current-meters or ultrasonic velocity-meters. Differences generally range from about $\pm 2\%$ to about $\pm 5\%$, but this can vary depending on flow and channel conditions (Gordon [1989]).

Floats

Floats are the simplest tools for measurement of flow velocity. The time it takes the float to drift over a known distance between two previously fixed transversal lines is a measure of the flow velocity. Examples of surface floats and subsurface floats are shown in Figure 8.11.

Two disadvantages of surface floats are that they measure the flow velocity at the water surface only and that they are influenced by the wind. Better information on the mean velocity in the vertical can therefore be obtained using subsurface floats.

The various types of floats have conversion factors varying from 0.85 to 0.95; these values, for conversion of the float velocity to mean flow velocity, have been obtained by simultaneous measurements on floats and propeller current-meters. Floats in particular are of practical use for streamflow measurements during floods.

8.2.4 Current meter measurements by wading

Current meter measurements by wading are preferred if conditions permit. Wading measurements with the current meter supported on a graduated wading rod, which rests on the bed of the stream are normally more accurate than those from cableways or bridges as the operator has more control over the general gauging procedure.

A measuring tape or tag line is stretched across the river at right angles to the direction of flow; the spacing of verticals is determined by the required accuracy. The positions of successive verticals used for depth and velocity are located by horizontal measurements from a reference marker (initial point) on the bank, usually defined by a pin or a monument. The gauging starts at the water edge of the near bank, where depth and velocity may or may not be zero. At each chosen vertical the depth is measured and the value used to compute the setting or settings of the current meter depending on the method to be used (usually 0.6 or 0.2 and 0.8 depth).



Fig. 8.12: Current meter by wading

The position of the operator is important to ensure that the operator's body does not affect the flow pattern when approaching the current meter. The best position is to stand facing one of the banks, slightly downstream of the meter and an arm's length from it. The rod is kept vertical throughout the measurement with the meter parallel to the direction of flow (see Fig. 8.12).

8.2.5 Suspension systems

An alternative to wading is lowering the flow measurement equipment by means of a cable from a supporting structure. In general it can be stated that proper positioning of the equipment from a cable in vertical and horizontal direction causes much more problems than with wading. To avoid dragging of the suspended cable with the current, usually a weight is attached to the cable or current meter.

The cable with the current meter can for instance be moved by means of a cableway that crosses the river. Alternatively river crossing bridges are used to lower the measuring equipment.

Current meter measurements from cableways

Cableways are normally used when the depth of flow is too deep for wading, when wading in a swift current is considered dangerous, or when the measuring section is too wide to string a tag line or tape across it.

There are two basic types of a cableway:

1. Those with an instrument carriage controlled from the bank by means of a winch, either manually or electrically operated (Fig. 8.14);
2. Those with a manned personnel carriage, commonly known as a cable car, in which the operator travels across the stream to make the necessary observations; the car may be pulled manually across the river by means of a cable car puller, or it may be electrically operated

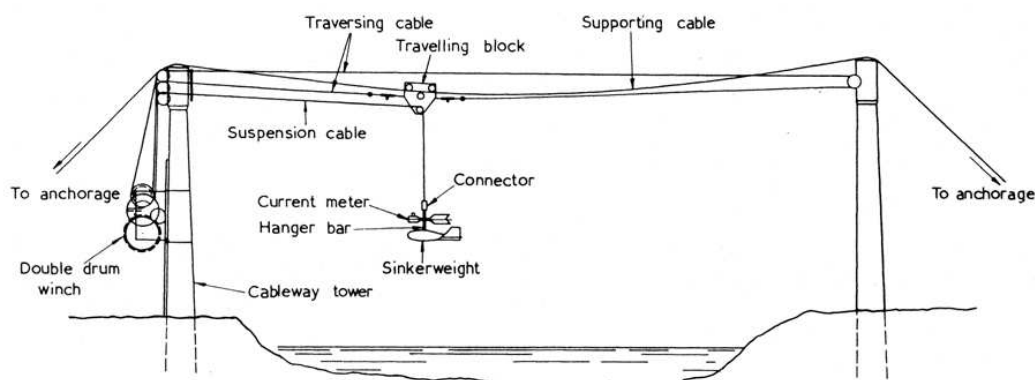


Fig. 8.13: Schematic arrangement of unmanned cableway and suspension assembly

The general gauging procedure is similar, except that in the case of the non-manned cableway the instrument carriage, suspended from the track cable, moves the current meter and sinker weight across the stream between the cable supports. The operator remains on the bank and operates the gauging winch, which is provided with both distance and depth counters for placing the current meter at the desired position. The electrical pulses from the current meter are returned through the core conductor of the suspension cable and registered on a revolution counter. The manned cableway, on the other hand, is provided with a support for a gauging reel, a guide pulley for the suspension cable, and a protractor for reading the vertical angle of the suspension cable.

Line suspension from bridges

From higher bridges and for greater depths, the current meter and weight are suspended on a cable. The cable is controlled by a gauging reel mounted on a bridge crane or on a bridgeboard (see Fig. 8.14). A handline may be used with the smaller weights. The gauging procedure is essentially the same as that for measurements from a cable car.

Sinker weights

The size of the sinker weight, attached to the current meter by means of a hanger bar, requires being sufficiently heavy to maintain the current meter suspension cable in an approximate vertical position. It is usually decided on by experience, common weights in operation vary from about 7 to 150 kg depending on the velocity and depth of flow. On the Qintong River in the Zhjiang Province of China, for example, depths are as much as 70 meter and velocities are of the order of 7 m/s, and a sinker weight of 750 kg is required. This, however, is an exception but weights of 250 kg are common in the Yangtze River catchment. Also in the Yangtze catchment the Bureau of Hydrology in China has introduced a combined sediment sampler and current meter equipped with an ultrasonic depth sounder. The facility of the ultrasonic transducer enables depth to be measured without the necessity of having to make air-line and wet-line corrections although the weight of the sampler requires to be sufficient to place the device at the appropriate location in the vertical to make the velocity measurements.

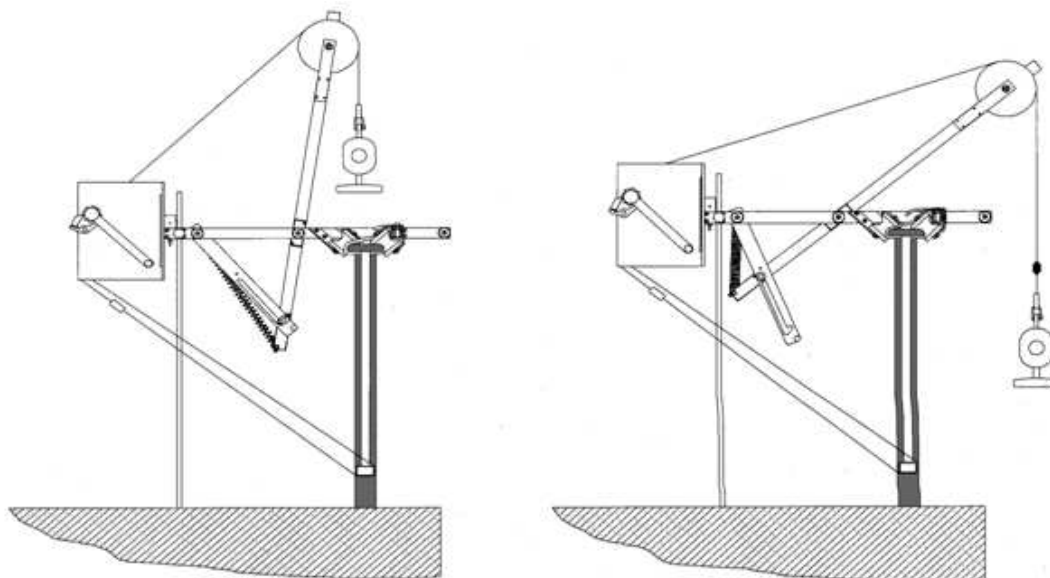


Fig. 8.14: Line suspension from bridge

Sinker weights are designed to a streamline form and furnished with tail fins to orient them parallel with the current so as to cause the minimum interference to the flow.

8.2.6 Moving boat

Frequently on larger streams and in estuaries conventional methods are impractical and involve costly and tedious procedures. This is particularly true during floods when facilities may be inundated or inaccessible, at remote sites where no facility exist, or at locations where unsteady flow conditions require that measurements be made as rapidly as possible. In other cases floating obstacles or river traffic require that measurements be made as rapidly as possible. The instruments that are most used with moving boat flow measurements are the ADCP and the propeller current meter (see subsection 8.2.3).

The moving boat technique is applicable to rapid measurements of rivers. In tidal rivers or estuaries, where density currents occur, the technique using a propeller current meter, with only limited information in the vertical, can not be applied. The river water in the upper layer can flow seawards while in the underlayer seawater will flow inland. The ADCP, on the contrary, is more suitable under these conditions. Traditionally the term moving boat is mainly associated with the measurements using the propeller current meter and will be as such used in the remainder of this chapter.

The moving boat technique is based on the velocity area method of determining discharges. According to this method the total area of the cross-section is divided in sub-areas for which a representative velocity is determined. The principal difference between a conventional measurement and the moving boat measurement is in the method of data collection. The mean velocity, in the segments of a cross-section of the stream in case of a conventional technique, is determined by point velocities or by an integrated mean velocity in the vertical. The moving boat technique measures the velocity over the width of a segment by suspending the current meter

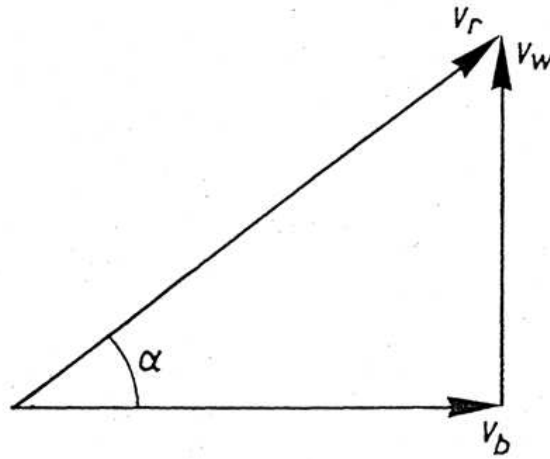


Fig. 8.15: Vector diagram

at a constant depth during the traverse of the boat across the stream. The measured velocity and the additional information of the depth sounding gives the required data for determining the discharge.

The velocity measurement taken at each of the observation points in the cross-section is a vector quantity, which represents the relative velocity of water past the current meter. This velocity v_r is the vector sum of v_w , the component of the time integrated stream velocity perpendicular to the boat path in the interval, and v_b , the velocity of the boat with respect to the streambed along the selected path. As this vector sum is the relative velocity of the water past the current meter assembly. The vector diagram, Figure 8.15, demonstrates this relationship.

Three types of data are required:

1. Location of observation points across the stream
2. Stream depth
3. Stream velocity

During the traverse an echo-sounder normally records the geometry of the cross-section and a continuously operating current meter senses the combined stream and boat velocities. A third set of data is needed to determine the location of the boat in the cross-section. This can be done by various methods. One method is to measure the angle between the boat and the cross-section that is traversed. Due to the current the boat will drift from the section if not corrected by steering. As a result the boat will move in an angle with the traversed path. The angle can be measured and results, in combination with the measured velocity, in a position of the boat (method 1). Alternatively the location is directly measured relatively to a grid or beacons (method 2).

The two methods are described as being representative for the different approaches. Combinations of the described techniques are of course possible. In method 1 (as it is called in the following) the current meter is located at a fixed depth below the water surface. The determination of the location of the observation points in the cross-section is based on observations of the

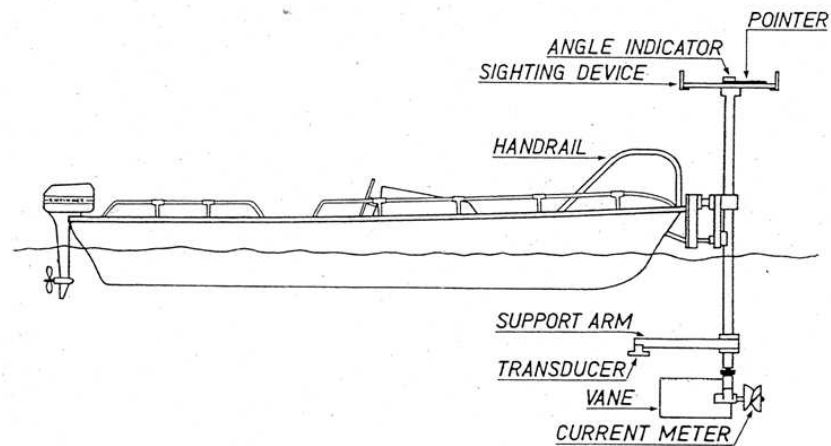


Fig. 8.16: Possible layout of equipment on board of a boat

angle between the section and the orientation of the current meter. In (the afterwards called) method 2 the current meter is freely suspended while the location of the observation points is directly measured with for example sextant readings.

In the following a more detailed description is given of the two methods, the way of measurement and the principle of the calculation procedure.

Method 1

Equipment and measurements A specially equipped boat is used as indicated in Figure 8.16. A vane with an indicating mechanism is mounted on the bow. The angles (α) between the direction of the vane and the cross-section are read via a pointer mounted in line with the vane. A sighting device attached to the free swivelling dial provides a means of aligning the index point on the dial with the cross-section.

The propeller current-meter (OTT) is mounted on the leading edge of the vane, whereas an electronic counter is used as pulse indicator. A stopwatch is used to time interval measurements. Finally an echosounder is installed for depth registration.

A crew of four persons is required:

1. A boat operator.
2. An angle observer.
3. A revolution counter operator.
4. A note keeper, echosounder operator, stopwatch operator.

After selection of the site and installation of the reference marks or beacons that define the orientation of the cross-section, the width of the stream and the location of the beacon(s) near the river are determined for example by triangulation. For rivers with a width of more than about 600 meter alignment reverends are used on both banks (see Fig. 8.17).

The location of the water line is fixed in relation to a nearby beacon. Using method 1, the exact locations of the starting and finishing position of the boat have to be determined (A and B).

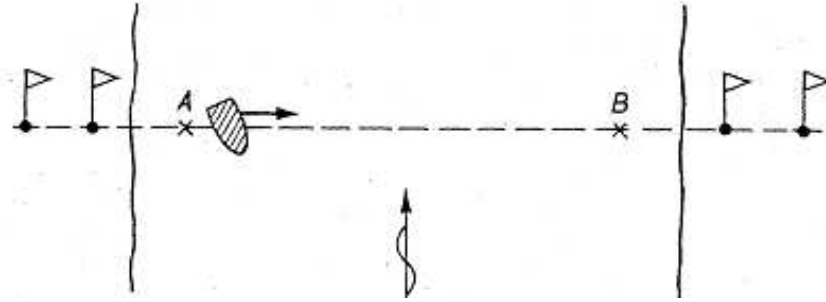


Fig. 8.17: Stream, boat and beacon

This can be done by rangefinder observations or sextant readings. If a third reference point on the bank(s) is available Buoys can be located in A and B. Starting in A the revolution counter and vane direction indicator are read and the echosounder registration is marked simultaneously. The observations can be done at regular time intervals for calculation purposes (20 or 30 sec); it is not essential for the method itself. However, a minimum of 25 à 30 observations is required. For this purpose and, the boat velocity is estimated more or less equal to the water velocity.

Computation The boat velocity is calculated by:

$$v_b = v_r \cdot \cos(\alpha) \quad (8.10)$$

With:

v_b boat velocity (m/s)

v_r measured relative water velocity (m/s)

α angle between cross section and the longitudinal axes of the boat (degrees)

ΔL is the distance covered in the time interval Δt with:

$$\Delta L = v_b \Delta t \quad (8.11)$$

The total distance L between A and B is calculated as the sum of the distances ΔL :

$$L = \sum^n v_b \Delta t \quad (8.12)$$

with n = number intervals.

Knowing the real distance between A and B (L_r) a correction factor k_l can be determined:

$$k_l = \frac{L_r}{L} \quad (8.13)$$

The water velocity is calculated leading to

$$v_w = v_r \cdot \sin \alpha \quad (8.14)$$

where v_w = water velocity,

and the partial areas and discharges as:

$$\Delta A = \Delta L \cdot d \quad (8.15)$$

$$\Delta Q = \Delta A \cdot v_w \quad (8.16)$$

where d = average depth between two observation points.

The total area and discharge between A and B (n intervals) is calculated according to

$$A_{AB} = \sum_n \Delta A \quad (8.17)$$

$$Q_{AB} = \sum_n \Delta Q \quad (8.18)$$

The corrections for the areas and partial discharges between the points A and B and the banks are made assuming a straight bottom slope between the water line and the depth in A or B and using a parabolic velocity distribution. Taking into account these corrections, the total area and discharge A_{tot} and Q_{tot} are calculated.

Two more adjustments are made:

1. Adjustment for the mean velocity in the vertical (k_v). It is assumed that in larger streams the relation between the velocity on the depth of the current-meter and the mean velocity in the vertical can be considered as fairly constant. In order to arrive at a representative average value of k_v several vertical velocity distributions have to be determined in strategically placed verticals. k_v is calculated as a weighed average with weights in proportion to the discharge in the segments. As the coefficient depends on the average water depth, these kinds of measurements have to be repeated at several stages in a non-tidal river and at various moments in a tidal river or estuary. It is, however, not necessary that k_v is determined for each different discharge measurement. k_v normally ranges between 0.85 and 0.92, and depending on the required accuracy of the measurement it seems that a good estimation is obtained using $k_v = 0.90$.
2. Width adjustment. The correction factor k_l is used to correct both the calculated area (A_{tot}) and discharge (Q_{tot}).

Summarized the real area (A_r) and discharge (Q_r) are calculated with the following formula:

$$A_r = k_l \cdot A_{tot} \quad (8.19)$$

$$Q_r = k_v \cdot k_l \cdot Q_{tot} \quad (8.20)$$

Method 2

Equipment and measurements No special equipment with reference to the conventional techniques is required in the most basic execution form of method. The current-meter is freely suspended in the same way as for a conventional discharge measurement and distances are determined by rangefinder or sextant. However, it is recommended to use an echosounder for

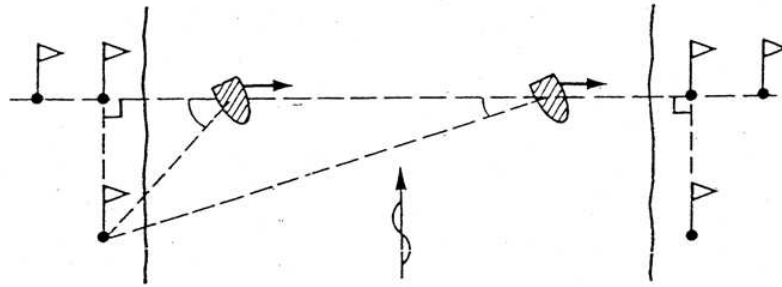


Fig. 8.18: Stream, boat and beacons for sextant reading

simultaneous depth registration and special counting device for revolutions and time interval observations; the objective of the special counter is to 'freeze' for a moment the observations that have to be copied. Two counters that operate alternatively or one counter with a special memory system can do this. Due to computational difficulties in cases that observation errors are made, a one counter system with a memory is highly recommendable. A crew of four persons is required:

1. A boat operator
2. A sextant or rangefinder observer.
3. A revolution, time interval observer.
4. A note keeper, echosounder operator.

Field practice showed that for experienced groups, dependent; however, on the facilities offered by the counting device, a crew of three persons is sufficient. As far as the site selection is concerned reference is made to the description given above for method 1. The reference points on one bank consist of 3 beacons, two for alignment of the launch and two as a base for the sextant readings. For rivers over about 600 meters wide these reference marks are installed on both banks (see Fig. 8.18). No special measurements as described in method 1 are required to locate points A and B.

Computation The computational procedure is slightly different for method 1. ΔL results directly from the location determined by the sextant readings and v_b is calculated with

$$v_b = \frac{\Delta L}{\Delta t} \quad (8.21)$$

With:

- v_b boat velocity (m/s)
- ΔL the distance between the observation points (m)
- t the time interval between two readings (s)

The water velocity is determined by

$$v_w = \sqrt{v_r^2 + v_b^2} \quad (8.22)$$

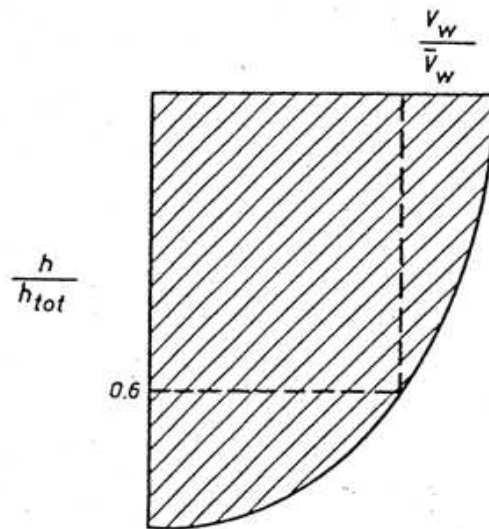


Fig. 8.19: Vertical velocity distribution

With:

v_r the measured relative water velocity (m/s)

v_w the water velocity (m/s)

The mean velocity adjustment is made directly after the computation of v_w (and before calculation of the partial discharges) by way of a unitary-velocity distribution in the vertical, relating the relative depth with the relative velocity.

With:

\bar{v}_w mean water velocity (m/s)

h depth of the current meter (m)

\bar{h}_{tot} total depth (m)

8.3 Dilution gauging

8.3.1 Principles

Dilution gauging is, as is the velocity area method, a method to obtain a near instantaneous value of the discharge of a river. The principle of dilution gauging is simple. Added to a constant unknown discharge Q , is a smaller discharge $\Delta Q(t)$ that exists of a watery solution of a substance of which the concentration (t) is measurable. From the known data, $\Delta Q(t)$ and $\phi(t)$ the value of Q is derived.

8.3.2 Constant rate injection method

Constant rate injection is the simplest case of the dilution gauging. The injection consists of a constant discharge ΔQ , with concentration 1 that is added to the river discharge Q , during a long enough time period. If on the reach L (see Fig. 8.20) there is sufficient mixture, than after a certain time period a constant concentration 0 will be measured at the end of the reach. From

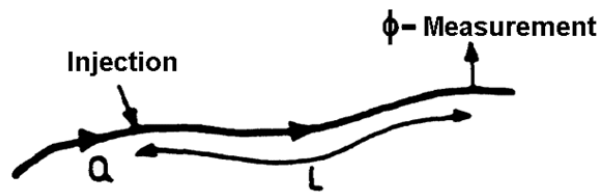


Fig. 8.20: Dilution gauging for reach L

the mass-balance of the concentrations, it follows by approximation (when $\Delta Q \ll Q$):

$$\phi_0 = \frac{\Delta Q}{Q} \phi_1 \quad (8.23)$$

For a good measurement a couple of conditions have to be met, the most important are described below. Also André and Molinari [1979] pays attention to this kind of measurements.

Requirements of the tracer

- Naturally, the tracer has to dissolve in water
- The concentration of the tracer still has to be measurable after a sufficient dilution ($\Delta Q \ll Q$).
- No density flows may occur. Almost all solutions meet this requirement. Even NaCl-solutions do because of $\Delta Q \ll Q$ possible.
- The tracer may not attach to floating sediment. Therefore the colouring agent Rhodamine (concentration determination with colorimeter) is normally not suitable. Only suitable is Rhodamine WT (= 'watertracer').
- The unmarked water should have low concentrations of the tracer. This is why NaCl is not always suitable.

Requirements of the river reach

- Within the reach (see Fig. 8.20) no water flows into nor out of the river
- Within the reach length L the mixture has to be as good as possible.
- During the measurement steady flow ($Q=\text{constant}$) needs to occur

The length L can be roughly determined with an experimental equation (Eq. 8.24):

$$L > 0.13K \frac{B^2}{a} \quad (8.24)$$

With:

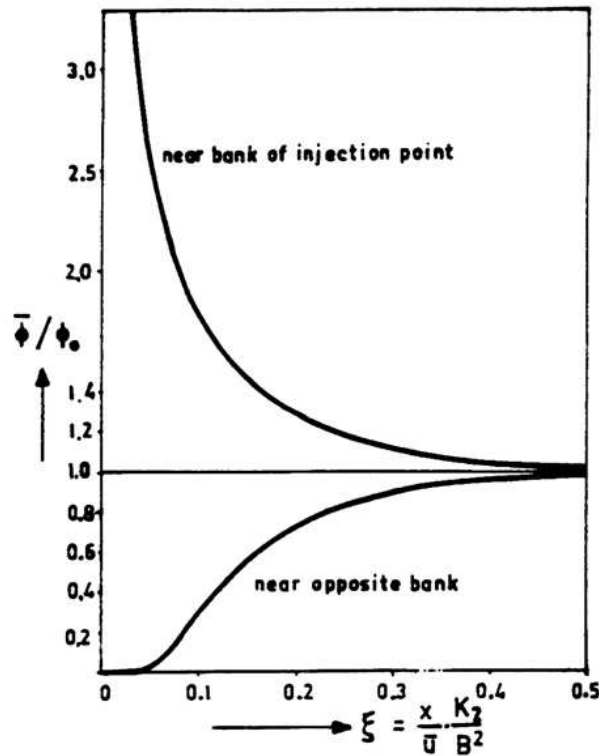


Fig. 8.21: $\frac{\bar{\phi}}{\phi_0} = f(\xi)$

$$K = \frac{C(0.7C + 2\sqrt{g})}{g} \quad \text{for} \quad 4.8 < \frac{C}{g} < 16 \quad (8.25)$$

With:

C Chezy roughness ($\text{m}^{1/2}/\text{s}$)

B river width (m)

a river depth (m)

van Mazijk [1996] has analytically examined the relationship between the concentration near the banks and the average concentration when the injection takes place at one bank (see Fig. 8.21). It is assumed that complete mixture occurs when the concentration on the opposite bank (ϕ), is 95% of the average concentration in the whole cross-section (ϕ_0).

For the accompanying length $L_{0.95}$ it is found that:

$$\frac{L_{0.95}}{B} = 0.4 \frac{\bar{u}B}{K_2} \quad (8.26)$$

Whereby K_2 is the transversal dispersion coefficient with $K_2 \approx \alpha a u^*$

Together with Equation 8.26 applies,

$$L_{0.95} = \frac{0.4}{\alpha} \frac{C}{\sqrt{g}} \frac{B^2}{a} \quad (8.27)$$

because

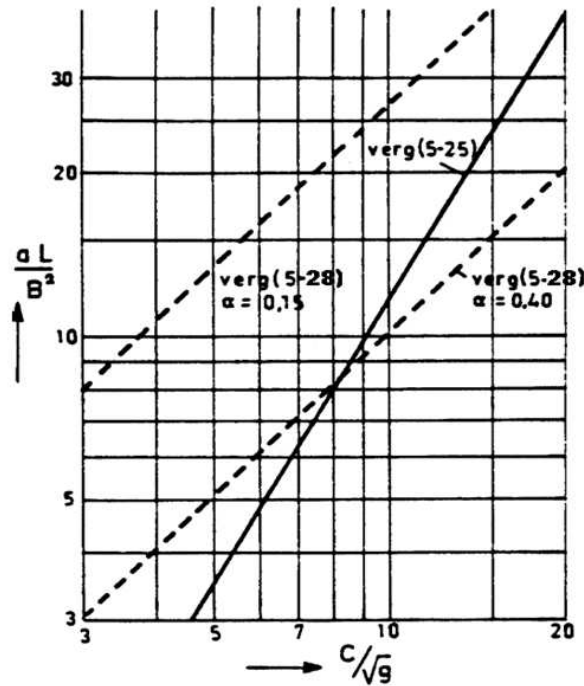


Fig. 8.22: Determining reach length

$$\frac{\bar{u}}{u_*} = \frac{C}{\sqrt{g}} \quad (8.28)$$

For a rectangular profile applies $\alpha \approx 0.15$ and for an arbitrary profile applies $\alpha \approx 0.6$ (see also de Vries, 1984). For Equation 8.26 and 8.27 generally goes:

$$L > \beta \frac{B^2}{a} \quad (8.29)$$

With $\beta = \frac{0.4}{a} \left(\frac{C}{\sqrt{g}} \right)$

Both Equation 8.29 and 8.27 give a functional relation between the dimensionless parameter $\beta = aL/B^2$ and C/\sqrt{g} (Fig. 8.22). Because the dilution gauging is mostly used for irregular watercourses ($\alpha = 0.4$), it appears that both criteria for the length L of the river reach do tally. The length L does not need to be chosen longer than necessary. After all the timespan θ over which one has to inject depends on the length L . It appears that $\theta = 10$ à 15 minutes is sufficient. This could be checked with a test-measurement.

Execution of the measurement

For the constant rate injection method, it is important to keep ΔQ constant. This is possible by injecting the tracer into the river with an adjustable pump. It is also possible to use the principle of the bottle of Mariotte (1620-1684) (see Fig. 8.23) This is the principle that is also used for drinking water bottles in birdcages. When the water level starts to lower, automatically air is let into the bottle, as much as to keep the flow opening under a constant pressure. The discharge

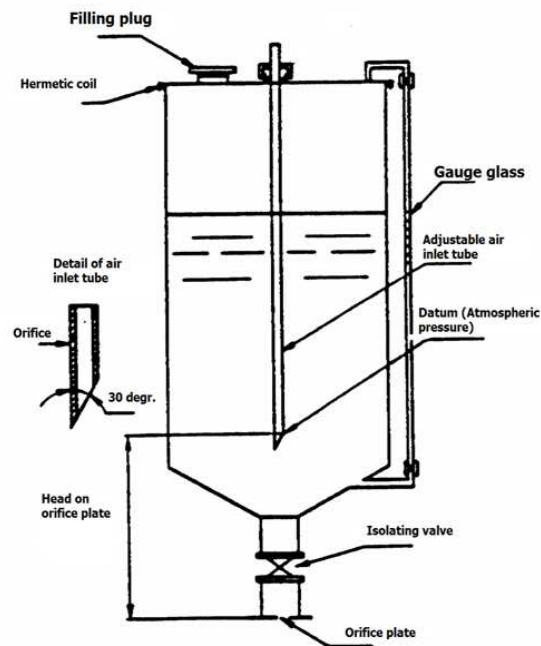


Fig. 8.23: Bottle of Mariotte

ΔQ depends on the pressure at the flow opening and thus is independent of the amount of fluid left in the bottle.

The concentration depends on the used tracer. For colouring agent (e.g. rhodamine WT or fluorescent) a colorimeter is being used. For salt solutions (e.g. cooking salt) the conductivity is being measured.

Comment:

For the sake of completeness, the use of radioactive tracers will also be mentioned. The necessary expertise and often-rigorous safety rules make the use of this kind of tracer troublesome.

It is wise to verify that a uniform dilution of the added concentration occurs at the measurement site. Obviously the necessary length of the reach is shortest if one injects in the centre of the watercourse. Because this is not always possible, Figure 8.22 assumes adding of the concentrate and measurement of the dilution from the banks. Dilution gauging works best in strong turbulent water (and thus good mixture). For mountain creeks this method is ideal. In fact, other methods based on velocity measurements in mountain creeks are usually less suitable, due to the irregular cross-sections. The method of dilution gauging is also very suitable for the determination of the capacity of pumping stations (the pump will take care of the necessary mixture).

8.3.3 Sudden or Gulp injection method

As a variant on the discussed method of the constant rate injection, the method of sudden or Gulp injection has to be mentioned. By this method on $t = 0$ a tracer mass (M) is instantaneously injected in the river. On a distance L downstream (where the concentrate is assumed uniformly diluted) the mass concentration is being measured. The following formula applies here:

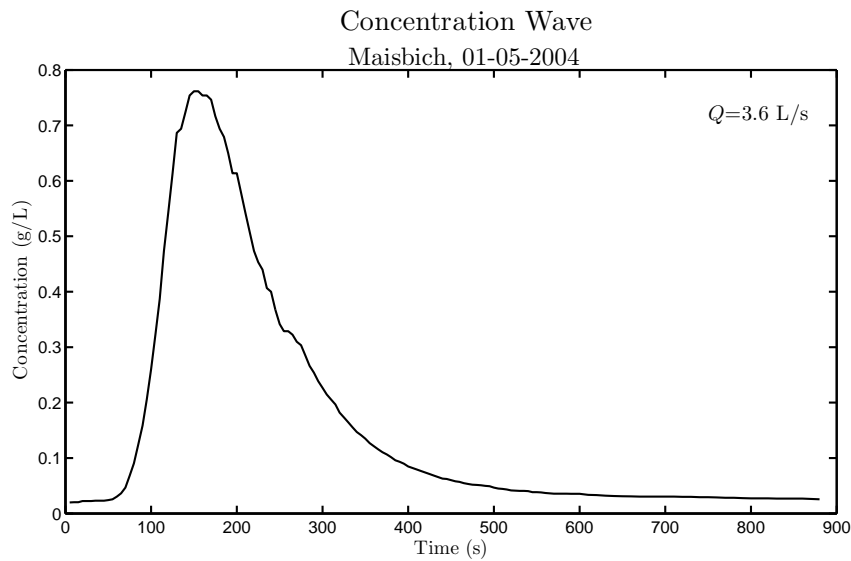


Fig. 8.24: Example of a concentration wave from a sudden injection of 500 gram of salt

$$M = Q \int_0^{\infty} (\phi(t) - \phi_1) dt \quad (8.30)$$

Where ϕ_1 is the possible existent natural concentration in the watercourse, which can be determined upstream from the injection point. Theoretically ϕ_1 can be a function of time. The condition that $\phi_1 \ll \phi$ does apply. When M is known and both $\phi(t)$ en $\phi_1(t)$ are measured, the discharge Q in Equation 8.30 is the only unknown.

8.3.4 Range and accuracy

The dilution gauging is preferably suitable for small watercourses with a lot of turbulence as well as for pumping stations. Nevertheless, accurate measurements were achieved with discharges up to 2000 m³/s. With precise execution the relative error in the discharge can be in the order of 1%.

8.4 Ultra-sonic streamflow measurement

Ultrasonic streamflow measurement is a method to determine an instantaneous value of the discharge of a river.

8.4.1 Theory

When there is no flow in a watercourse ($v = 0$), the time T_{AB} it takes for an acoustic pulse to go from A to B is the same as the time T_{BA} to go from B to A. The time T_{AB} and T_{BA} equals L/c , where L is the distance between A and B, and c is the speed of sound in water (about 1500 m/s).

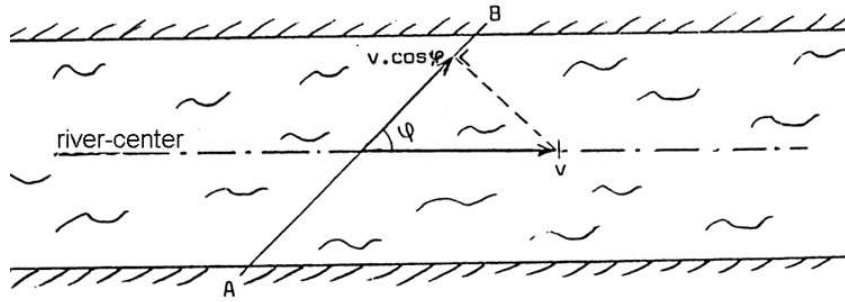


Fig. 8.25: Speed of sound in flowing water

When there is flow in the watercourse ($v \neq 0$), then the sound from A to B will have an extra velocity $v \cos \phi$ (see Fig. 8.25). The total dynamics of the sound which goes from A to B will be $c + v \cos \phi$, hence

$$L = (c + v \cos \phi) T_{AB} \quad (8.31)$$

A sound pulse from B to A is slower (with a fraction $v \cos \phi$), so the dynamics of the sound which goes from B to A is equal to $c - v \cos \phi$, and hence

$$L = (c - v \cos \phi) T_{BA} \quad (8.32)$$

From these equations follows (elimination of c):

$$v = \frac{L}{2 \cos \phi} \left(\frac{1}{T_{AB}} - \frac{1}{T_{BA}} \right) \quad (8.33)$$

The flow velocity can be calculated from Equation 8.33 if L and T_{AB} and T_{BA} are known, and T_{AB} and T_{BA} have been measured. However when put into practice two important problems occur:

- To derive Equation 8.33 from Equation 8.31 and 8.32, it is assumed that the speed of sound for both measurements (from A to B and vice versa) is exactly the same; this however is often not the case.
- The streamflow direction is never exactly along the river centre.

Both problems will be discussed.

The motion of sound is not a real constant, but depends on different conditions of the water:

- The water temperature and water pressure.
- The salinity (=salt concentration in the water).
- The concentration, size and distribution of air bubbles.

Because the measurements are made in two directions along the same sound path, the conditions for both are similar. Furthermore, from a good flow measurement utility, one has to expect it will measure both measurements simultaneously (otherwise conditions could change).

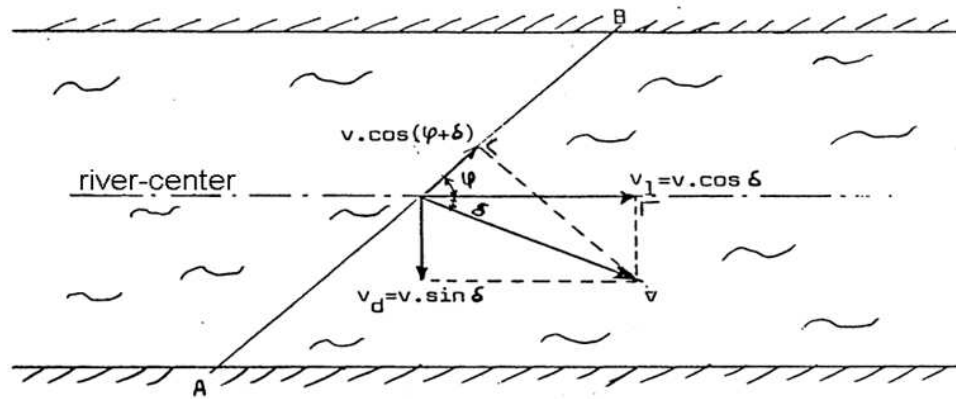


Fig. 8.26: Flow with lateral component

In Equation 8.31, $v \cos \phi$ is the component of the streamflow velocity assuming the direction of the streamflow velocity along the river centre. In an arbitrary watercourse (normally) this direction is not along the river centre, but makes an angle δ with the line following the centre (see Fig. 8.26).

The component v_1 is now equal to $v \cos \delta$ and the component v_d is $v \sin \delta$. The streamflow-component along AB is now $v \cos(\phi + \delta)$. Hence Equation 8.33 still applies, on condition that ϕ is replaced by $(\phi + \delta)$:

$$v = \frac{L}{2 \cos(\phi + \delta)} \left(\frac{1}{T_{AB}} - \frac{1}{T_{BA}} \right) \quad (8.34)$$

Using simple geometry¹ we get:

$$v \cos \phi \cos \delta - v \sin \phi \sin \delta = \frac{L}{2} \left(\frac{1}{T_{AB}} - \frac{1}{T_{BA}} \right) \quad (8.35)$$

For a second measuring line CD (see Fig. 8.27) under the same angle with the centre line, but mirrored, it follows that:

$$v \cos \phi \cos \delta - v \sin \phi \sin \delta = \frac{L}{2} \left(\frac{1}{T_{DC}} - \frac{1}{T_{CD}} \right) \quad (8.36)$$

From adding Equation 8.35 with 8.36 we get:

$$v \cos \delta = \frac{1}{2} \frac{L}{\cos \phi} \left(\frac{1}{T_{DC}} - \frac{1}{T_{CD}} + \frac{1}{T_{AB}} - \frac{1}{T_{BA}} \right) \quad (8.37)$$

The left side of this equation is the component of the flow velocity along the river centre, v_l , and the right side of this equation is the average of Equation 8.33, for two measuring lines AB and CD. Lateral components can thus be eliminated using the 'measuring-cross'. Using Equation 8.35 and 8.36 also the component v_d can be calculated.

$$v \sin \delta = \frac{1}{2} \frac{L}{\sin \phi} \left(\frac{1}{T_{DC}} - \frac{1}{T_{CD}} - \frac{1}{T_{AB}} + \frac{1}{T_{BA}} \right) \quad (8.38)$$

¹ $\cos(\phi \pm \delta) = \cos \phi \cdot \cos \delta \pm \sin \phi \sin \delta$

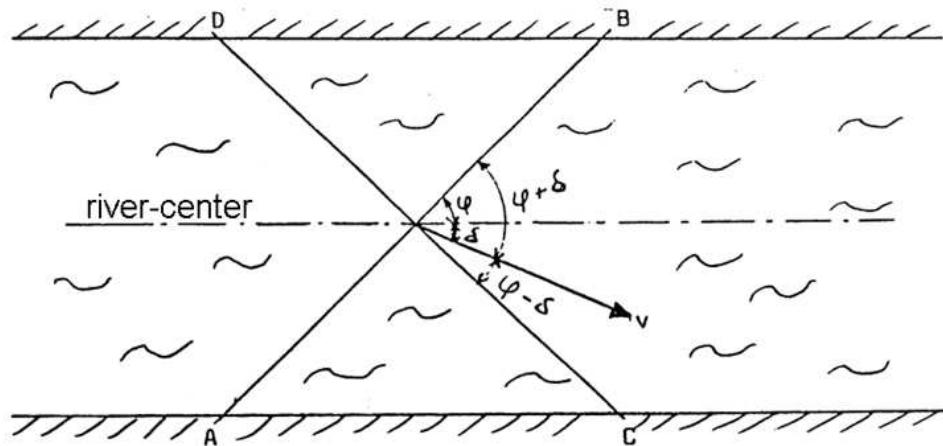


Fig. 8.27: Measuring cross

8.4.2 Site selection

When making a decision as to whether or not a site is suitable for an ultrasonic streamflow gauge the following basic factors need to be true:

1. A reliable source of power is available; a portable system is now marketed, however, which is battery operated.
2. The channel width is in the range 20-300m, although the system operates outside this range, this range is normally considered economically feasible.
3. The channel is free of weed growth at all times as weeds disperse the beam.
4. Generally, as a guide, sections having concentrations of over 1000 mg suspended solids/litre, for significant periods of time are avoided. Suspended solids may have a significant effect on the signal attenuation caused by both reflection and scatter from sediment particles suspended in the stream.
5. Other causes of attenuation need also be avoided; attenuation of the acoustic signal may also be caused by reflection and scatter from entrained air usually caused by rapids or waterfalls.
6. Upstream inflows to the river at different temperatures or high salt content are not advisable; they may cause the beam to be refracted.
7. The measuring reach is one, which is preferably straight and uniform, and at cross-sections in the reach, between the upstream and downstream transducers, the velocity distribution is similar.
8. The bed is stable.
9. Wide shallow rivers are avoided, otherwise the beam may reflect from the surface or channel bed and cause gross uncertainties.

8.4.3 Instrumentation

If there was no sound absorption in water, the highest possible operating frequency could be used as this increases the system timing accuracy and allows closer spacing between the acoustic path and the surface or bottom of the channel. However, sound absorption by particulate matter and entrained air increases with increasing frequency. While increasing transmitter power helps somewhat, there is an upper limit achievable and a compromise is therefore reached in determining the operating frequency. Generally the frequency range used in ultrasonic systems varies between 200 and 500 kHz, the lower frequencies being used in wide rivers. Manufacturers, however, are able to modify their systems in order to use the appropriate frequency for the given conditions of the site.

As stated earlier, special problems arise for the paths nearest to the surface and bed (the reason to avoid shallow rivers). If the transducers are too near these boundaries, reflected signals from the boundary can interfere with the direct transmission and causes inaccuracies in the time measurement. Sound is reflected from the water surface and, to a lesser extent, from the channel bed. The bed may even be a net absorber of sound. As an acoustic wave propagates across a river it will intersect with the water surface and be reflected, suffering a 180 phase change in the process. The secondary wave will proceed across the river and arrive at the opposite bank. The target transducer will sense its arrival later than the direct wave, and the difference in arrival time will be a function of the difference in the respective lengths of the direct and indirect paths. Errors in signal timing will occur if the secondary signal interferes with the first cycle of the direct signal. To avoid this effect, the difference in the two paths should exceed one acoustic wavelength (speed of sound divided by the frequency). This will be achieved if the depth of water above the acoustic path exceeds that given by the equation:

$$H = 24\sqrt{\left(\frac{L}{f}\right)} \quad (8.39)$$

With:

- H is the minimum depth (m)
- L is the path length (m)
- f is the transducer frequency (Hz)

A similar restriction may apply to the channel bed, particularly if it is smooth and, hence, reflects rather than absorbs an acoustic signal.

Single/multiple path systems

In the single path system, measurement of velocity is made at one depth only with the pair of transducers normally set at 0.6 of the most frequently occurring depth. If the transducers are movable, they are used to calibrate the system by taking line velocity measurements throughout the depth as in the vertical velocity distribution method. Instead of using verticals, horizontal paths are scanned at an infinite number of 'verticals'. If the transducers are fixed, a relation is established between flow, as measured by current meter, and the ultrasonic line velocity. The

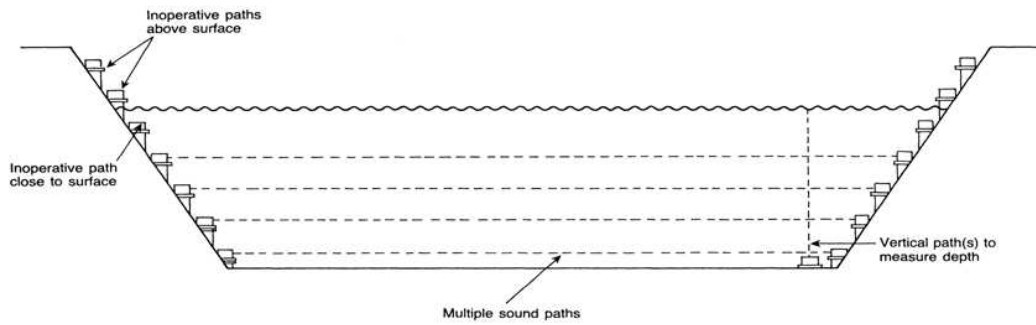


Fig. 8.28: Diagrammatic illustration of multi-path ultrasonic system (Also shown is an ultrasonic depth gauge)

single path system is normally used when the variation in stage is small for a larger percentage of the time.

The more common multi-path system incorporates several pairs of transducers to provide velocity measurements at various water depths and is particularly suitable for rivers having a wide range in stage or with irregular velocity distributions.

Maintenance

Working with an ultrasonic streamflow measurement system requires little maintenance. Yearly, the transducers need to be cleaned and the altitude-measurement must be checked. Periodically the float shafts and supply shaft of the altitude-measurer, needs to get flushed and cleaned (removal of obstacles, bank growth and such more). Obviously, it needs to be checked regularly if the, in the discharge measurement system, imported profiles and correction-factors still agree with reality. It speaks for itself, the facilities need maintenance too.

8.4.4 Accuracy

The streamflow velocity is determined by: the angle (ϕ), the distance L and the time periods T_{AB} and T_{BA} (see Eq. 8.33). The accuracy with which the streamflow velocity is determined is also determined by the accuracy of these components. Without going into any details the following can be said about the accuracy.

The accuracy of the determined time periods (T_{AB} and T_{BA}) is for the standard 200 kHz-transducers better than 15 ns (1ns = 10^{-9} s). Converted to the velocity this means accuracy within circa 0.5mm/s for a measuring line length of 50m. For longer measuring lines the accuracy gets proportionally better (e.g. for $L = 250$ m the accuracy is better than 0.1mm/s). The other way around, for smaller lengths the accuracy gets proportionally worse (better than 2.5mm/s for $L = 10$ m). For very small measuring lines the accuracy can be improved 5 times by using special transducers.

The measuring line L can normally be established within the 0.5% accuracy. The maximum error for the velocity measurement as a result of the accuracy of L is than also 0.5%.

The angle can be established within 0.1% accuracy. For a measuring line angle of $\phi = 45^\circ$, this means the maximum error in the streamflow velocity determination is 0.2%.

8.4.5 Existing installations

Despite the high initial costs of measurement equipment and measurement facilities, Rijkswaterstaat expands the use of ultrasonic streamflow measurements. This because the method gives:

- Continuous information about the discharge and therefore is suitable for operational watermanagement.
- Exact information, as well for high discharges as low discharges, and thus can be used for a broad scale of purposes.
- Reliable information, due to internal controls.
- Digital information and thus can be used for modern means of data transport and data processing.

Finally the equipment is maintenance friendly and the exploitation costs are low.

8.5 Electromagnetic streamflow measurement

8.5.1 Theory

According to Faraday's law of electromagnetic induction, the motion of water flowing in a river cuts the vertical component of the earth's magnetic field and an electromotive force (emf) is induced in the water. This emf can be sensed by electrodes ('probes') on each side of the river and is found to be directly proportional to the average velocity of the flow in the cross-section. Therefore, unlike the ultrasonic method (see section 8.4) which measures velocity across paths, the electromagnetic method performs integration over the entire cross-section. However, although measurements have been conducted using the earth's magnetic field, usually in tidal estuaries, these have had a large uncertainty due to the fact that the emf induced by the earth's field is too small to be distinguished from other electrical interference. This interference normally created by 240 V mains, electrical motors and other ambient electrical noise present in some form or another in the ground. Therefore, to induce a measurable potential in the electrodes, a vertical magnetic field is generated by means of a coil buried in the riverbed, or placed over it, through which an electric current is driven. The potential generated is proportional to the width of the river (m) multiplied by the magnetic field (T) multiplied by the average velocity of flow (ms^{-1}).

The electromagnetic technique has been used for many years for gauging full pipes where the area of flow is constant. The basic principle is shown schematically in Figure 8.29. The pipe flow meter is manufactured in units of practically any required diameter sizes, the largest in practice being about 2 meter diameter. The coil is incorporated in the form of a saddle around

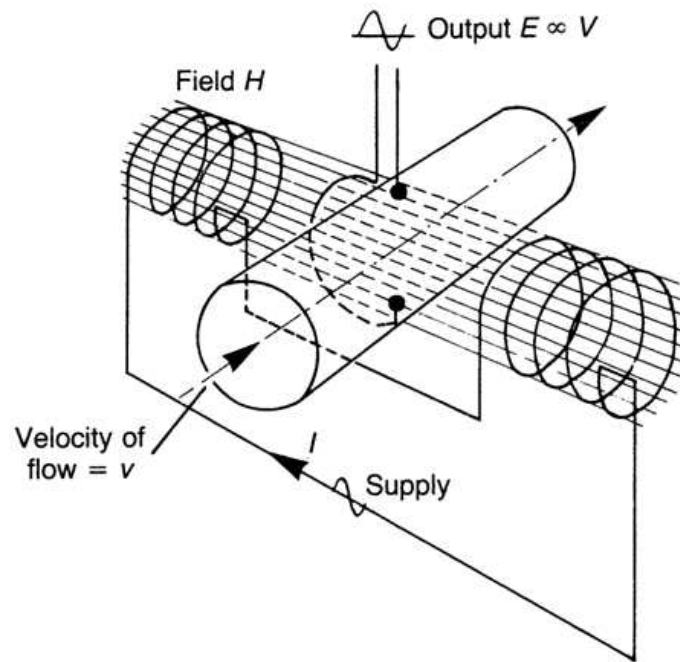


Fig. 8.29: Basic principle of fluid flow measurement in pipes by electromagnetic induction

the pipe section and the electrodes are inserted in the pipe wall flush with the inside wall. In streamflow measurement, however, the stage varies and therefore the cross-sectional area of flow is not constant. In addition, stream channels are much wider than pipes and hence the electromagnet forms a large part of the cost; velocities in rivers are normally much slower than in water flowing in full pipes since the former are flowing under gravity whilst full pipes are normally under pressure. In addition, electrical interference is generally higher near rivers than in pipes, particularly at the mains distribution frequency. All of these factors make open channel electromagnetic gauging much more complex than those in full pipes.

Referring to Figure 8.29 Faraday's law of electromagnetic induction relates the length of a conductor moving in a magnetic field to the emf generated, by the equation:

$$E = B\bar{v}b \quad (8.40)$$

With:

E is the emf generated (V)

B is the magnetic flux density in teslas (T)

\bar{v} is the average velocity of the conductor in the cross-section (ms^{-1})

b is the length of the conductor and is equal to the river width (m)

Now in the case of an operational gauge having an insulated bed and a square coil just wider than the channel, the voltage generated is approximately 0.8 times that given by Equation 8.40. This reduction in voltage is caused by the shorting effect of the water upstream and downstream from the magnetic field. Numerically the empirical relation ($\pm 3\%$) is:

$$E' \approx \bar{v}bH \quad (8.41)$$

Where E' is the electrode potential (μV) and H is the average magnetic field strength in amperes per meter. (Note: the physical relationship between B and H in free space, air or water is given by:

$$B = H4\pi10^7 \quad (8.42)$$

In the ideal case where the magnetic field strength is constant over the entire wetted section, the discharge, Q (m^3s^{-1}), is given by:

$$Q = \bar{v}bh \quad (8.43)$$

With h the water depth. From Equation 8.41 and 8.42 follows the equation for the discharge:

$$Q = \frac{E'h}{H} \quad (8.44)$$

Operationally this equation may take the form:

$$Q = K \left(\frac{E'h}{I} \right)^n \quad (8.45)$$

where I is the coil current in amperes and K and n are constants. If the coil is mounted above the channel the water near the bed will move in a less strong magnetic field relative to that near the surface. Normally the relation is expressed in the form:

$$Q = (K_1 + h + K_2h^2) \frac{E'}{H} \quad (8.46)$$

The current meter calibration graph may take several forms; it may be a single straight line when transposed logarithmically, or have several straight lines with inflexions or it may be curvilinear. It can be seen that the discharge from Equation 8.44 and 8.45 or 8.46 is obtained by the velocity-area principle in which the velocity is inferred from the electrode potential and multiplied by the cross-sectional area of flow. The area is a function of the recorded water level and the equations contain dimensional constants established empirically. The river width factor does not appear in the equations and is accounted for in the design of the coil, which extends the full width of the channel, and in the empirical calibration.

8.5.2 Site selection

The following are the main considerations in selecting a site for an electromagnetic gauge:

1. Due to cost considerations, the maximum width of the river is in the order of 30m. This limit is mainly set by the need to insulate the channel with a membrane.
2. A site survey is carried out to measure any external electrical interference (e.g. power cables, radio stations, electric railways). Areas of high electrical interference are preferably avoided.
3. A 2kW source of electrical energy is available. For continuous operation a power supply of 110-240 V is necessary but the system can operate on a 12 V supply for short periods,

4. The site requires adequate on-bank working space for handling the membrane and cable.
5. There is good access to the site for installation, operation and maintenance.
6. The site characteristics are such that the calibration of the station can be checked by current meters.
7. Sites are selected where there is no spatial variation of water conductivity. The accuracy is degraded if the spatial conductivity is not uniform across the section. Temporal variations are unimportant provided the spatial uniformity of the conductivity is maintained. This requirement makes an electromagnetic gauge unsuitable for channels where fresh water flows over saline water, which often occurs in small estuaries. Provided these requirements are met, the quality of the water, ranging from mountain streams to foul sewage, will not affect the operation of the gauge and, similarly, the conductivity of the water will not affect the operation of the gauge.

8.5.3 Design and construction

The electromagnetic gauging station consists of (see also Fig. 8.30):

1. A field coil installed below or above the channel;
2. A pair of electrodes one on each side of the channel;
3. An insulating membrane;
4. An instrumentation unit including a coil power supply unit;
5. A water-level measuring gauge;
6. A reference gauge and station benchmark.

The coil

The coil is wound with a determined number of turns of wire which will depend on: the accuracy required, the river width, the minimum velocity and the coil power supply, but normally a coil of between 50 and 300 turns is required. The field to be generated by the coil is made of sufficient magnitude to cause the induction of a measurable voltage between the two electrodes at the minimum water velocity. For a rectangular channel the relationship between the electrode voltage and the electromagnet is $500\text{mV}\cdot\text{s}^{-1}$ water velocity for a 1000 A turn (AT) coil. To establish a minimum number of ampere-turns to be provided, the measurable voltage, which is typically 0.5mV , is related to the minimum voltage obtained at the minimum velocity. For example, consider a typical river situation where the minimum velocity to be measured is 0.03ms^{-1} and the resolution of measurement required is 5%. This accuracy of 5% corresponds to a velocity of 0.0015ms^{-1} . If this velocity corresponds to a minimum voltage measurement of 0.5mV an electromagnet is required with:

$$1000 \cdot \frac{0.5}{500} \cdot \frac{1}{0.0015} \text{AT} \approx 660\text{AT} \quad (8.47)$$

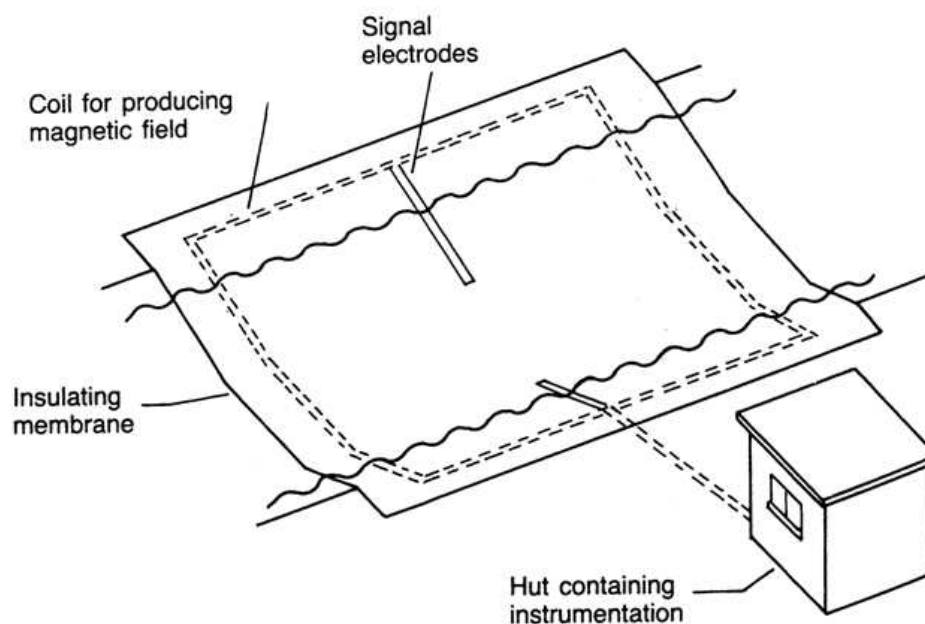


Fig. 8.30: Schematic view of electromagnetic gauge with coil installed below channel bed

8.6 Flood surveys

To handle the damage that floods can cause it is essential to be able to quantify its magnitude. This is in terms of the maximum discharge and/or flood levels as well as the flood volume. This would need flood surveys to link stage and discharge. Measuring discharge under extreme flow conditions is not easy. Typical methods that can deliver estimates of stage and discharge under even the most extreme flood conditions are the slope area method and measurements by floats.

8.6.1 Floats

Contrary to what most hydrologists and hydrometrists wish to believe floats are the most reliable and scientifically most appropriate instruments for measuring discharges during peak flows. The hydrometrist often considers floats below his/her professional standard and thinks incorrectly that his / her current meter is the most accurate instrument for determining peak discharges. Floats, well positioned, and with a resistance body at the right depth (see Fig.8.31) are best for the following reasons:

- Floats move at the same velocity as the surrounding water (provided they are made as in Figure 8.31) and integrate the velocity in the longitudinal direction; they thus provide an accurate sample of the real mean velocity. Current meters, that integrate the velocity over time at a fixed position, may be affected by local accelerations (e.g. due to bed forms). Moreover, current meters do not always measure the point velocity accurately.
- Floats are stagnant in relation to the moving water, thus the vertical position of the resistance body in the flow is correct. The vertical position of a current meter in the

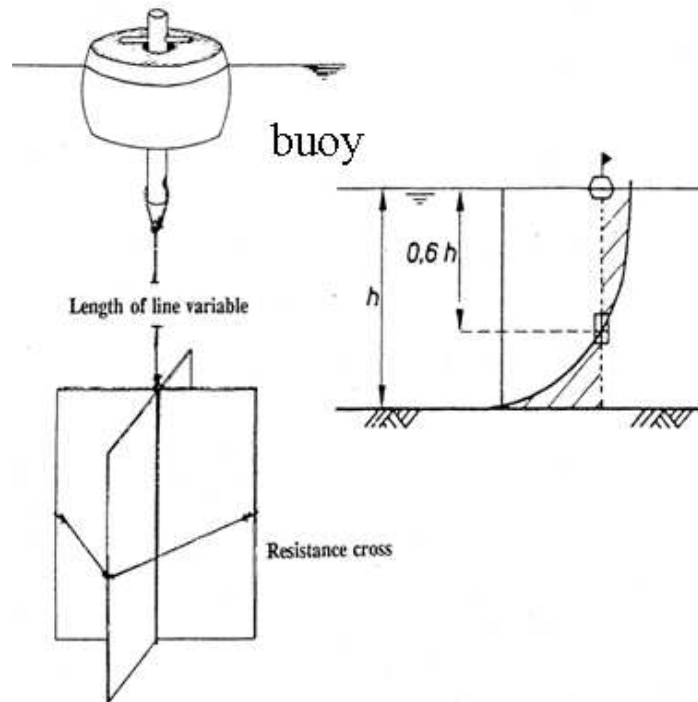


Fig. 8.31: Float with resistance body and the location of the resistance body in the vertical

stream, on the other hand, is not certain. Often velocities are so high that the instrument just 'takes off' after touching the water surface.

- A float measurement can be carried out in a shorter period of time than a current meter measurement, which is an advantage under rapidly changing conditions.
- Floats are cheap compared to current meters; it is not a disaster if one gets lost.
- At the peak of the flood, the river is full of debris; use of a current meter then is completely impossible. If no professional floats are available, it is easy to improvise.

If one arrives at the site unprepared, it is always possible to clock the velocity of floating debris. The larger the debris (e.g. trees) the better they describe the mean velocity in the vertical. A float measurement is briefly described underneath.

A straight reach is selected of 100m length (see Fig. 8.32). The width is divided into approximately eleven equal distances in which ten measuring points are established. If there are no constraints in time or resources, try as many points as possible. At each measuring point a float is used with a resistance body at 60% of the average depth at that point.

Beacons, placed on both banks in a line perpendicular to the flow, mark two measuring sections at the upstream and downstream end of the measuring reach. On each bank of a measuring section the two beacons should stand with sufficient distance between them to allow the observer to determine his position from a boat (if a boat is used). At night the floats and the stacks should carry lights. A float measurement is carried out by launching a float at a particular point in the cross-section. The positioning can be done from a cable mounted across the river, from markings on a bridge (if present) or if necessary by sextant. The float should be launched (from

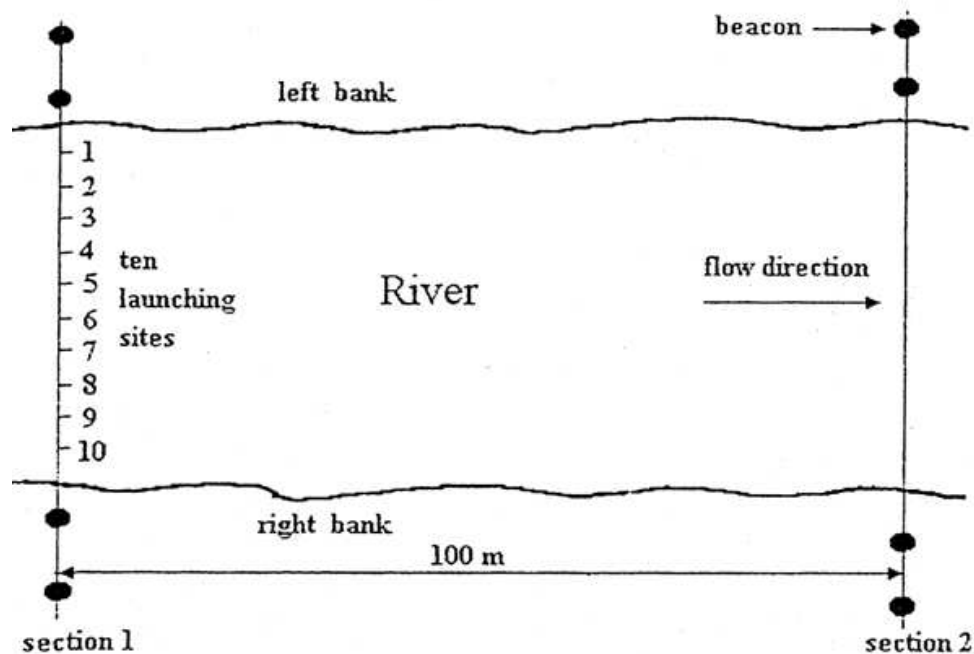


Fig. 8.32: Layout of float measurement

a bridge or from a boat) at least 10 m upstream from the cross-section where the measurement starts, to allow the float to adjust itself to the flow velocity. When a boat is used, the observer should stay with the float, keeping next to it. When the float enters the measuring section, the observer starts the stopwatch; he/she then follows the float until the measuring cross-section 100 meters downstream where he/she stops the stopwatch. He/she notes down the time and (if using a boat) recovers the float to return and repeat the measurement at the next observation point. The advantage of a boat moving with the float is that only one observer is needed per float and no communication problems occur. The disadvantage is that the determination of the moment in which the float passes the section is less accurate. If no boat is available, floats should be launched from a bridge, and followed along the bank. More observers could work at the same time, and one observer could clock more than one float. The advantage of this method is a greater degree of accuracy when starting and stopping the stopwatch; the disadvantage, however, is the more complicated communication and that the floats are lost.

A float measurement over a distance of 100 meters has a relative error, in the measurement of the velocity, of 1%. A current meter does not have that degree of accuracy. Moreover, by following the flow trajectory, the velocity is correctly averaged in the longitudinal direction. The only problem remains getting the average over the cross-section. The variation over the cross-section may be substantial. The variation over the width appears to be the largest source of errors. Therefore, one should select at least ten measuring positions in the cross-section.

This still leaves the problem of determining the cross-sectional area. Only if one has an echosounder at one's disposal (it might get lost) and the river is navigable the cross-sectional area

can be determined. Normally, however, determining the cross-sectional area has to be left for the 'morning after' program.

8.6.2 Slope area method

The slope area method is a method to estimate the discharge of a river. Application of the slope-area method, which is much less accurate than the other methods should only be considered as an ad hoc method if the other methods are not feasible, for example when floods occur.

Flood marks

For the slope area method the cross-sectional area, the hydraulic radius and water slope, which occurred during the flood, need to be determined. Immediately after the flood peak has passed one should go to the field and search for flood marks. Flood marks can be found in the color of mud on bridges, pillars, or (in case of extreme flooding) on the walls of buildings. Also the presence of small floating debris in trees and bushes are good indications of the flood level. One should take into account that bushes bend under the force of the flow and that, considerable waves could have occurred. Both actions indicate higher flood levels than actually occurred. Flood marks on the banks, where wave action and run-up form surge are at a minimum, are generally preferable to those in bushes and trees. However, they disappear fast.

The first action, which has to be taken, is to paint the observed flood marks on walls and trees, where possible accompanied by the date of occurrence of the flood. A record of flood marks on the wall of a solid structure is an important future source of information.

Try to get as many reliable flood marks as possible along the river. Also in areas which at the time are not yet developed. A good survey of flood marks of an extreme flood is an invaluable asset for the planning of future projects.

Sometimes flood marks are difficult to find, principally because one is too late and rains have cleared the coloring, or winds have cleared the debris from the trees. A good method then is to install a leveling instrument at the suspected flood level and to look through the instrument towards different objects. If the instrument is indeed at the approximate flood mark position, then the accumulation of, sometimes insignificant, marks may help to verify the flood level.

If one is really too late to find back any traces of the flood, one should gather information from people living in the area. Needless to say that such information is much less reliable.

Finally, where possible, take photographs of flood marks, or of people indicating a flood mark.

Computation

For a good slope area computation one should look for a fairly straight stable clean channel, without pools, rapids, island or sharp curves. No bridges or other obstructions should be downstream of the reach.

The reach to determine the cross-sectional area should be about ten times the width of the river; one should survey approximately five to ten cross-sections. The flood mark survey should be over a long enough distance to determine the water level and slope accurately. Taking into account the error of reading, this will often amount to a distance of several kilometers.

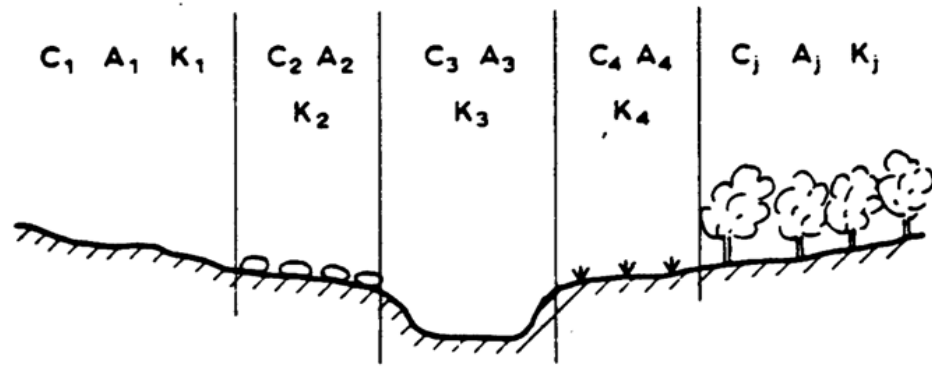


Fig. 8.33: Slope area

The following procedure is used to determine the discharge: first, area A_j and hydraulic radius R_j of parts of the cross-section are determined. The parts are selected in such a way that the roughness coefficient C_j in a part can be considered as a constant. The river slopes for all the different parts of the cross-section are considered to be equal. For every section applies Chézy (Eq. 8.48).

The hydraulic calculations are based on Chzy's formula:

$$Q_j = \bar{u}_j A_j = C_j A_j R_j^{1/2} i^{1/2} = K_j i^{1/2} \quad (8.48)$$

With:

- $K_j = C_j A_j R_j^{1/2}$ (-)
- C_j Chézy coefficient ($m^{1/2}$)
- R_j Hydraulic radius (m)
- A_j Cross sectional area (m^2)
- i bedslope (-)

The factor K_j , the so-called conveyance, contains the geometrical quantities. When using the Manning sand roughness (n), C_j reads,

$$C_j = \frac{R_j^{1/6}}{n_j} \quad (8.49)$$

By estimating the values of K_j the discharge can be calculated with:

$$Q = i^{1/2} \sum^j K_j \quad (8.50)$$

In the above method the greatest difficulty lies in the determination of channel roughness. It is very difficult for even an experienced surveyor to arrive at an objective value. Indicative values for channel roughness are provided in Table 8.1.

8.6.3 Simplified slope area method

A remarkable method developed by H.C. Riggs Riggs [1976] may be used to overcome the difficulty of subjectivity. Riggs postulates that in alluvial streams slope and roughness are

related. In more popular terms this means that the river adjusts its roughness (through bed forms) to the slope, or that the river adjusts its slope (through meandering) to the roughness. Experiments have shown that there indeed is a relation between roughness and slope, although the relation shows considerable scatter. However, Riggs showed that the error in the relation between slope and roughness is less than the error made by experienced surveyors in estimating the roughness.

The equation of the simplified method reads:

$$\log Q = 0.188 + 1.33 \log(A) + 0.05 \log(S) - 0.056 (\log S)^2 \quad (8.51)$$

In this equation the value of A should be representative for the reach under study. The cross-sectional area A should be determined on the basis of five to ten cross-sections:

$$A = \frac{\sum A_i}{N} \quad (8.52)$$

where N is the number of sections surveyed. The equation was tested in 64 rivers in the USA with discharges ranging from $2\text{m}^3/\text{s}$ to $2500\text{m}^3/\text{s}$, and with Chézy coefficients ranging from 14 to $65\text{ m}^{1/2}/\text{s}$. The method is extremely useful, also as a check on the previously mentioned slope area method.

8.7 Structures

8.7.1 Principles

On small rivers it is often convenient to measure flow by means of a weir or flume. Such structures have the advantage that they are less sensitive to the downstream conditions, the channel roughness and the influence of backwater than the velocity-area method for example.

The philosophy of the method is founded on the premise that the relation of discharge to water level is found empirically or is based on physical principles.

The water level, or head, is measured at a prescribed distance upstream of the structure. For the simple, and usual case, where the downstream water level is below some limiting condition and where it does not affect the upstream head, there is a unique relation between head and discharge. This condition is termed the free-flow or modular condition. If, however, the tailwater level affects the flow, the weir is said to be drowned, or submerged, and operates in the non-modular condition. For this condition an additional downstream measurement of head is required and a reduction factor must be applied to the modular or free-flow discharge equation. When the flow in the non-modular condition increases until the weir is almost or wholly submerged, the structure no longer performs as a measuring device.

There is a significant degradation in the accuracy of discharge measurements in the non-modular flow condition. This degradation is due mainly to the difficulty in measuring the downstream head because of turbulence and the uncertainty in the coefficient of discharge in the non-modular range.

Tab. 8.1: Values of Manning's n and Chzy's C

Type of channel and description	Manning coefficient (n)	Chézy's coefficient			
		$R_h = 1\text{m}$	$R_h = 2.5\text{m}$	$R_h = 5\text{m}$	$R_h = 10\text{m}$
Excavated or dredged					
(1) Earth, straight and uniform					
(a) Clean, recently completed	0.016 to 0.020	63 to 50	72 to 58	81 to 65	91 to 73
(b) Clean, after weathering	0.018 to 0.025	55 to 40	64 to 46	72 to 52	81 to 59
(c) Short grass, few weeds	0.022 to 0.033	45 to 30	53 to 35	59 to 40	67 to 44
(2) Rock cuts					
(a) Smooth and uniform	0.025 to 0.040	40 to 25	46 to 29	52 to 33	59 to 37
(b) Jagged and irregular	0.035 to 0.050	29 to 20	33 to 23	37 to 26	42 to 29
Natural streams					
Minor streams (top width at flood stage less than 30 m) on plains; clean, straight, full stage, no rifts or deep pools	0.025 to 0.033	40 to 30	46 to 35	52 to 40	59 to 44
Flood plains					
(1) Pasture, no brush					
(a) Short grass	0.025 to 0.035	40 to 29	46 to 33	52 to 37	59 to 42
(b) High grass	0.030 to 0.050	33 to 20	39 to 23	44 to 26	49 to 29
(2) Rock cuts					
(a) No crop	0.020 to 0.040	50 to 25	58 to 29	65 to 33	73 to 37
(b) Mature row crops	0.025 to 0.045	40 to 22	46 to 26	52 to 29	59 to 33
(c) Mature field crops	0.030 to 0.050	33 to 20	39 to 23	44 to 26	49 to 29
(3) Brush					
(a) Scattered brush, heavy weeds	0.035 to 0.070	29 to 14	33 to 17	37 to 19	42 to 21
(b) Light brush and trees (without foliage)	0.035 to 0.060	29 to 17	33 to 19	37 to 22	42 to 24
(c) Light brush and trees (with foliage)	0.040 to 0.080	25 to 12	29 to 14	33 to 16	37 to 18
(c) Medium to dense brush (without foliage)	0.045 to 0.110	22 to 9	26 to 10.5	29 to 12	33 to 13
(d) Medium to dense brush (with foliage)	0.070 to 0.160	14 to 6.5	17 to 7.5	19 to 8	21 to 9
(4) Trees					
(a) Cleared land with tree stumps, no sprouts	0.030 to 0.050	33 to 20	39 to 23	44 to 26	49 to 29
(b) Same as above, but with heavy growth of sprouts	0.050 to 0.080	20 to 12	23 to 14	26 to 16	29 to 18
(c) Heavy stand of timber, a few felled trees, little undergrowth, flood stage below branches	0.080 to 0.120	12 to 8.5	14 to 9.5	16 to 11	18 to 12
(d) Same as above, but with flood stage reaching branches	0.100 to 0.160	10 to 6.5	12 to 7.5	13 to 8	15 to 9
(e) Dense willows in midsummer	0.110 to 0.200	9 to 5	10.5 to 6	12 to 6.5	13 to 7.5

In order to increase the range of a structure in the free-flow condition, it is sometimes convenient to raise the design height; otherwise for a weir the device may be used as a section control in the non-modular condition, and rated by a current meter in this range.

The installation of a measuring structure in a river requires major civil engineering work and each device needs to be designed as such with due attention to foundations. Ground conditions may require sheet piling and cut-offs to prevent the seepage of water under or around the structure or risks to stability. If provision for energy dissipation downstream is not included in the construction, for example, there may be a tendency to scour depending on the ground conditions. If this becomes excessive the stability of the structure will be in danger. If the structure, however, is founded on rock, for example, such problems may not be severe but nevertheless due attention may still be required with regard to energy dissipation. The energy downstream of a structure is normally dissipated by a hydraulic jump and generally design and construction considerations involve the installation of a stilling basin and a suitable elevation for the floor of the basin.

The capital cost of installing a measuring structure is much greater than the capital cost of installing a velocity-area station but the operational costs of a structure are very much lower. This is due to the calibration costs in manpower in establishing the stage-discharge relation for a velocity-area station. The advantage, in this respect, of a standard measuring structure is that records of discharge are obtained immediately on completion of the installation.

A weir or a flume is basically a section control designed and built to specific criteria. The rating equation for a stage discharge relation and measuring structure, therefore, take the same form, which is:

$$Q = Ch^n \quad (8.53)$$

Ideally the flow conditions upstream of a measuring structure are governed by the geometry of the structure and the approach channel, and by the physical properties of the water. They are not affected by the flow conditions in the channel downstream or by the roughness and geometry of the channel upstream.

At the control section critical flow conditions occur, where for a given discharge the depth is such that the total head is a minimum. The total head is the total energy of the flow per unit weight of water and, by Bernoulli's theorem; this is the sum of the potential head, the pressure head and the velocity head. It is generally referred to the crest of the structure as a datum.

In presenting the theoretical analysis for the establishment of the discharge equation the broad-crested weir is used (see Fig. 8.34). Taking the critical section to occur where the flow is parallel near the end of the crest of the weir, then the Bernoulli equation gives:

$$H = d + \frac{u^2}{2g} \quad (8.54)$$

With:

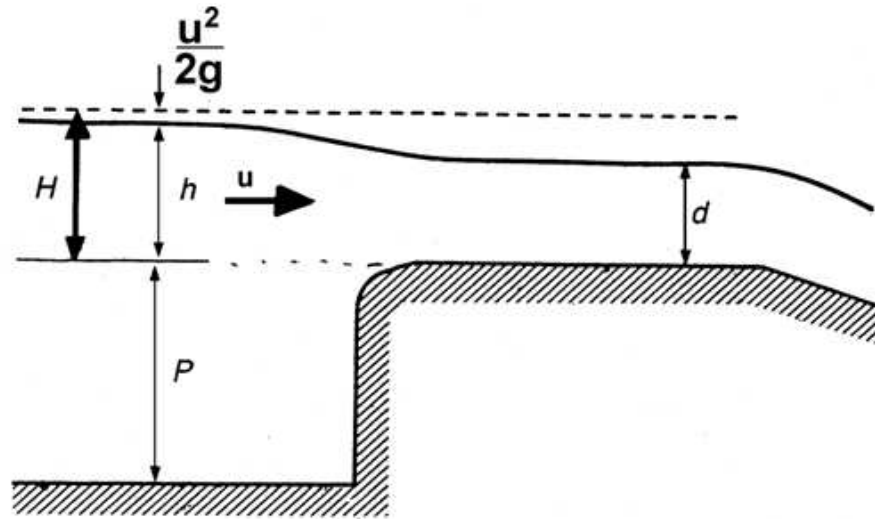


Fig. 8.34: Schematic illustration of principle and theory of flow over broad crested weir

- H the total head (m)
 g the acceleration due to gravity (m/s^2)
 u the velocity on the streamline (m/s)
 d depth of flow over the crest (m)
 h depth of flow in front of the weir (m)

If the approach channel is deep, the total head H is the same for all streamlines and it follows from Equation 8.54 that the velocity at the critical section is constant with depth and equal to \bar{u} , the mean velocity. The discharge over a width b is:

$$Q = b d \bar{u} \quad (8.55)$$

and substituting from Equation 8.54

$$Q = b d \sqrt{2g(H-d)} \quad (8.56)$$

Differentiating Equation 8.56, treating H as a constant and putting $dq/dd=0$ gives the following equation for critical flow conditions

$$d_c = \frac{2}{3} H \quad (8.57)$$

or

$$Q = \left(\frac{2}{3}\right)^{2/3} b \sqrt{g} H^{3/2} \quad (8.58)$$

Equation 8.58 is derived from theoretical concepts and calibration of a structure imposes on the equation a coefficient of discharge. The equation then becomes:

$$Q = \left(\frac{2}{3}\right)^{2/3} C_d b \sqrt{g} H^{3/2} \quad (8.59)$$

Since the total head H cannot be measured in practice, an iterative procedure is necessary to compute the discharge from Equation 8.59. In order to avoid this cumbersome procedure the discharge equation can be presented as

$$Q = \left(\frac{2}{3}\right)^{2/3} C_d C_v b \sqrt{g} H^{3/2} \quad (8.60)$$

This is the basic equation for measuring structures with:

C_v the dimensionless coefficient for the velocity of approach (-)

C_d the coefficient of discharge ($\text{s/m}^{1/2}$)

From an inspection of Equations 8.59 and 8.60 it can be seen that:

$$C_v = \left(\frac{H}{h}\right)^{2/3} \quad (8.61)$$

The Bernoulli equation relates H and h as follows:

$$H = h + \frac{\bar{u}^2}{2g} = h + \frac{Q^2}{2gA^2} \quad (8.62)$$

The energy head H and measured water level in front of the structure will be practically equal if \bar{u} is negligible. For a large range of discharges this will be the case if A is large. This is the reason that a stilling basin of water upstream of the structures often is part of installation requirements.

With each of the discharge equations for measuring structures, limitations are imposed as to their use in practice. Such limitations concern in range in head under which a laboratory calibration was made, the distance upstream to the head measurement section, the limits on certain ratios such as h/P , where P is the height of the weir, and others which will be presented later. The values and uncertainties of the coefficients of discharge and velocity are dependent on maintaining these limitations in the field installation. If the limitations are relaxed for any reason the measuring structure may still produce a record of streamflow but the uncertainty of the measurement will be impaired. In most, if not all, of these cases no data are available to give values of uncertainties in the coefficients, and therefore in the discharge measurements where the specified limitations have been relaxed. The only resort in these circumstances is to field calibration.

8.7.2 Description of structures

Measuring structures may be divided into the following categories:

- Thin/sharp crested weirs
- Broad crested weirs
- Flumes
- Compound measuring structures
- Non-standard weirs

As an overview the main concept in each category of structures will be discussed, with the relevant discharge formulae. For more details or specific designs numerous handbooks exist and must be consulted for specific installations or flow conditions.

For the various discharge formulae provided below the following conventions were adopted.

- Q discharge (m^3/s)
- g acceleration due to gravity (m/s^2)
- C coefficient of discharge (-)
- b length of a notch or weir and breath of a flume (m)
- h gauged head (m)
- P level of top of weir above the bottom (m)

Thin/Sharp crested weirs

A number of sharp crested weirs are depicted in Figure 8.35. The sharp crested weirs are either rectangular or formed as a V with a certain angle. The rectangular weirs can be contracted or suppressed. For all thin plate weirs it is essential that the plates (or angle iron) are kept clean and smooth so that the nappe does not cling to the downstream side.

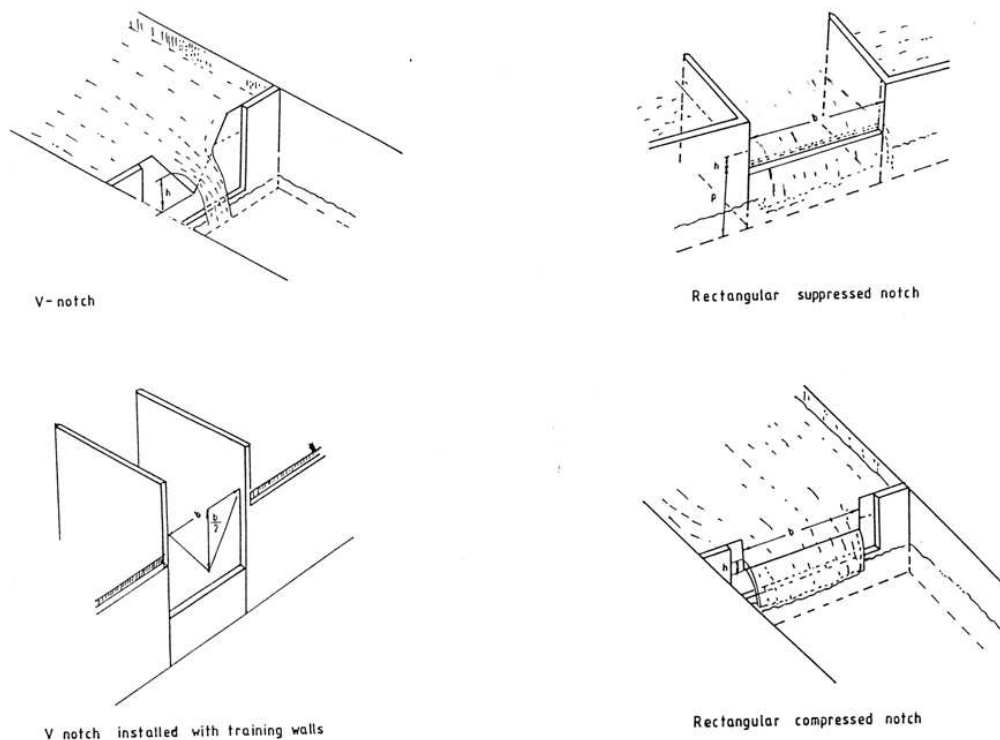


Fig. 8.35: Examples of thin plate weirs

V-notch The most common V notch has an angle of $\theta = 90^\circ$. In that case the dimension across the top is twice the vertical depth. The discharge formula reads.

$$Q = \frac{8}{15} \sqrt{2g} C_d \tan \frac{\theta}{2} h^{5/2} \quad (8.63)$$

approximated by

$$Q = 1.34h^{2.5} \quad (8.64)$$

Other V-notches are the ‘half’ and ‘quarter’ V-notch, with $\tan(\theta/2)=0.5$ and $\tan(\theta/2)=0.25$ respectively.

Rectangular contracted or compressed notch The width, b , of the notch does not completely extend over the full width, B , of the river. The vertical sides of the cross-section at the notch are thin plated as well. The general discharge equation reads:

$$Q = \frac{2}{3} \sqrt{2g} C b h^{3/2} \quad (8.65)$$

A more useful equation that awards the calculation of the coefficient of discharge is:

$$Q = 0.554(1 - 0.0035 \frac{h}{P})(b + 0.0025) \sqrt{g}(h + 0.001)^{3/2} \quad (8.66)$$

Rectangular surpressed notch This is a notch without side contraction (in contrary to a contracted or compressed notch). It also applies when a weir is subdivided into sections that are separated by training walls. The general formula reads:

$$Q = 2.95(0.602 + 0.0832 \frac{h}{P}) b h^{3/2} \quad (8.67)$$

With $h/P = 0.25$ the equations turns into the Rehbock formula:

$$Q = 1.84b h^{3/2} \quad (8.68)$$

The Kriel factor In all standard formulae for thin-plate weirs it is assumed that they are really ‘thin plated’ i.e. the thickness of the crest is only 1-2 mm. Often many of the crests are considerably thicker as they are made from commercial irons, and because of this a correction factor has to be introduced. The calculated discharge for rectangular notches is multiplied by this so-called Kriel factor when the head is below 0.6m.

Kriel factor: $1 + \frac{0.012}{h^{0.8}}$ for $h < 0.6\text{m}$.

Broad Crested Weirs

With broad crested weirs the critical flow conditions are achieved by raising the bottom of the stream according to a certain profile. Different shapes of crests have been designed with different names often related to the shape and specific discharge formulae.

Sometimes broad crested weir formulae are also applied when the flow through flumes and the sharp crested weirs contained within a gauging structure exceeds the design capacity. The most

common method in that case is to assume that the cut-off wall acts as a broad crested weir. The accuracy of the flows calculated in this way is low. Some typical broad crested weirs and discharge formulae are described below.

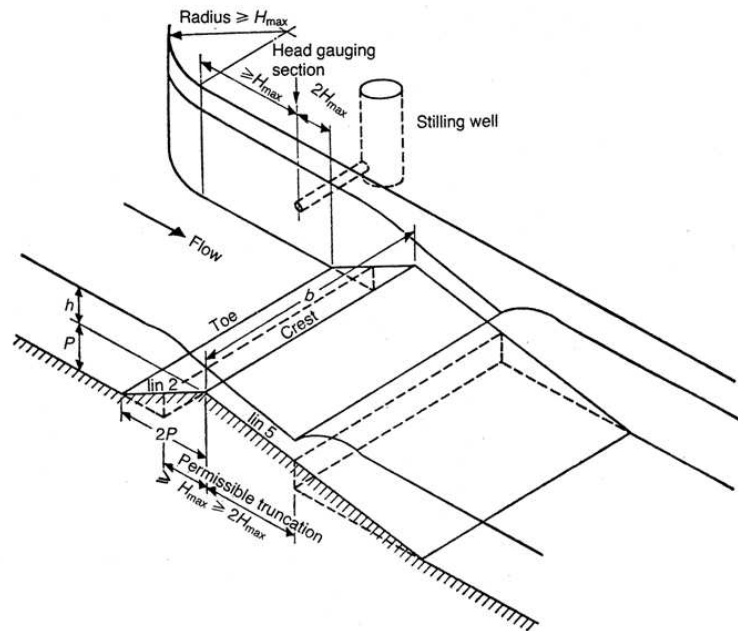


Fig. 8.36: The triangle profile (Crump) weir

The triangle profile (Crump) weir The weir has a slope 1:2 on the upstream face and 1:5 on the downstream face.

Discharge formula:

$$Q = 0.633\sqrt{gb}H^{3/2} \quad (8.69)$$

The flat V weir The flat V weir has the same section as the triangular profile weir, 1:2 upstream slope and 1:5 downstream slope, but in elevation has a crest slope of 1:10, 1:20 or 1:40 so that it takes the form of a shallow V when viewed in the direction of flow. With this geometry, it is therefore sensitive to low flows but at the same time has a wide flow range.

A diagrammatic illustration of the basic weir form is shown in Figure 8.37. The discharge over a flat V weir may be within the V, above the V and within vertical side walls, or above the V and within trapezoidal side walls. To allow for these conditions, a shape factor, Z , is included in the discharge equation. The equation of discharge is:

$$Q = \frac{4}{5}C_dC_v\sqrt{gm}Zh^{5/2} \quad (8.70)$$

In terms of total head the discharge equation is:

$$Q = \frac{4}{5}C_d\sqrt{gm}ZH^{5/2} \quad (8.71)$$

The rectangular profile weir Of all the pre-calibrated broad crested weirs in operational use today there has probably been more research carried out on the rectangular profile weir than on any other. This has not been because of the merit of the weir as a gauging structure but rather due to the hydraulic considerations in the variable coefficient range. Indeed, reported installations of the weir have been few compared to other types of weir. However, there are many existing rectangular profile weirs, which are used for operational purposes such as irrigation devices or for compensation water measurement from reservoirs, which were built before the International Standard on the weir was published. Some of these weirs might conform, even approximately, to the limitations given later although degradation in the uncertainty in discharge has to be accepted. The weir is one of the easiest to construct in the field, the main requisite being that it has to have sharp right-angle corners. The main disadvantages of the weir are that silt and debris collect behind the structure and it has a low modular limit. A diagrammatic illustration of the weir form is shown in Figure 8.38.

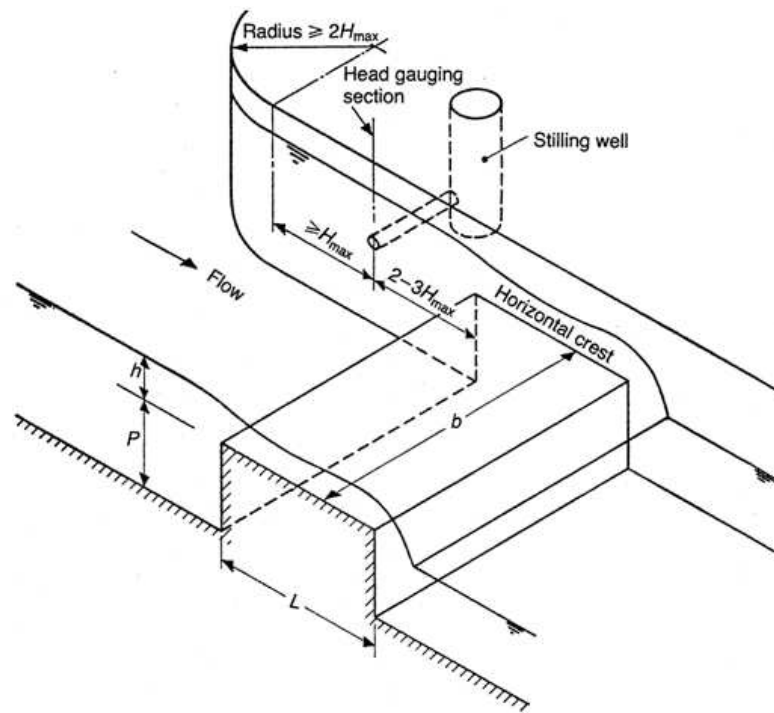


Fig. 8.38: The rectangular profile weir

The equation of discharge is:

$$Q = \left(\frac{2}{3}\right)^{3/2} C \sqrt{gb} H^{3/2} \quad (8.76)$$

The coefficient of discharge C is a constant value of 0.86 in the range

$$\frac{h}{p} \leq 0.5 \text{ and } \frac{h}{L} \leq 0.3$$

where L (m) is the length of the weir in the direction of flow.

For computer processing C may be obtained from the following equation:

$$C = 0.888 - 0.093y + 0.133y^2 - 0.021y^3 - 0.151x + 0.102xy - 0.065xy^2 + 0.310x^2 + 0.028x^2y - 0.102x^3 \quad (8.77)$$

With: $x = h/L$ $y = h/P$

Other practical limitations for the use of Equation 8.76 are:

h should not be less than 0.06m;

b should not be less than 0.3m;

P should not be less than 0.15m;

L/P should not be less than 0.15 nor greater than 7.0;

h/P should not be greater than 2.5 (variable coefficient range);

h/L should not be greater than 2.4 (variable coefficient range)

The location of the head measurement section is at 3-4 times H_{max} upstream from the weir block.

Flumes

A flume is a flow measurement device, which is formed by a constriction in a channel. The constriction is a narrowing in the channel mostly combined with a hump.

Flumes are in particular recommended in streams where siltation of a weir is expected to be a mayor problem. However, it should be realized that the construction is complex (and costly) and that attention must be given to the appropriate rating.

It is essential to construct the flumes to the dimensions as specified in the standard designs. For the same reason the heads should be measured at the positions specified.

A typical design of a flume is provided in Figure 8.39, which has rectangular cross-sections.

There are variations to this design with different cross-sectional shapes such as U-shaped trapezoidal shaped cross-sections.

An example of a short throated flume is the Parshall flume. It has a rectangular cross-section and comprises three main parts; a converging inlet section with a level floor, a throat section with a downward sloping floor and a diverging outlet section with an upward sloping floor (see Fig. 8.40). The control section of the flume is not located in the throat as on the previous flumes mentioned but near the end of the level floor, or crest in the converging section.

Flumes are supposed to operate under free flow conditions, i.e. the flow is unaffected by the downstream water level and only the upstream level (h_1) needs to be measured. If the downstream water level h_b exceeds a certain level, free flow conditions no longer exist and the flume is said to be submerged. The level that must not be exceeded depends on the size of the flume, and is for 1ft to 8ft (0.30m to 2.4m) flumes $0.7h_1$ and for 10ft to 50ft (3.0m to 15.2m) flumes $0.8h_1$. If the flume becomes submerged, h_b must be measured and the flow adjusted accordingly.

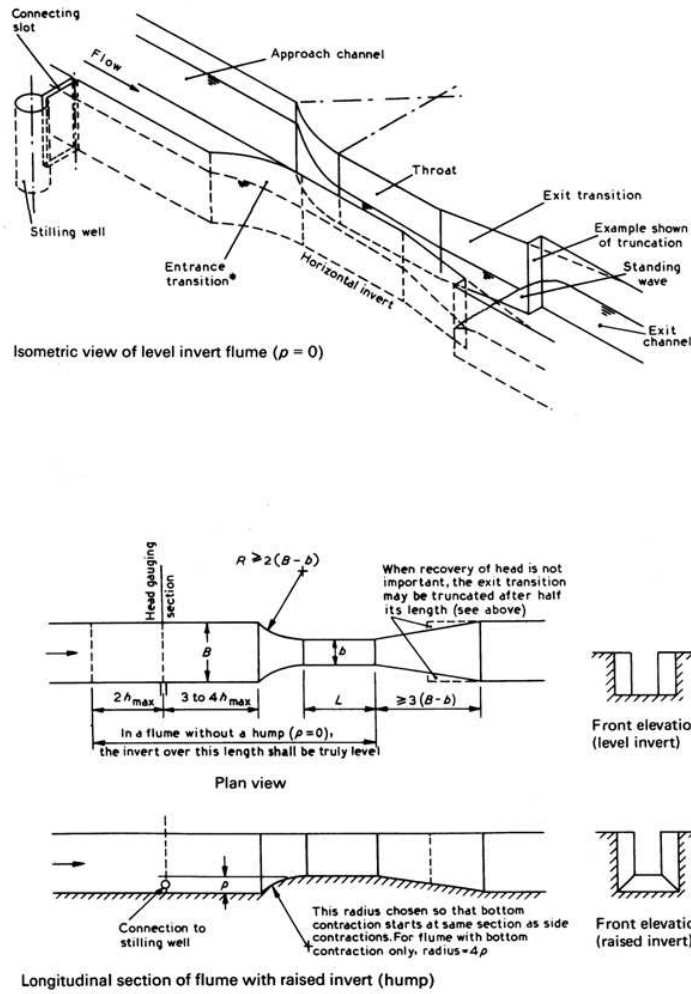


Fig. 8.39: Typical design of a flume

In case of high risk of submergence a tapping for measuring the downstream water level is used. Different sizes of Parshall flumes, related to the design discharges to be measured, can be applied. Their typical dimensions and discharge formulas have been well investigated (see Tab. 8.2 and 8.3). A Parshall flume is typically identified by the width of the throat. One will talk of an 8ft Parshall flume.

The discharge equation of a Parshall flume is:

$$Q = Kh_1^n \tag{8.78}$$

where K and h are derived from the table to the applicable flume.

At some gauging stations there is a combination of flumes and sharp-crested weirs. The head is then not measured at the prescribed point in the flume, but upstream of the flume. Experiments at some flumes have indicated that the relation between the head in the flume and the upstream head is ± 0.83 . When the upstream pool level is measured 0.83 is therefore used as a conversion factor.

Tab. 8.2: Dimensions for Parshall flumes

Parshall flume dimensions (mm).

b	Dimensions as shown in Figure																	
	A	a	B	C	D	E	L	G	H	K	M	N	P	R	X	Y	Z	
1 in	25.4	363	242	356	93	167	229	76	203	206	19	—	29	—	—	8	13	3
2 in	50.8	414	276	406	135	214	254	114	254	257	22	—	43	—	—	16	25	6
3 in	76.2	467	311	457	178	259	457	152	305	309	25	—	57	—	—	25	38	13
6 in	152.4	621	414	610	394	397	610	305	610	—	76	305	114	902	406	51	76	—
9 in	228.6	879	587	864	381	575	762	305	457	—	76	305	114	1080	406	51	76	—
1 ft	304.8	1372	914	1343	610	845	914	610	914	—	76	381	229	1492	508	51	76	—
1 ft 6 in	457.2	1448	965	1419	762	1026	914	610	914	—	76	381	229	1676	508	51	76	—
2 ft	609.6	1524	1016	1495	914	1206	914	610	914	—	76	381	229	1854	508	51	76	—
3 ft	914.4	1676	1118	1645	1219	1572	914	610	914	—	76	381	229	2222	508	51	76	—
4 ft	1219.2	1829	1219	1794	1524	1937	914	610	914	—	76	457	229	2711	610	51	76	—
5 ft	1524.0	1981	1321	1943	1829	2302	914	610	914	—	76	457	229	3080	610	51	76	—
6 ft	1828.8	2134	1422	2092	2134	2667	914	610	914	—	76	457	229	3442	610	51	76	—
7 ft	2133.6	2286	1524	2242	2438	3032	914	610	914	—	76	457	229	3810	610	51	76	—
8 ft	2438.4	2438	1626	2391	2743	3397	914	610	914	—	76	457	229	4172	610	51	76	—
10 ft	3048	—	1829	4267	3658	4756	1219	914	1829	—	152	—	343	—	—	305	229	—
12 ft	3658	—	2032	4877	4470	5607	1524	914	2438	—	152	—	343	—	—	305	229	—
15 ft	4572	—	2337	7620	5588	7620	1829	1219	3048	—	229	—	457	—	—	305	229	—
20 ft	6096	—	2845	7620	7315	9144	2134	1829	3658	—	305	—	686	—	—	305	229	—
25 ft	7620	—	3353	7620	8941	10668	2134	1829	3962	—	305	—	686	—	—	305	229	—
30 ft	9144	—	3861	7925	10566	12313	2134	1829	4267	—	305	—	686	—	—	305	229	—
40 ft	12192	—	4877	8230	13818	15481	2134	1829	4877	—	305	—	686	—	—	305	229	—
50 ft	15240	—	5893	8230	17272	18529	2134	1829	6096	—	305	—	686	—	—	305	229	—

Tab. 8.3: Discharges for Parshall flumes

Throat width b	Discharge characteristics of Parshall flumes					
	Discharge range		Equation $Q=kh_1^n$ (metric)	Head Range (meters)		Modular limit h_2/h_1
	Min.	Max.		Min.	Max.	
	l/s					
1 in	0.09	5.4	$0.0604h^{1.55}$	0.015	0.21	0.50
2 in	0.18	13.2	$0.1207h^{1.55}$	0.015	0.24	0.50
3 in	0.77	32.1	$0.1771h^{1.55}$	0.03	0.33	0.50
6 in	1.50	111	$0.3812h^{1.58}$	0.03	0.45	0.60
9 in	2.50	251	$0.5354h^{1.53}$	0.03	0.61	0.60
1 ft	3.32	457	$0.6909h^{1.52}$	0.03	0.76	0.70
1 ft 6 in	4.80	695	$1.0560h^{1.538}$	0.03	0.76	0.70
2 ft	12.1	937	$1.4280h^{1.550}$	0.046	0.76	0.70
3 ft	17.6	1427	$2.1840h^{1.566}$	0.046	0.76	0.70
4 ft	35.8	1923	$2.9530h^{1.579}$	0.06	0.76	0.70
5 ft	44.1	2424	$3.7320h^{1.587}$	0.06	0.76	0.70
6 ft	74.1	2929	$4.5190h^{1.595}$	0.076	0.76	0.70
7 ft	85.8	3438	$5.3120h^{1.601}$	0.076	0.76	0.70
8 ft	97.2	3949	$6.1120h^{1.607}$	0.076	0.76	0.70
	m ³ /s					
10ft	0.16	8.28	$7.4630h^{1.60}$	0.09	1.07	0.80
12ft	0.19	14.68	$8.8590h^{1.60}$	0.09	1.37	0.80
15ft	0.23	25.04	$10.960h^{1.60}$	0.09	1.67	0.80
20ft	0.31	37.97	$14.450h^{1.60}$	0.09	1.83	0.80
25ft	0.38	47.14	$17.940h^{1.60}$	0.09	1.83	0.80
30ft	0.46	56.33	$21.440h^{1.60}$	0.09	1.83	0.80
40ft	0.60	74.70	$28.430h^{1.60}$	0.09	1.83	0.80
50ft	0.75	93.04	$35.410h^{1.60}$	0.09	1.83	0.80

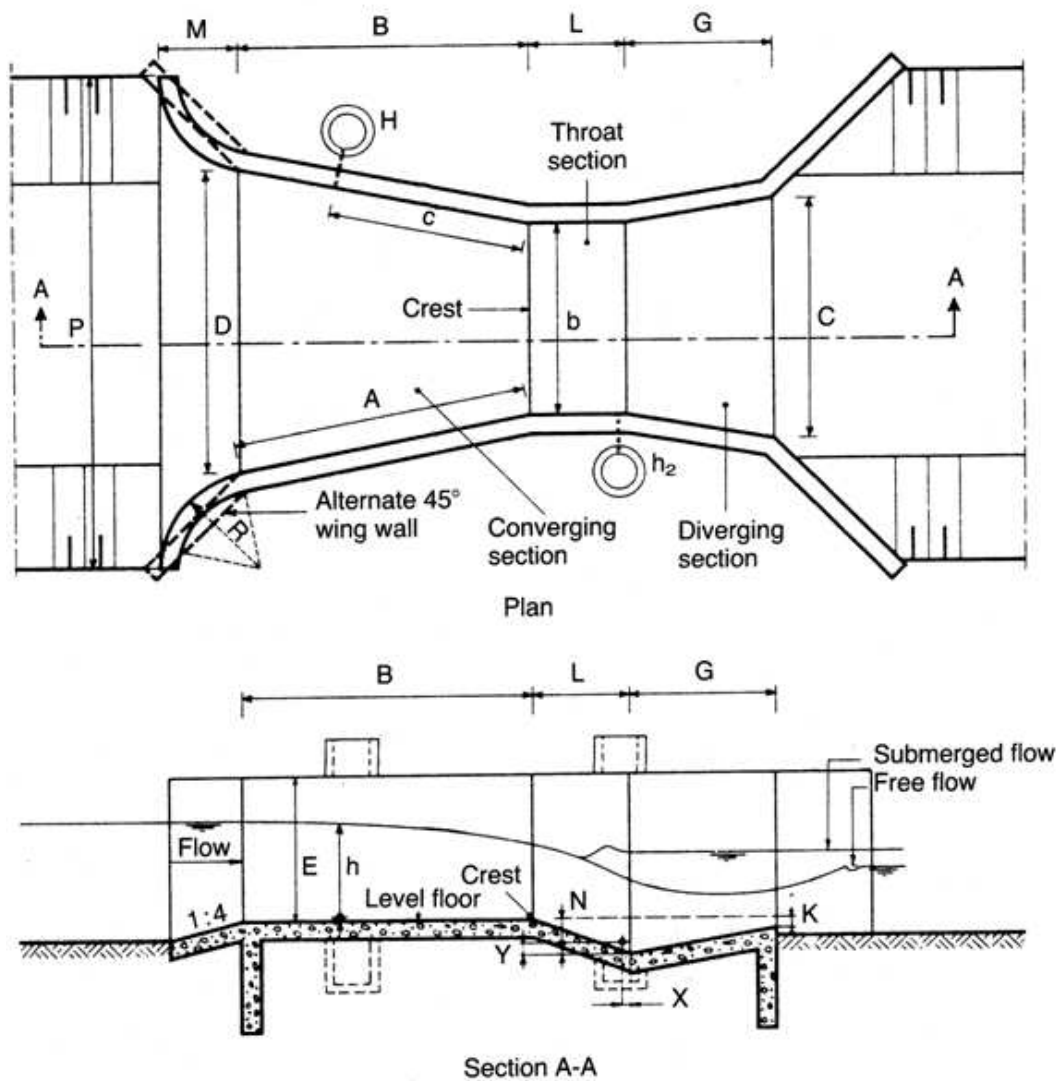


Fig. 8.40: Diagrammatic illustration of the Parshall flumes

Compound measuring structures

Compound structures are combinations of measuring devices in one and the same structure. This can be any combination of sharp-crested weirs, broad crested weirs and flumes. The applied combination is usually doctored for specific reasons and applies under specific conditions. Two main reasons can be mentioned for compound stations:

1. The structure has to be accurate for both low and high flows. Accurate low flow measurements need sufficient head above the structure. This is obtained by narrowing the profile. To the contrary, flood flows would need a sufficient cross-sectional area (width) over the structure. The ideal solution is a structure where the cross-sectional width increases with increasing discharge. A triangular shape of the cross-sectional area of the measuring structure fulfills this requirement. That is the reason that for low to moderate flows the V-notches are applied. For constructional reasons a V-notch is not suitable for

large flows. The alternative is a stepwise increasing profile, where each step has a sharp crest. The typical lay-out for a compound station that measures low and high flow in that case is a V-notch for the lower stages, and a stepwise profile that takes over at higher stages, see Figure 8.41 and Figure 8.42. The various sections so created can be separated by training walls.

Note that the rating equation for a compound station is also a compound of equations for the different stages. Usually the zero stage is at the lowest notch, or the bottom of the notch in case of a V-notch. For every stage where a next notch will have discharge the rating equation changes with the contribution of this notch.



Fig. 8.41: Compound gauging weir under construction (Zimbabwe, Mupfure catchment)

2. The structure needs to pass a considerable sediment load. In case of considerable sediment loads a flume is the right solution. Flumes are not easy to construct and get easily drowned. Combining a flume with a weir in one and the same structure provides the opportunity to pass high flows, create more head and pass the sediment load.

Stand alone large flumes have been constructed. They can handle large flows and large sediment loads. To compensate for the poor accuracy with low flows, a V-notch can be added, down or upstream of the flume. In general structures placed in series (one behind the other) are referred to as composite stations. They are not much favored, as the different stages that are measured at such a composite station are reason for confusion. Together with the measurement of actual stages it must be clearly indicated to which structure they apply. At some composite stations stages are measured for each structure separately, but also sometimes the measurement of stages is combined through complicated plumbing arrangements.



Fig. 8.42: Discharging compound gauging weir (Zimbabwe, Sebakwe river)

Non-standard structures

Most non-standard structures are structures that have been developed for other purposes than discharge measurements, but provide an opportunity to determine the discharge. The discharge relation in that case might not have been standardized and therefore should be carefully established. Examples of such structures are conduits, orifices, sluices and spillways. Also a volume change of a reservoir can be used for discharge estimation of a river or catchment. Obviously releases, seepage and evaporation from the reservoir have to be considered. Depending on the moment (no releases) or the timescale (hours, days) these could be negligible.

Generally, spillways have the advantage that only the upstream level is required, which is the reservoir level. It might well be that the levels of a reservoir are closely monitored anyway, as to keep track of the reservoir's volume. The general equation for discharge over spillways is:

$$Q = Cbh^{3/2} \quad (8.79)$$

With:

$$C \text{ for circular weirs} = 2.03 \left(\frac{h}{R}\right)^{0.07}$$

and

$$C \text{ for parabolic weirs} = 1.86h^{0.01}$$

Practical limits are:

h should not be less than 0.05m

h/p_1 should not be less than 3 (p_1 height of weir above upstream bed)

h/p_2 should not be less than 1.5 (p_2 height of weir above downstream channel)

b/h should not be less than 2

h_2/h should be less than 0.3 (h_2 downstream head above crest level)

h should be measured at a distance 2 to 3 times h_{max} upstream from the weir face

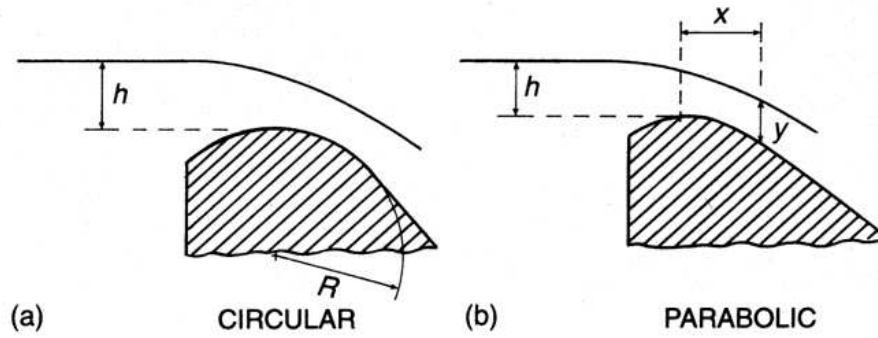


Fig. 8.43: Round crested weirs

The equations provided apply to spillways with vertical upstream faces. For sloping upstream faces correction factors for the discharge have to be applied.

9

Tracer Hydrology

The following articles, which are online available on Blackboard, give a good overview on the fundamentals of tracer hydrology.

9.1 General overview on tracer hydrology

Leibundgut, C., Seibert, J., 2011. *Treatise on Water*. Oxford: Academic Press, Ch. Tracer Hydrology, pp. 215–236

9.2 Applications

Wenninger, J., Uhlenbrook, S., Tilch, N., Leibundgut, C., 2004. Experimental evidence of fast groundwater responses in a hillslope/floodplain area in the Black Forest Mountains, Germany. *Hydrological Processes* 18, 3305–3322

Uhlenbrook, S., Frey, M., Leibundgut, C., Maloszewski, P., 2002. Hydrograph separations in a mesoscale mountainous basin at event and seasonal timescales. *Water Resources Research* 38

Gonzales, A. L., Nonner, J., Heijkers, J., Uhlenbrook, S., 2009. Comparison of different base flow separation methods in a lowland catchment. *Hydrology and Earth System Sciences* 13, 2055–2068

Uhlenbrook, S., Didszun, J., Wenninger, J., 2008. Source areas and mixing of runoff components at the hillslope scale - a multi-technical approach. *Hydrological Sciences* 53, 741–753

10

Interpolation techniques

Hydrology, being an earth science, has to cope with parameters that are geographically distributed, e.g. rainfall, evaporation, infiltration. The related issue of spatial heterogeneity of these parameters is usually an issue that has to be handled in hydrologic analysis, e.g. as to obtain a proper water balance. A point-observation of such a parameter is a single draw from the spatially distributed event. Nevertheless, estimated values at non-observed locations are required to be able to spatially integrate the event over the area of investigation. Estimates at non-observed locations and integration into an areal estimate can be obtained by various techniques, referred to as interpolation techniques. Well-known interpolation techniques are through methods known as:

- Inverse distance;
- Thiessen polygonse;
- Contouring;
- Kriging.

All these techniques to a certain extent introduce an error in the result compared to the true (unknown) areal value. The magnitude of the error varies per technique. However, it should be realised that only with few techniques a measure for error can be determined. The method known as Kriging applies a stochastic approach and therefore provides the opportunity to specify an error of the estimate in terms of the variance for the error of the areal estimate.

10.1 Inverse distance

The estimate at any point without observation is obtained from the sum of weighted observations in the neighbourhood. The weights are inverse proportional to the distance through a mathematical definition. This can be described by:

$$z'(x_0) = \sum \lambda_i \cdot z(x_i) \tag{10.1}$$

With:

$$\lambda_i = \frac{1/D_i^b}{\sum_{j=1}^n 1/D_j^b} \quad (10.2)$$

With:

- $z(x_i)$ Observation in point x_i
- λ_i Weight for observation $z(x_i)$
- $z'(x_0)$ Estimate at x_0
- D_i Distance between x_0 and x_i
- b exponent (e.g. 2)

This process is repeated for the total area and hence will result through areal integration into the areal value.

10.2 Thiessen polygons

Lines are drawn to connect the reliable observation points, including those just outside the area of study. The connecting lines are bisected perpendicularly to form a polygon around each point. The value of the observation point is assumed valid for the whole of the area of the polygon.

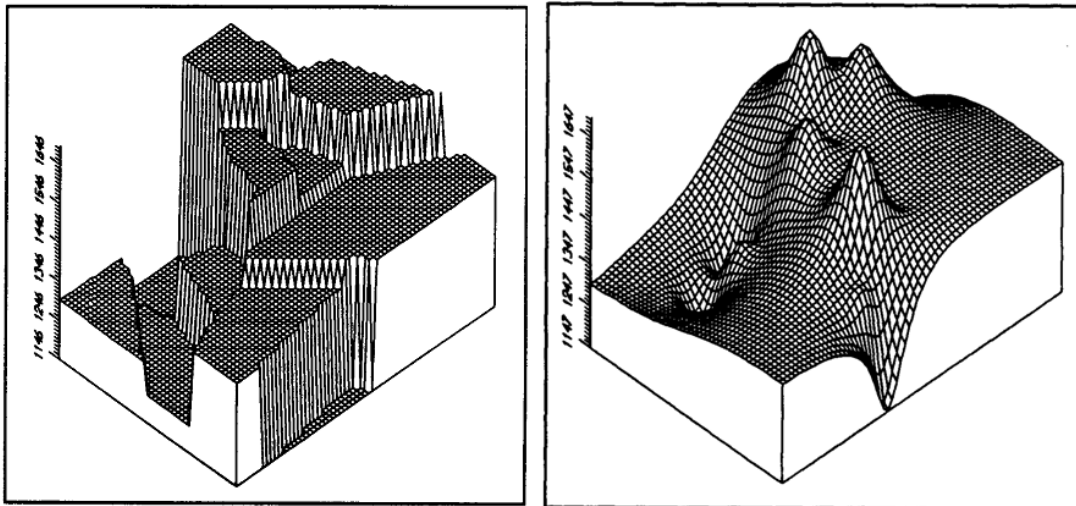


Fig. 10.1: Left: Thiessen polygon, Right: Inverse distance (b=2)

10.3 Contouring

Observations are plotted on the map and contours of equal values (iso-lines) are drawn. The average value between contours is assumed representative for the area between the contours.

10.4 Kriging

As is the case with the method of inverse distance, the estimate at any point is obtained from the sum of weighted observations in the neighbourhood. This can be described by:

$$z'(x_0) = \sum \lambda_i \cdot z(x_i) \quad (10.3)$$

With:

- $z(x_i)$ Observation in point x_i
- λ_i Weight for observation $z(x_i)$
- $z'(x_0)$ Estimate at x_0

The weights λ_i are now obtained by minimizing the variance (or standard error) of the error $\varepsilon = z'(x_0) - z(x_0)$. This can be mathematically solved, although in different ways for various types of Kriging. Different types of Kriging can be introduced for specific conditions, e.g. where clear spatial trends exist (rainfall on mountain slopes), or when specific mathematical schemes to solve the equations are assumed.

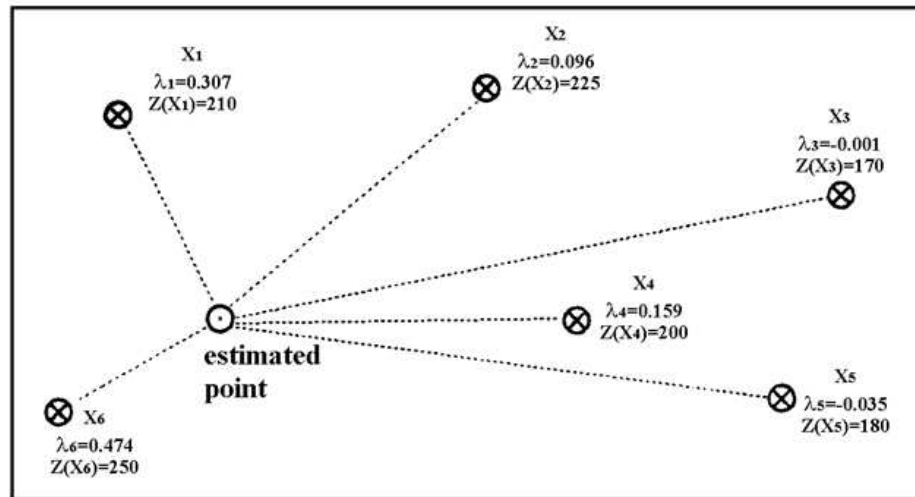


Fig. 10.2: Kriging weights

The most common type is ‘Ordinary Kriging’. In that case it can be demonstrated that:

$$\sum \lambda_i = 1 \quad (10.4)$$

The weights, λ_i , also define the contribution from each observation to the total variance σ_ε^2 for the error of the estimate at location x_0 . For ordinary Kriging it reads:

$$\sigma_\varepsilon^2 = \sum \lambda_i \cdot \gamma_i + \mu \quad (10.5)$$

With:

- σ_ε^2 the variance for the error of the estimate at location x_0
 λ_i weighing factor
 γ_i the variance for the error from the observation at x_i
 μ the Lagrange operator

The variance for the error, γ_i is a function of the distance h between x_i and x_0 and is obtained from the known values at point of observations:

$$\gamma(h) = \frac{1}{2} \frac{\sum (z(x+h) - z(x))^2}{N} \quad (10.6)$$

N represents the number of observations that are all a distance h apart. For practical reasons h is often divided in classes. The equation 10.6 delivers the variogram. Constructing the variogram is usually the first step in a Kriging analysis. The variogram based on observations delivers a scatter plot of h against γ . When calling a best fit line a model, distinct models of variograms can be defined, see Figure 10.3.

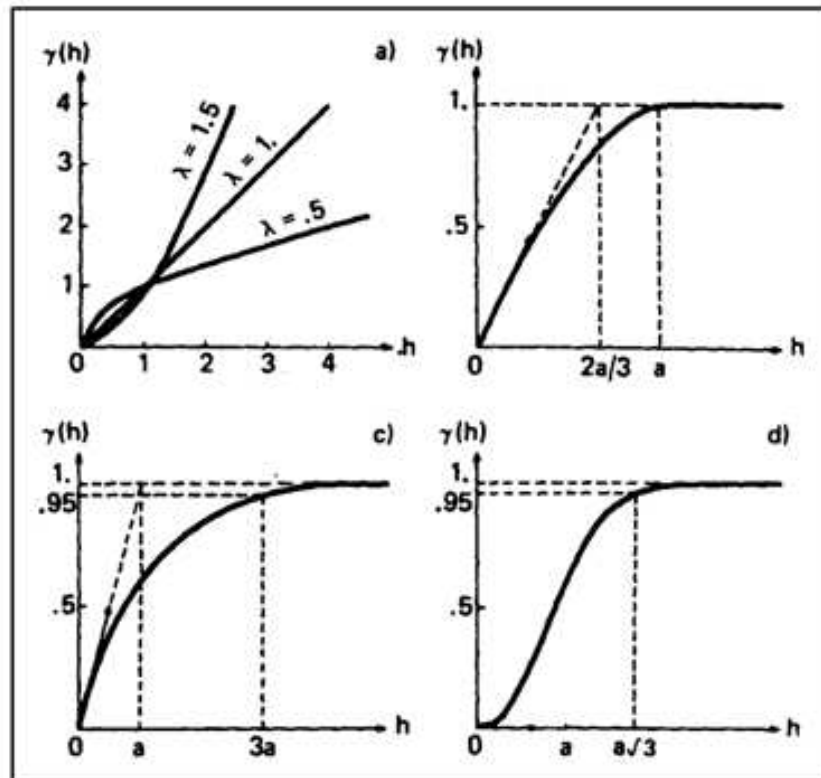


Fig. 10.3: Distinct models of the variogram

Important further characteristics of the models are the sill and the nugget. If a sill can be defined, it sets the maximum for γ . A sill indicates that the effect of observations further away diminishes. The nugget is a measure for the randomness of observations at one and the same location, see Figure 10.4.

With ordinary Kriging the weights, λ_i , are obtained from solving the following set of equations, presented in matrix notation in Equation 10.7.

Tab. 10.1: Distinct models of the variogram

Type	Formula	Slope at the origin Range		Sill
Nugget effect	$\gamma(h) = C (1-\delta)$	∞	0	C
Monomial	$\gamma(h) = \omega h ^\lambda$	∞	∞	∞
Spherical	$\gamma(h) = \begin{cases} \omega \left[\frac{3}{2} \frac{ h }{a} - \frac{1}{2} \left(\frac{ h }{a} \right)^3 \right] & h \leq a \\ \omega & h > a \end{cases}$	$0 < \lambda < 1$	∞	∞
		$\lambda = 1$	ω	∞
		$1 < \lambda < 2$	0	0
Exponential	$\gamma(h) = \omega [1 - \exp(- h /a)]$	ω/a	$3a$	ω
Gaussian	$\gamma(h) = \omega [1 - \exp(- h ^2/a^2)]$	0	$a\sqrt{3}$	ω

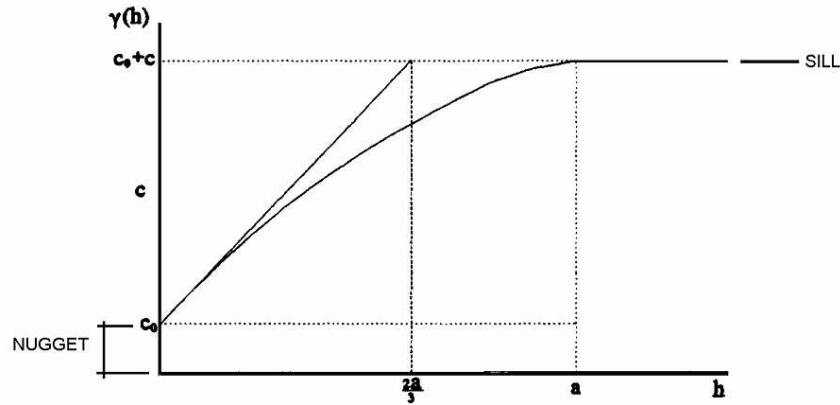


Fig. 10.4: Spherical variogram model, definition of sill and nugget

$$\begin{bmatrix} \gamma(x_1, x_1) & \gamma(x_1, x_2) & \dots & \gamma(x_1, x_n) & 1 \\ \gamma(x_2, x_1) & \gamma(x_2, x_2) & \dots & \gamma(x_2, x_n) & 1 \\ \vdots & \vdots & \vdots & \vdots & \vdots \\ \gamma(x_n, x_1) & \gamma(x_n, x_2) & \dots & \gamma(x_n, x_n) & 1 \\ 1 & 1 & \dots & 1 & 0 \end{bmatrix} \cdot \begin{bmatrix} \lambda_1 \\ \lambda_2 \\ \vdots \\ \lambda_n \\ \mu \end{bmatrix} = \begin{bmatrix} \gamma(x_0, x_1) \\ \gamma(x_0, x_2) \\ \vdots \\ \gamma(x_0, x_n) \\ 1 \end{bmatrix} \tag{10.7}$$

With:

$\gamma(x_i, x_j)$ γ according to a distance h between x_i, x_j

$\gamma(x_0, x_j)$ γ according to a distance h between x_0, x_j

All the required values for γ in the equations can be obtained from the variogram model. When writing the equations as $A\lambda = C$, the values for γ (and μ) are obtained by inverting matrix A and perform the operation $\lambda = CA^{inv}$.

10.4.1 Validation of Kriging results

Also at locations of observations an estimated value can be obtained through the Kriging process. Comparing the observations and the estimates gives the opportunity to verify the results. This is referred to as cross validation. The statistical parameters KAE and $KRMSE$ are defined to quantify the results of cross validation.

The Kriging Average Error (KAE):

$$KAE = \frac{1}{n} \sum_{i=1}^{i=n} \varepsilon_i(x_i) \quad (10.8)$$

With:

$$\varepsilon_i = z'(x_i) - z(x_i) \quad (10.9)$$

For satisfactory results KAE should approach zero.

The Kriging Reduced Mean Square Error ($KRMSE$):

$$KRMSE = \frac{1}{n} \sum_{i=1}^{i=n} \left(\frac{\varepsilon_i(x_i)}{\sigma_i(x_i)} \right)^2 \quad (10.10)$$

With:

$$\varepsilon_i^2 = (z'(x_i) - z(x_i))^2$$

σ_i^2 variance of error of the estimate derived from the Kriging process

For satisfactory results the $KRMSE$ should approach 1.

The usual procedure is to calculate KAE and $KRMSE$, adjust the parameters of the model variogram, and repeat the process until KAE and $KRMSE$ are acceptable close to zero and one, respectively.

Tab. 10.2: Example of cross validation

Station Name	UTM Easting [km]	UTM Northing [km]	Measured Mean Annual Rain [mm]	Estimated Mean Annual Rain [mm]	ε_i [mm]	σ_i [mm]	$(\varepsilon_i/\sigma_i)^2$
Murewa	422	8048	610	700	-90	130	0.5
Liemba	347	8003	640	560	80	120	0.4
Chiremwaremwa	382	7744	700	760	-60	150	0.2
Tandavel	475	7796	1150	950	200	140	2.0
Weleglegen	495	7808	1020	980	40	130	0.1
Makosa	447	8087	520	690	-170	140	1.5
Garuso	517	7902	1040	910	130	120	1.2
Mapai	397	7477	660	820	-160	200	0.6
Revue	503	7904	1000	900	100	130	0.6
Mazoi	500	8159	640	680	-40	160	0.1
				Sum	30		7.2

11

Design of networks

In order to be able to design or evaluate a measuring network, a criterion for the performance is required. This would allow comparing different network layouts. A useful criterion is the accuracy of the areal value derived from point observations. This can be expressed in terms of the variance of the error of estimate. By areal integration this parameter can directly be derived from the Kriging process that defines the variance of error at locations x_0 in the x, y plane. Under specific conditions also the negative exponential correlation function (as derived by Kagan) can deliver the variance of the error of the areal estimate.

11.1 Kriging

The Kriging process delivers at every point x_0 a value σ_ε^2 for the error of estimate. This indeed allows to obtain the areal error of estimate, but also indicates what region of the area has the largest error. Obviously this is the area where the network needs improvement, e.g. additional stations. By inserting fictitious stations the performance of the network can be reassessed and improved. This process is demonstrated in Figure 11.1 and Figure 11.2. When locating two additional stations in the upper zone the variance of the estimates in the upper zone of the region diminishes, obviously resulting in a more accurate estimate of the rainfall for the whole area.

11.2 Kagan

The negative exponential correlation function for data between neighbouring stations, as derived by Kagan, provides an opportunity to define the error of estimate. When the measured value, x , is used for the estimate, \hat{y} , a distance r away, the estimation formula is: $\hat{y} = ax$, with $a = 1$. According to the theory of regression and correlation (Chapter 2.4.2) it reads:

$$\sigma_\varepsilon^2 = a^2 \left(\frac{1}{\rho^2} - 1 \right) \sigma_x^2 \quad (11.1)$$

Substitution of the negative exponential correlation function and $a = 1$ delivers:

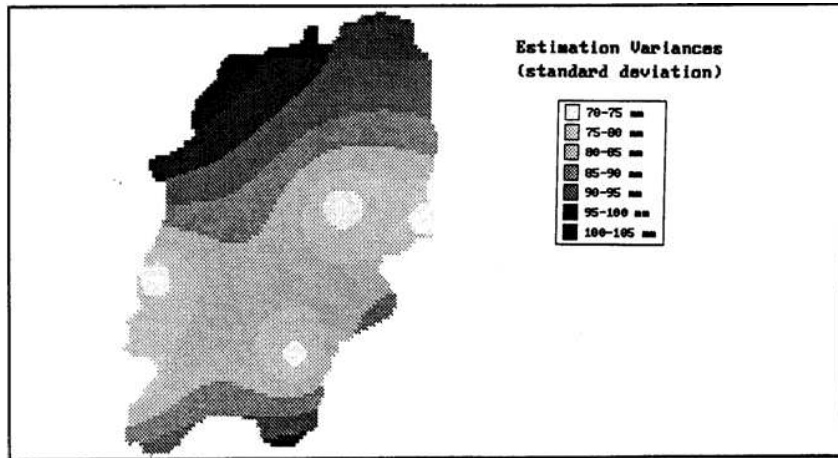


Fig. 11.1: Kriging estimation variances

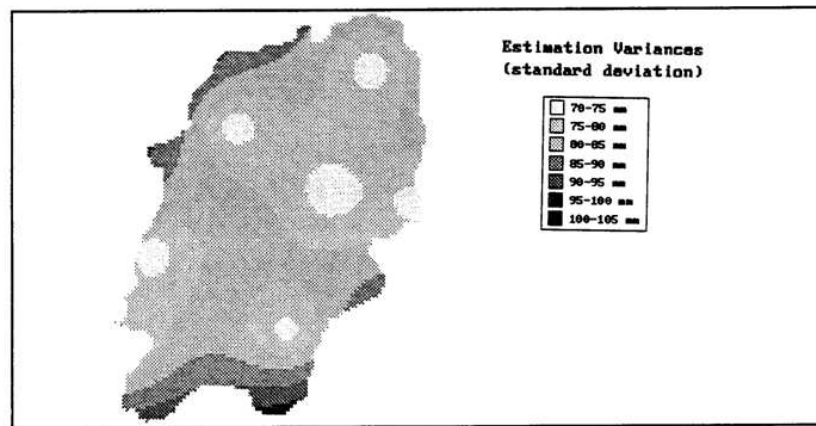


Fig. 11.2: Kriging estimation variances with two additional stations

$$\sigma_{\varepsilon}^2 = \left(\frac{e^{\frac{2r}{r_0}}}{\rho_0^2} - 1 \right) \sigma_x^2 \quad (11.2)$$

This applies to locations a distance r away from the location of observation. σ_x^2 is the variance of the measured (independent) data, x , at the location of observation. It can be shown through areal integration that the variance for a square area A reads:

$$E^2 = \sigma_x^2 \left((1 - \rho_0) + 0.23 \frac{\sqrt{A}}{r_0} \right) \quad (11.3)$$

This integration only holds if the data is isotope and homogeneous throughout the area A . The point of observation is assumed located in the middle of the square. The formula for the relative error is:

$$Z = CV_x \sqrt{(1 - \rho_0) + 0.23 \frac{\sqrt{A}}{r_0}} \quad (11.4)$$

With:

$$Z = E/\bar{x}$$

$$CV_x = \sigma_x/\bar{x} \text{ (=coefficient of variation of } x\text{)}$$

Assume that an area S has N stations and that the isotropy and homogeneity assumption holds throughout the area. Firstly this means that the area $A = S/N$. Secondly this means that the measurement is repeated in N stations and that the relative error reduces by a factor $1/\sqrt{N}$. Hence, for an area S with N stations the relative error is:

$$Z = CV_x \sqrt{\frac{1}{N} \left((1 - \rho_0) + 0.23 \frac{\sqrt{S/N}}{r_0} \right)} \tag{11.5}$$

This relation is depicted in the following Figures for rainfall over periods of observation of 1, 5, 10 days and a month.

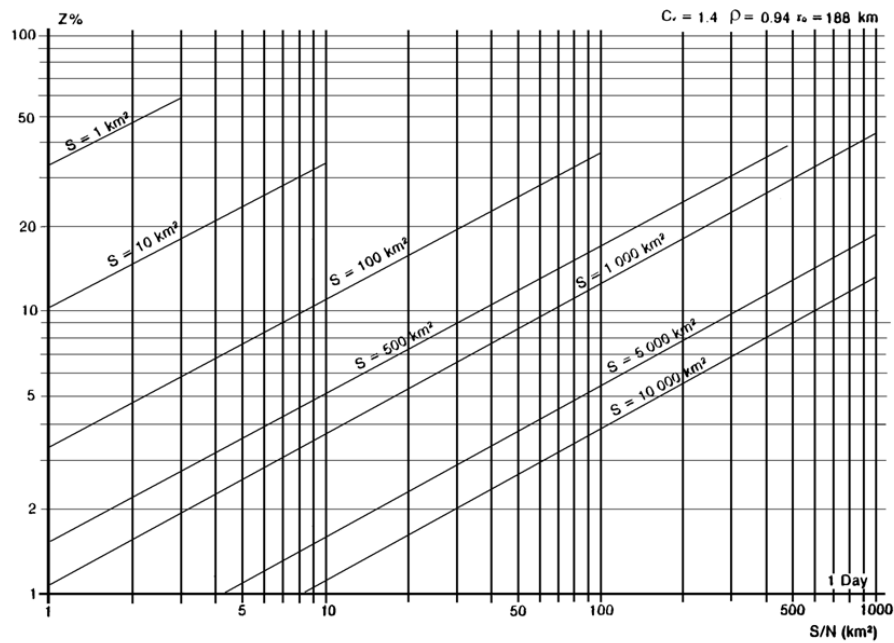


Fig. 11.3: Relation 11.5 depicted for rainfall over period of observation of 1 day

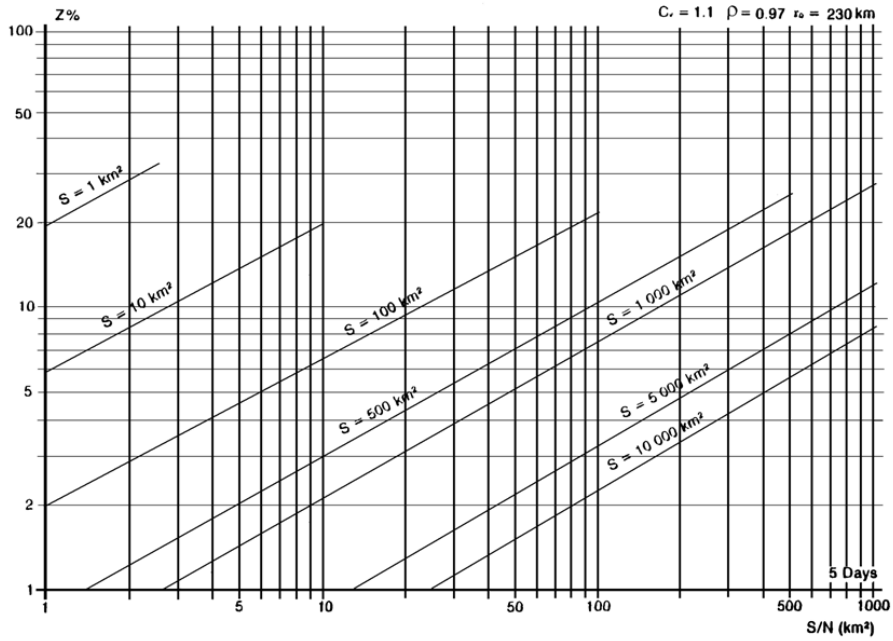


Fig. 11.4: Relation 11.5 depicted for rainfall over period of observation of 5 days

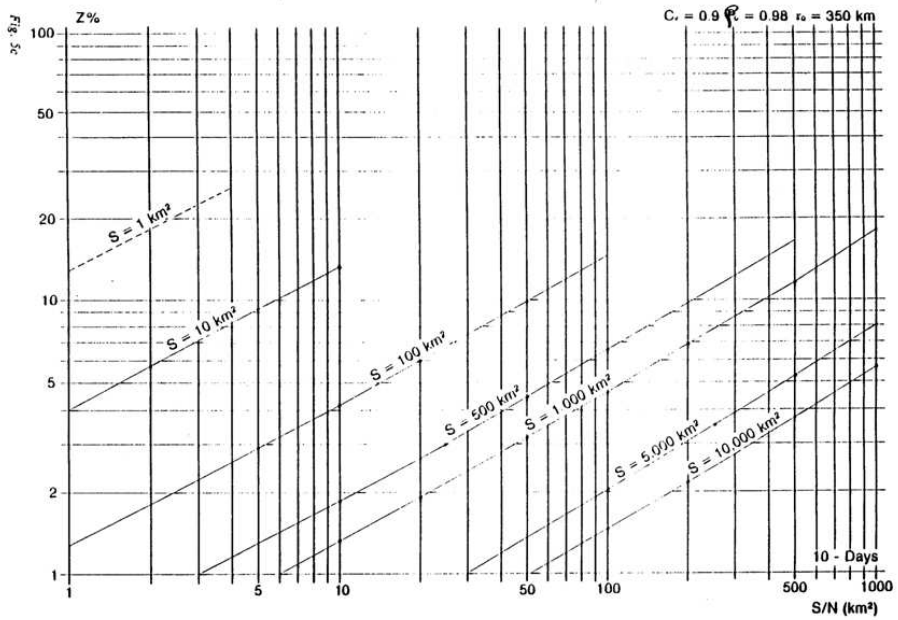


Fig. 11.5: Relation 11.5 depicted for rainfall over period of observation of 10 days

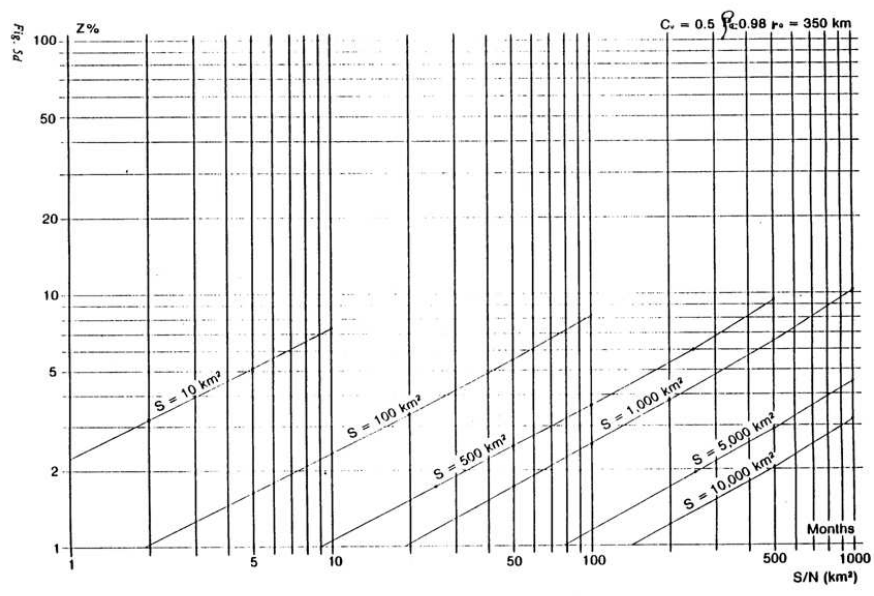


Fig. 11.6: Relation 11.5 depicted for rainfall over period of observation of a month

APPENDIX

A

Examples of statistical methods and distributions

A.1 Detection of spatial inhomogeneities

Table A.1 shows an example for detecting spatial inhomogeneities with the inverse distance method

Tab. A.1: Detection of spatial inhomogeneities, using inverse distance weights

Year	Measured Rainfall				Estimated rainfall				P _{est} - P _{meas}	P _{est} / P _{meas}
	P _{5,feb}	P _{425,feb}	P _{6,feb}	P _{5/(r_{119-ε})²}	P _{5/(r₁₁₉₋₄₂₅)²}	P _{5/(r_{119-ε})²}	P _{119,feb}			
58/59	92.6	204.2	31.2	0.1688	0.3021	0.0255	127.41	34.81	0.73	
59/60	85.8	65.9	149.8	0.1619	0.0975	0.1223	97.98	12.18	0.88	
60/61	108.0	48.8	32.2	0.0661	0.0722	0.0263	42.24	65.76	2.56	
61/62	26.3	7.2	10.4	0.0115	0.0154	0.0012	7.22	19.08	3.64	
62/63	204.6	91.9	97.9	0.2016	0.1359	0.0799	107.16	97.44	1.91	
63/64	42.2	30.8	43.2	0.0493	0.0639	0.0829	50.32	8.12	0.84	
64/65	69.0	36.1	30.4	0.0534	0.0534	0.0248	33.80	35.20	2.04	
65/66	124.9	96.2	128.0	0.1907	0.1423	0.1045	112.31	12.59	1.11	
66/67	353.6	197.7	261.3	0.3592	0.2925	0.2133	222.03	131.57	1.59	
67/68	227.9	76.0	270.3	0.1216	0.3817	0.2207	185.83	42.07	1.23	
68/69	58.2	258.0	64.0	0.0925	0.0658	0.0522	54.05	4.15	1.08	
69/70	47.2	49.1	45.5	0.1384	0.0726	0.0371	63.71	16.51	0.74	
70/71	63.4	71.6	28.4	0.1370	0.1059	0.0232	68.30	4.90	0.93	
71/72	327.1	208.3	157.0	0.2888	0.3081	0.1282	186.13	140.97	1.76	
72/73	141.8	87.5	57.8	0.1381	0.1294	0.0472	80.78	61.02	1.76	
73/74	107.7	5.1	52.3	0.0197	0.0075	0.0427	17.95	89.75	6.00	
74/75	356.5	277.0	212.3	0.4798	0.4098	0.1733	272.85	83.65	1.31	
75/76	255.4	148.1	108.5	0.1138	0.2191	0.0886	108.18	147.22	2.36	
76/77	580.5	308.3	528.5	0.3952	0.4561	0.4314	329.27	251.23	1.76	
77/78	86.9	30.0	49.1	0.1232	0.0444	0.0401	53.31	33.59	1.63	

ρ = .75 ρ₀ = .98 r₀ = 1500km

r₁₁₉₋₅ 25 km
 r₁₁₉₋₄₂₅ 26 km
 r₁₁₉₋₆ 35 km
 r_{max} 401 km
 Σ (1 / r²) 0.003895616

A.3 Students-t distribution

Table A.3 shows the points of the students-t distribution for a 5% level of significance.

Tab. A.3: Students-t distribution for 5% level of significance

$p=P(t \leq t_p):$		0.025	0.975
v:	4	-2.78	2.78
	5	-2.57	2.57
	6	-2.54	2.54
	7	-2.36	2.36
	8	-2.31	2.31
	9	-2.26	2.26
	10	-2.23	2.23
	11	-2.20	2.20
	12	-2.18	2.18
	14	-2.14	2.14
	16	-2.12	2.12
	18	-2.10	2.10
	20	-2.09	2.09
	24	-2.06	2.06
	30	-2.04	2.04
	40	-2.02	2.02
	60	-2.00	2.00
	100	-1.98	1.98
	160	-1.97	1.97
	inf	-1.96	1.96

Note: It is customary to take the next higher v-value in case the needed number of degrees of freedom is not listed in a table. It is evident that this practice results in a more severe test.

A.4 The Spearman's rank test

Table A.4 shows an example for the spearman's rank test performed on the yearly rainfall in station P6

Tab. A.4: Spearman's rank test for yearly rainfall in P6

Year	Xobs	Xrank	Kxi	Kyi	Di	Di^2	
46/47	521.2	473.3		1	6	-5	25
47/48	524.7	475.4		2	7	-5	25
48/49	770.8	502.4		3	26	-23	529
49/50	801.8	502.7		4	28	-24	576
50/51	650	508.2		5	19	-14	196
51/52	528.6	521.2		6	8	-2	4
52/53	850.9	524.7		7	34	-27	729
53/54	597.9	528.6		8	15	-7	49
54/55	921	529.6		9	36	-27	729
55/56	828.9	537.1		10	29	-19	361
56/57	734.2	559.7		11	23	-12	144
57/58	593.8	570.2		12	13	-1	1
58/59	594.2	593.8		13	14	-1	1
59/60	570.2	594.2		14	12	2	4
60/61	836	597.9		15	32	-17	289
61/62	508.2	619.5		16	5	11	121
62/63	830.7	626.7		17	31	-14	196
63/64	473.3	638.5		18	1	17	289
64/65	502.4	650		19	3	16	256
65/66	971.9	650.4		20	38	-18	324
66/67	768	657.3		21	25	-4	16
67/68	657.3	702.7		22	21	1	1
68/69	800.1	734.2		23	27	-4	16
69/70	529.6	760		24	9	15	225
70/71	475.4	768		25	2	23	529
71/72	988.2	770.8		26	39	-13	169
72/73	626.7	800.1		27	17	10	100
73/74	830.9	801.8		28	30	-2	4
74/75	896.1	828.9		29	35	-6	36
75/76	839.9	830.7		30	33	-3	9
76/77	1,179.80	830.9		31	40	-9	81
77/78	702.7	836		32	22	10	100
78/79	619.5	839.9		33	16	17	289
79/80	537.1	850.9		34	10	24	576
80/81	954.8	896.1		35	37	-2	4
81/82	638.5	921		36	18	18	324
82/83	502.7	954.8		37	4	33	1,089.00
83/84	760	971.9		38	24	14	196
84/85	650.4	988.2		39	20	19	361
85/86	559.7	1,179.80		40	11	29	841

Rsp	0.08
t	0.49
tcr	+,- 2.02

A.6 Split record tests

Table A.6 shows an example of a split record test for yearly rainfall in station P6

Tab. A.6: Example split record test

X1		X2	
46/47	521.2	66/67	768.0
47/48	524.7	67/68	657.3
48/49	770.8	68/69	800.1
49/50	801.8	69/70	529.6
50/51	650	70/71	475.4
51/52	528.6	71/72	988.2
52/53	850.9	72/73	626.7
53/54	597.9	73/74	830.9
54/55	921.0	74/75	896.1
55/56	828.9	75/76	839.9
56/57	734.2	76/77	1,179.8
57/58	593.8	77/78	702.7
58/59	594.2	78/79	619.5
59/60	570.2	79/80	537.1
60/61	836.0	80/81	954.8
61/62	508.2	81/82	638.5
62/63	830.7	82/83	502.7
63/64	473.3	83/84	760.0
64/65	502.4	84/85	650.4
65/66	971.9	85/86	559.7
Xavg	680.5		725.9
s	158.654		183.9288
Var	25171.1		33829.81

F-TEST, FOR STABILITY OF THE VARIANCE

Ft	=	0.744051
Fcr(0.025)		0.39
Fcr(0.975)		2.63

T-TEST, FOR STABILITY OF THE MEAN

tt	=	-0.834679
tcr	=	+,- 2.02

Bibliography

- Allen, R. G., Pereira, L. S., Raes, D., Smith, M., 1998. Crop evapotranspiration - Guidelines for computing crop water requirements. Vol. 56. FAO - Food and Agriculture Organization of the United Nations.
- André, J. C., Molinari, J., 1979. Physico-chemical conditions which affect the concentration measurements of fluorescent tracers and their practical consequences in hydrology. *Journal of Hydrology* 30, 257–285.
- Arkin, P. A., Meisner, B. N., 1987. The relationship between large-scale convective rainfall and cold cloud over the Western hemisphere during 1982-84. *Monthly Weather Review* 115, 51–74.
- Campbell, C. S., Calissendorff, C., Williams, J. H., 1991. Probe for measuring soil specific heat using a heat-pulse method. *Soil Science Society of America Journal* 55, 291–293.
- de Jeu, R. A. M., Wagner, W., Holmes, T. R. H., Dolman, A. J., van de Giesen, N. C., Friesen, J., 2008. Global soil moisture patterns observed by space borne microwave radiometers and scatterometers. *Surveys in Geophysics* 29, 399–420.
- Drusch, M., Wood, E. F., Gao, H., Thiele, A., 2004. Soil moisture retrieval during the Southern Great Plains Hydrology Experiment. *Water Resources Research* 40, –.
- Entekhabi, D., Njoku, E. G., O'Neill, P. E., Kellogg, K. H., Crow, W. T., Edelstein, W. N., Entin, J. K., Goodman, S. D., Jackson, T. J., Johnson, J., Kimball, J., Piepmeier, J. R., Koster, R. D., Martin, N. McDonald, K. C., Moghaddam, M., Moran, S., Reichle, R., Shi, J. C., Spencer, M. W., Thurman, S. W., Tsang, L., Van Zyl, J., 2010. The soil moisture active passive (SMAP) mission. *Proceedings of the IEEE* 98, 704–716.
- Ferraro, R. R., Marks, G. F., 1995. The development of SSM/I rain-rate retrieval algorithms using ground-based radar measurements. *Journal of Atmospheric Oceanic Technology* 12, 755–770.
- Gonzales, A. L., Nonner, J., Heijkers, J., Uhlenbrook, S., 2009. Comparison of different base flow separation methods in a lowland catchment. *Hydrology and Earth System Sciences* 13, 2055–2068.
- Gordon, R. L., 1989. Acoustic measurements of river discharge. *ASCE Journal of Hydraulic Engineering* 115, 925–936.
- Grismer, M. E., Orang, M., Snyder, R., Matyac, R., 2002. Pan evaporation to reference evapotranspiration conversion methods. *Journal of Irrigation and Drainage Engineering* 128, 180–184.
- Henderson, F. M., 1963. Flood waves in prismatic channels. *Proc. ASCE* 89, 39–67.
- Jansen, P. P., van Bendegom, L., van den Berg, J., de Vries, M., Zonen, A., 1979, reprint 1994. Principles of river engineering - The non-tidal alluvial river. Delftse uitgevers maatschappij.

- Kerr, Y. H., Waldteufel, P., Wigneron, J. P., Martinuzzi, J. M., Font, J., Berger, M., 2001. Soil moisture retrieval from space: The soil moisture and ocean salinity (SMOS) mission. *IEEE Transactions on Geoscience and Remote Sensing* 39, 1729–1735.
- Leibundgut, C., Seibert, J., 2011. *Treatise on Water*. Oxford: Academic Press, Ch. Tracer Hydrology, pp. 215–236.
- Monteith, J. L., 1965. Evaporation and the environment. In: *Symp. Soc. Expl. Biol.* Vol. 19. pp. 205–234.
- Njoku, E. G., a. E. D., 1996. Passive microwave remote sensing of soil moisture. *Journal of Hydrology* 184, 101–129.
- Penman, H. L., 1948. Natural evaporation from open water, bare soil and grass. *Proceedings of the Royal Society of London* 193, 120–146.
- Riggs, H., 1976. A simplified slope-area method for estimating flood discharges in natural channels. *Journal of research of the US Geological Survey* 4, 285–291.
- Robinson, D. A., Campbell, C. S., Hopmans, J. W., Hornbuckle, B. K., Jones, S. B., Knight, R., Ogden, F., Selker, J., Wendroth, O., 2008. Soil moisture measurements for ecological and hydrological watershed-scale observatories: a review. *Vadoze Zone Journal* 7, 358–389.
- Uhlenbrook, S., Didszun, J., Wenninger, J., 2008. Source areas and mixing of runoff components at the hillslope scale - a multi-technical approach. *Hydrological Sciences* 53, 741–753.
- Uhlenbrook, S., Frey, M., Leibundgut, C., Maloszewski, P., 2002. Hydrograph separations in a mesoscale mountainous basin at event and seasonal timescales. *Water Resources Research* 38.
- van Mazijk, A. D., 1996. One-dimensional approach of transport phenomena of dissolved matter in rivers. Ph.D. thesis, TU Delft.
- Vereecken, H., Huisman, J. A., Bogaen, H., Vanderborght, J., Vrugt, J. A., Hopmans, J. W., 2008. On the value of soil moisture measurements in vadose zone hydrology: a review. *Water Resources Research* 44, –.
- Wagner, W., Scipal, K., 2000. Large-scale soil moisture mapping in Western Africa using the ERS scatterometer. *IEEE Transactions on Geoscience and Remote Sensing* 38, 1777–1782.
- Wagner, W. G., Blöschl, G., Pampaloni, P., Calvet, J. C. and Bizzarri, B., Wigneron, J. P., Kerr, Y., 2007. Operational readiness of microwave remote sensing of soil moisture for hydrologic applications. *Nordic Hydrology* 38, 1–20.
- Wenninger, J., Uhlenbrook, S., Tilch, N., Leibundgut, C., 2004. Experimental evidence of fast groundwater responses in a hillslope/floodplain area in the Black Forest Mountains, Germany. *Hydrological Processes* 18, 3305–3322.
- Winsemius, H. C., 2009. Satellite data as complementary information for hydrological models. Ph.D. thesis, Delft University of Technology.

Zhao, L., Weng, F., 2002. Retrieval of ice cloud parameters using the Advanced Microwave Sounding Unit. *Journal of Applied Meteorology* 41, 384–395.